Funded by the European Union

LILAS4SOILS

CARBON FARMING

LILAS4SOILS D4.1 – Protocol for Sampling and Data Collection

Author(s):	*Mercedes Román Dobarco, Patricia Gallejones Bringas, Ainara Artetxe Arrien, Arrate Lacalle Gutiérrez, Lur Epelde Sierra, Aitor Anitua Martínez, Mikel Anza Hortala, Oscar del Hierro Cerezo, Olatz Unamunzaga Galarza, NEIKER*
Version:	*First Version – **This is a draft version subject to the approval of EC.***
Quality review:	*María Alonso-Ayuso (ITACYL), Jose Luis Gabriel Pérez (INIA-CSIC), Marta Goberna (INIA-CSIC), Regina Menino (INIAV), Ana Marta Paz (INIAV), José Antonio Rodríguez Martin (INIA-CSIC), Benjamín Sánchez Gimeno (INIA-CSIC)*
Submission Date:	*DD/04/2025*
Dissemination level:	*PU*
Grant Agreement N°:	101157414
Starting Date:	01-09-2024
Duration:	60 months
Coordinator:	Javier Gonzalez, EIT Food South
Contact details:	javier.gonzalez@eitfood.eu

Funded by the European Union. Views and opinions expressed are however those of the author(s) only and do not necessarily reflect those of the European Union or LILAS4SOILS. Neither the European Union nor the granting authority can be held responsible for them.

Table of Contents

Abbreviations 2
Summary 3
1. Introduction 4
1.1 Synergies and trade-offs between SOC storage and other soil functions 5
1.2 Target spatial scale 7
1.3 Minimum detectable difference and number of samples 7
1.4 Space-time sampling designs 8
2. Soil sampling approaches 9
2.1 Simple Random Sampling 9
2.2 Area-Frame Randomized Soil Sampling (AFRSS) 10
2.3 Stratification with Compact Geographical Strata 11
2.4 Stratification with clusters defined from environmental covariates 14
2.5 Targeted sampling 19
2.6 Conditioned Latin Hypercube Sampling 19
2.7 OSPATS+ 20
2.8 Allocation of soil samples among strata 21
2.9 Choice of sampling design 21
3. SOC Sampling and Monitoring Protocol 24
3.1 Spatial boundaries of intervention area 24
3.2 Protocol for spatial sampling 25
3.3 Soil properties measured at different soil monitoring times 28
3.4 Protocol for field sampling 30
3.5 Laboratory analyses and calculations of soil properties for estimating SOC stocks 35
3.6 Calculation of SOC stocks 40
3.7 Equivalent soil mass 41
3.8 Calculation of SOC stock change 42
3.9 Measuring and modelling changes in SOC 43
3.10 Establishment of baseline SOC values 44
3.11 Available resources and tutorials on sampling design and implementation in R 45
References 46
Annex A 52
Applying the soil sampling protocol with R 52

Abbreviations

AFRSS	Area-Frame Randomized Soil Sampling
C	Carbon
CF	Carbon farming
cLHS	Conditioned Latin Hypercube Sampling
CRCF	Carbon Removals and Carbon Farming
CRS	Coordinate Reference System
ICOS	Integrated Carbon Observation System
IS	Independent synchronous
GHG	Greenhouse gas
GIS	Geographic information system
LL	Living lab
LUCAS	Land Use/Cover Area frame statistical Survey
MAOM	Mineral-associated organic matter
MDD	Minimum detectable difference
MRV	Monitoring, reporting and verification
NDVI	Normalized difference vegetation index
PMN	Potential mineralizable nitrogen
POM	Particulate organic matter
RP	Rotating panel
SA	Serially alternating
SIC	Soil inorganic carbon
SOC	Soil organic carbon
SP	Supplemented panel
SRS	Simple random sampling
SS	Static-synchronous
TC	Total carbon
TWI	Topographic wetness index

Summary

This deliverable supports the planning and implementation of soil sampling design across participant demo-sites from five living labs in the context of LILAS4SOILS (*Fostering Carbon Farming Practices through LIving LAbS in the Mediterranean & Southern EU for the healthy future of European SOILS*). The target end-users of the soil sampling and data collection protocol involves farmers and agricultural managers interested in setting up carbon farming projects. The deliverable includes field and laboratory protocols to measure several soil properties beyond soil organic carbon stocks, indicators of several soil functions.

The deliverable is structured by providing a brief introduction to the objectives of LILAS4SOILS and some aspects of space-time monitoring of soil organic carbon, followed by an overview of some methods for soil spatial sampling approaches, the instructions for spatial sampling design, field sampling, laboratory analyses and calculations within LILAS4SOILS, and a short tutorial for implementing spatial sampling with the free and open software R.

The authors would like to thank Alexandre M.J.-C. Wadoux (INRAE, France), Andrea Ferrarini (UNICATT, Italy), Jose Luis Gabriel Pérez (INIA, Spain) and Benjamín Sánchez Gimeno (CSIC, Spain) for their valuable help with spatial soil sampling strategies at the early stages of designing this protocol.

This document is a draft version for expert consultation and subject to the approval of the European Commission.

1. Introduction

Soils are the main reservoir of carbon in terrestrial ecosystems (Dixon et al., 1994), with a combined pool of organic and inorganic carbon (C) of approximately four times the atmospheric C pool and seven times the biotic C pool (Lal, 2010). The global soil organic carbon (SOC) stock for the first metre of soil is estimated in 1500 Pg C (Jobbágy and Jackson, 2000) with other estimates ranging from 504 to 3000 Pg C (Scharlemann et al., 2014). The soil carbon stocks increase to 2400 Pg C for SOC (Batjes, 1996) and more than 2300 Pg for soil inorganic carbon (SIC) in the first two metres (Zamanian et al., 2021). Soils can be a sink or a source of C. Hence, even small changes in SOC dynamics and storage can alter the ecosystem C balance with an impact on atmospheric CO_2 levels at the regional scale. The global C budget for 2023 estimated the net uptake of CO_2 by the land on 2.3 ± 1.0 Gt C yr^{-1}, while fossil emissions were 10.1 ± 0.5 Gt C yr^{-1} and land use change emissions 1.0 ± 0.7 Gt C yr^{-1} (Friedlingstein et al., 2025). Zickfeld et al. (2023) advised that reducing CO_2 or greenhouse gas (GHG) emissions should be prioritised over removals if we aim to achieve the goal of the Paris Agreement to limit global warming well below 2 °C and to pursue efforts to limit warming to 1.5 °C relative to pre-industrial levels. The rationale is that the effects of both processes (emissions and removals) on climate may not be equivalent due to differences in their biogeophysical effects, impermanence of sequestered C, non-CO_2 GHG and aerosol effects, and nonlinearities of the Earth system (Zickfeld et al., 2023). They posit that carbon neutrality may not mean climate neutrality. The implementation of removal technologies (including land use change and reforestation and afforestation practices, and C sequestration in the soil through agricultural practices) to an extent needed to achieve climate goals may not be feasible due to biophysical and economic constraints (Smith et al., 2016). Rather than promoting soil C sequestration as a universal remedy to compensate fossil emissions, the scientific community, agriculture and land managers, and different stakeholders should emphasize the beneficial effects of enhancing soil C sequestration on overall soil health and functions (Baveye et al., 2018). Indeed, the central role of SOC for soil multifunctionality encourages the adoption of agricultural practices increasing SOC storage (Kopittke et al., 2022). International initiatives like “4 per 1000” (https://4p1000.org/) aim at sequestering C from the atmosphere while enhancing soil functions and services, notably food security and resilience and adaptation to climate change.

Carbon farming (CF) encompasses several sustainable agricultural and forestry practices that target the reduction of greenhouse gas (GHG) emissions from soils and enhance C storage in soils and biomass. Besides the positive effects on climate change abatement and soil health, CF may become an additional source of income for farmers and foresters by the participation in voluntary C credit markets. The EU Carbon Removals and Carbon Farming (CRCF) Certification Regulation (European Parliament, Council of the European Union, 2024) laid the grounds for establishing the first EU-wide voluntary framework for certifying C removals, CF and carbon storage in products across Europe. Some carbon farming practices (CFPs) that are considered by the CRCF (Directorate-General for Climate Action, European Commission, 2025) and that can be applicable to the Mediterranean context include:

- Peatland management. Rewetting and restoring previously drained peatlands, keeping existing peatlands in good conservation status to avoid emissions, and adapted management of drained peatlands currently destined to productive uses which cannot be restored.
- Agroforestry and mixed farming. Increasing silvoarable and silvopastoral systems, integrating trees or shrubs with crop and/or livestock management, presence of hedgerows or field boundary tree cover.
- Improved fertilizer use efficiency management to reduce nitrous gas emissions (nutrient planning, use of nitrification inhibitors).

- Soil protection and SOC management practices like cover crops, conservation tillage, improved crop rotations, organic farming, etc.
- Reforestation respecting ecological principles for biodiversity and sustainable forest management.
- Livestock management. Grazing and grassland management, reducing enteric methane by improving feed digestibility and efficiency, reducing NO emissions through manure management.

The aim of this deliverable is to provide LILAS4SOILS and CF project planners with guidelines for selecting the soil sampling design more adequate to the characteristics of the project area (i.e., demo-sites at each living lab). The deliverable includes field and laboratory protocols to measure several soil properties during the course of the CF project, to assess the effects of CFPs on SOC stocks and other indicators of soil health, soil functions or threats to soil (Evangelista et al., 2023; Lehmann et al., 2020; Liptzin et al., 2022). A single soil sampling design will not be suitable across all sites due to inherent differences between agricultural systems (e.g., cropland, pastures, vineyards, *montado* or *dehesa,* olive groves, etc.), degree of spatial variability in soil properties, relief, and management history within the farms, and the type of CFPs implemented at each site. Considering the technical and financial constraints of any project, we propose a simplified protocol that will allow to estimate temporal changes on SOC stocks at a demo-site caused by the implementation of CFPs while providing a robust estimator of the spatial mean SOC stock.

The sampling protocol has the objectives of providing an unbiased estimator of the average temporal change in SOC stock per intervention area within a demo-site. The first sampling campaign (time 0) will set the baseline SOC stock value per demo-site at each living lab (LL) prior the implementation of the CFPs. The sampling strategy should be able to measure changes in SOC stock efficiently in the subsequent sampling times and to represent the spatial variability of the SOC stock in the intervention area. Thus, the preferred sampling protocols need to be:

- Design-unbiased, so we obtain a robust estimate of the change in SOC stock.
- Cost-effective, minimizing the number of samples analysed at the lab while providing reliable estimates of SOC stocks and SOC stock change at a desired confidence level.
- Easy to implement by the fieldwork team with the available resources of time and people.

Several soil sampling approaches require previous information on the spatial distribution of SOC content and its uncertainty at the farm level (De Gruijter et al., 2016) or environmental covariates, proxies of the soil-forming factors that influence SOC storage (Minasny and McBratney, 2006). This protocol aims to find a trade-off between sampling effort and statistical power while providing a design-unbiased estimator of the variance of the mean SOC change (Arrouays et al., 2018).

1.1 Synergies and trade-offs between SOC storage and other soil functions

There are several frameworks and definition of soil functions. Soil functions have been broadly defined as “bundles of soil processes that underpin the delivery of ecosystem services” (Bünemann et al., 2018). Evangelista et al. (2023) provides a list of soil functions that are an extension of those defined by Blum (2005) and the European Commission (Commission of the European Communities, 2006). According to Evangelista et al. (2023) the soil is:

- A producer of food and biomass.
- A store of carbon.

- A habitat for, and of, biodiversity.
- A store and regulator of nutrients.
- A store, purifier and regulator of water.
- A filter and remediator of contaminants.
- A source of raw materials.
- An archive of archæological artefacts.

The quantitative assessment of soil functions is complex, but a common element of different approaches begins with the identification of a minimum set of relevant indicators. These indicators are soil properties (dynamic or static) that inform of the soil potential and current performance of a function for given local conditions and management (Bünemann et al., 2018; Drobnik et al., 2018; Vogel et al., 2019). The list of indicators for soil functions, soil health and related concepts is quite extensive, but SOC or SOC related properties are common among all lists.

SOC is the main component of soil organic matter and is considered a general indicator of soil quality and soil health due to its correlation with multiple soil properties and critical role for soil functions, resilience and resistance to pressures (Herrick and Wander, 1998). Soil organic matter (SOM) influences physical soil properties like compactability, friability and increases soil water retention attributes, although the positive effect on available water capacity may be more limited than previously estimated (Minasny and McBratney, 2018). The interactions between plant roots, soil biota and SOC develop soil aggregates and structure, regulating air and water infiltration and movement through the profile, soil permeability and erodibility. The predominantly negative charge of organic matter's functional groups contributes to the soil cation exchange capacity, and weak acidic functional groups contribute to the soil buffering capacity, influencing the function of nutrient storage and regulation. SOM has high sorption capacity for several pollutants and heavy metals, leading to their immobilisation and preventing the contamination of groundwater and bioavailability, supplying the soil function of filter and remediator of contaminants (Kwiatkowska-Malina, 2018).

Vrebos et al. (2021) assessed the trade-offs and synergies between soil functions in agricultural lands from different pedoclimatic zones in Europe. Across the entire European Union, the function of climate regulation was positively correlated with drought protection and water purification and negatively correlated with waterlogging protection and nutrient cycling. The sign and magnitude of correlations between soil functions vary among climatic zones and land uses (e.g., arable land and grasslands) (Vrebos et al., 2021; Zwetsloot et al., 2021). For example, Zwetsloot et al. (2021) found positive correlations between climate regulation and biodiversity in grasslands and arable land in the Pannonian climatic region, whereas in Atlantic arable land the correlation between climate regulation and biodiversity was negative.

One of the objectives of LILAS4SOILS is to assess the potential synergies and trade-offs between soil functions resulting from the implementation of CFPs in agricultural and agroforestry systems and an increase on SOC storage. To that end, a set of soil indicators or soil properties used as input to model soil functions will be measured simultaneously to SOC stocks, namely: particle size distribution, coarse fragments, bulk density, SOC, TC, total nitrogen, carbonates, pH, potential mineralizable nitrogen (PMN), SOM fractions, soil moisture at field water capacity and at permanent wilting point, and 16S rRNA gene amplicon sequencing.

1.2 Target spatial scale

The spatial scale of this protocol refers to agricultural fields, pastures, or orchards within farms where CFPs are implemented, i.e., intervention areas (FAO, 2020). At a single farm or exploitation there may be several intervention areas where different CFPs are eligible. The scope of monitored areas by LILAS4SOILS is ideally one intervention area where homogeneous CFPs are implemented.

The sizes of the demo-sites range between less than one hectare to several hundred hectares. Regardless of the size of the demo-site, the intervention area will occupy between 1-5 ha (i.e., area where soil properties will be monitored). A factor that will influence the choice of the sampling approach is whether the intervention area will be subject to a single or different management plans. If different combinations of CFPs are implemented within a demo-site (e.g., no-till and cover crops, conversion from arable to grassland), these differences in management require to be treated as different intervention areas to assess the effect of different CPFs per site, or as different strata for planning the soil sampling. The stratification shall remain constant through the duration of the monitoring.

The methods for spatial sampling described in section 2 are applicable to larger farms or intervention areas, and to several intervention areas not necessarily spatially contiguous but in proximity (local scale) and that can be grouped into a single carbon farming project. The latter approach is used by many companies working on SOC monitoring, reporting and verification (MRV) projects (e.g., Agricarbon, SEQANA) as means to increase the cost efficiency of the soil sampling.

1.3 Minimum detectable difference and number of samples

To estimate the minimum detectable difference (MDD) in SOC stock for an acceptable level of uncertainty, we need measurements from two different times, t_0 and t_1 (FAO, 2020). To calculate the number of samples needed to achieve the desired MDD on SOC stock without available data for our study site, some authors recommend using values from the literature on the expected rate in SOC change associated with CFPs. Power analysis for a given confidence level can be applied to estimate the MDD:

$$MDD \geq \frac{S}{\sqrt{n}} x \left(t_{\alpha,v} + t_{\beta,v}\right)$$

where S is the standard deviation of paired differences in SOC stocks measured at t_0 and t_1, n is the number of samples, $t_{\alpha,v}$ is the two-sided critical value of the t-distribution at a given significance level (α) (often 5 to 10 %) for v degrees of freedom (v = n - 1), and $t_{\beta,v}$ is the one-sided quartile of the t-distribution corresponding to a probability of type II error β (being 1 − β the statistical power, often 80 to 90%) (FAO, 2020). Then, the minimum number of samples for a desired MDD would be:

$$n \geq \left(\frac{S\, x \left(t_{\alpha,v} + t_{\beta,v}\right)}{MDD}\right)^2$$

As an example, for a confidence level of 5 % and 2 degrees of freedom, $t_{0.025,2}$ (two-tailed, α = 0.05) is approximately 4.303. The $t_{0.2,2}$ (one-tailed, statistical power of 80%) is approximately 0.816 for 2 degrees of freedom. For a hypothetical MDD of 2 Mg C ha^{-1} between t_0 and t_1, and a standard deviation of paired differences in SOC stock of 1.5 Mg C ha^{-1}, the minimum number of samples would be 14.7. The sample size needs to be rounded to an integer, resulting on at least 15 soil samples.

Smaller values of MDD increase the minimum number of samples, whereas reducing the variance of the paired differences in SOC stocks would reduce the number minimum soil samples. FAO (2020) suggests carrying a preliminary sampling (5-10 samples) of the area of interest to estimate the spatial variability at farm scale, of the mean SOC. This is not the same as temporal variability but can give insight on the number of samples needed to capture the farm variability.

1.4 Space-time sampling designs

There are several types of synchronous space-time sampling designs that Brus (2022) and De Gruijter et al. (2006) classified and explained as:

- Static-synchronous (SS). The same sampling units are revisited in consecutive sampling campaigns.
- Independent synchronous (IS). A different probability sample is selected independently at each survey.
- Serially alternating (SA). Is a compromise between SS and IS. The sampling locations from the first survey are revisited at a later survey separated a determined time period, a multiple of the sampling interval (e.g., every 12 years for a sampling interval of 2 years, the period of revisits would be 6). Meanwhile, an independent sample is selected at the second survey which will be revisited after the same period, and so on. The sampling locations are revisited in the same order.
- Supplemented panel (SP). Another hybrid approach, only a subset of locations from the first survey is revisited at the subsequent surveys (permanent locations). The permanent locations are supplemented with an independent sample every survey.
- Rotating panel (RP). A proportion of the locations from the first survey (panel a) is revisited at the second survey and supplemented with additional locations (panel b). At the third survey, the locations that were only sampled at the previous time (panel b) are revisited and supplemented with a new sample (panel c). The same panel of locations is only sampled two consecutive times but replaced consecutively.

Depending on the persistence of the spatial pattern, Brus and De Gruijter (2013) made recommendations for choosing a space-time sampling design from a simulation study, that later Mudge et al. (2020) synthesized as follows: the SP is the best choice when there is strong persistence, whereas IS and SA are better choices for estimating the mean or the spatial trend in SOC for weak persistence of spatial patterns. In intermediate cases of moderate persistence, the choice depends on the objective of the monitoring. SS is more suitable for estimating the trend, IS is better for estimating the mean, whereas SP or SA are good choices when both parameters are of interest.

Mudge et al. (2020) summarised the advantages and disadvantages of the different designs for monitoring changes in SOC stocks in individual pastoral farms depending on if the objective of the monitoring is to estimate the mean or the trend of SOC stocks. Mudge et al. (2020) suggested that:

- Revisiting sampling locations generally improves the precision of the spatial mean estimate of change by reducing the sampling variance.

- Hence, the SS approach should reduce costs compared to IS for a required MDD in SOC. It is also simpler and easier.
- However, revising sampling locations is often avoided due to the risk of loss of market confidence out of fear of possible preferential agricultural practices near sampling locations.
- Hybrid designs like SP or SA may be better when no information on the spatial patterns of SOC are known, and we wish to estimate both the mean and trend of SOC.
- Hybrid approaches also reduce the risk of fraudulent practices since just a subset of locations are revisited and this risk is completely avoided with IS at the expense of increasing the number of required sampling locations for a desired MDC.

2. Soil sampling approaches

There are two main approaches that are generally used for monitoring soil properties over space and time, model-based and design-based. According to Brus (2021), the key differences between both approaches makes model-based approaches more appropriate for mapping, whereas design-based approaches are better when our aim is to estimate the mean or the total of a soil properties for a study area. Design-based sampling is generally stronger in terms of the validity of the estimate of the population mean and has a lower uncertainty for the same sample size than model-based approaches. The main difference between the two approaches is that whereas in design-based the random process needed to understand the spatial correlation originates from the random selection of sampling units (probability sampling), in model-based approaches the randomness is embedded in the statistical model of spatial variation, which is a stochastic model and therefore includes a random error term (Brus, 2014). There are also hybrid methods that combine the strengths of both approaches (Brus, 2021).

Some of the sampling approaches described in this section are protocols specifically defined for farm-scale carbon farming auditing (e.g., OSPATS (De Gruijter et al., 2019, 2016)), while most approaches are general designs for soil monitoring. There are many more types of sampling designs than those included here. For a detailed overview of sampling designs for soil survey we refer to Brus (2022) and De Gruijter et al. (2006).

2.1 Simple Random Sampling

Simple Random Sampling (SRS) is easy to implement, unbiased (probability sample), and it is one the most basic sampling designs. The sampling can be done with and without replacement. With replacement, a population unit can be selected more than once. SRS requires little to no prior information about the spatial distribution of the soil property of interest or environmental covariates. Hence, SRS is often done at preliminary step to calculate the number of samples needed for capturing the spatial variability and estimate the mean SOC stock at a given confidence level. The disadvantage of SRS is that it is not as efficient or accurate as other designs, and as it requires a larger sample size it increases the sampling costs (Soil Survey Staff, 2025). Because no information on the soil-forming factors is used, the sample may not represent the feature space. There is also risk of generating a clustered sample that does not cover the geographical space evenly (Soil Survey Staff, 2025).

2.2 Area-Frame Randomized Soil Sampling (AFRSS)

The Area-Frame Randomized Soil Sampling (AFRSS) protocol was designed by Stolbovoy et al. (2005) and updated (Stolbovoy et al., 2007) as a cost-efficient method to estimate changes in SOC stocks at croplands, pastures and forests. It does not require prior information on soil properties, relief attributes, management history, yield maps or other ancillary data. The AFRSS is a two-stage sampling design. In the first stage, a square grid of 100 cells that allows for a "modified" random sampling is overlayed with the agricultural field or area of interest, referred in this section as "plot" (Stolbovoy et al., 2007). The grid is numbered randomly (0-100) but avoiding that cells with consecutive numeration are too close to each other to avoid clustering of sampling units. The size of the grid is calculated from the extent of the field or plot. The longest X or Y axis (Maxis) is divided by 10 (Grid size = Gs = Maxis/10) (Stolbovoy et al., 2007). The randomized sampling template is adapted to the size of the plot. Then, depending on the size of the plot (Table 1), n primary sampling units are selected, starting with the cell with the lowest number located completely within the plot, and adding cells subsequently with the same criteria. This can be interpreted as that primary sampling units are selected randomly. The second phase consists of dividing each primary sampling unit into a 6 x 6 regular grid and locating 25 sampling points at the inner vertices (Figure 1). Hence, the sampling points are located at the centroid of the sampling unit and adding Gs/6 along N-S and E-W axes in both directions (Figure 1). Soil samples taken at the 25 points are combined into a composite, representative of the sampling unit variability.

Table 1: Recommended number of primary sampling units (cells of the grid) depending on the monitored area (Stolbovoy et al., 2007).

Size of the plot	Number of sampling units (n)
< 5 ha	3
5 – 10 ha	4
10 – 25 ha	5
> 25 ha	6

The AFRSS is some sort of two-stage random and systematic sampling design. The soils located near the edges of the plot have higher likelihood of falling in an incomplete grid cell. Hence, these areas will be undersampled. The probability that the soils located in edge cells to be sampled is zero, thus we cannot speak of a probability sample (Brus, 2022). The sampling units can be interpreted as a finite set of adjacent squares that replace the infinite population of soil samples. There is no design-unbiased estimator of the sampling variance with this type of designs (Brus, 2022). The number of subsamples per sampling unit (n = 25) generally captures well the variability of SOC within the sampling unit. The size of the sampling unit (grid size) is scalable with the size of the study area. This can be seen as a disadvantage when applied across different demo-sites because the spatial support of the sample will differ across sites. This approach has been applied to estimate changes in SOC stocks along chronosequences from agricultural lands, abandoned agricultural lands and forests (Bell et al., 2021), and to characterise the conservation of soil resources at agroecosystems at risk of desertification (Boschetto et al., 2010).

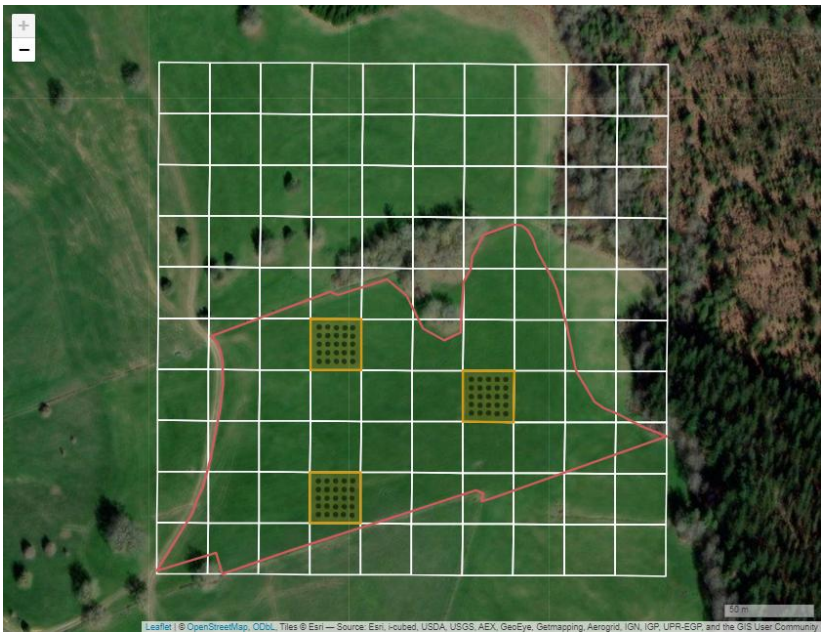

Figure 1: Sampling units selected with the Area-Frame Randomized Soil Sampling protocol for a pasture of 2.7 ha located at Behialde (Bizkaia). The selected grid cells (sampling units) are highlighted in orange, and the 25 sampling points to make a composite in black.

Compared to other sampling protocols that require between 5 to 11, the 25 subsamples per composite increase the time required for sampling a single demo-site. The comparison of mean SOC stocks calculated with composite samples made of 25, 13, or 12 aliquots per composite applying the AFRSS protocol (Stolbovoy et al., 2007) at three sites at the Basque Country (cropland, pasture, and forest) did not find significant differences between estimates of the mean SOC stocks (unpublished data). Thus, the Stolbovoy protocol can be simplified by reducing the number of soil cores (sampling points) used to make a composite sample from 25 to 13. In the context of LILAS4SOILS we prioritise having the same area for soil sampling units, and hence the simplified Stolbovoy will not be used, but it can be of interest for other carbon farming projects.

2.3 Stratification with Compact Geographical Strata

Some sampling designs can be advantageous when there is no prior information on the variability of the soil properties, SOC stocks, management history or other environmental factors that may influence SOC storage or when the area of interest is relatively homogeneous. Sampling designs with compact geographical strata are advantageous when no ancillary data on SOC storage is available (Chappell et al., n.d.; De Gruijter et al., 2006; Guerrero and Lorenzetti, 2021), or there is no possibility to explore other stratifications (e.g., lack of time or expertise for exploring stratification with proxies of yield, management history, relief, etc.). Another advantage is that as we take a probability sample, the sample mean is an unbiased estimator of the population mean (mean SOC), and we also obtain an unbiased estimate of the variance of the mean change in SOC.

The study area (field, pasture, orchard) is divided into strata that are geographically compact (i.e., strata are defined from the pixel coordinates, as groups of adjacent pixels) and of relatively equal size. Strata of the same size have the advantage that their weights are the same, and the sample mean is an unbiased estimator of the population mean (Brus, 2022). Stratification based on geographical strata improves the spatial coverage of the sample. Once the strata are defined, the sampling design for collecting the samples within each stratum can vary among multiple methods. The compact geographical strata can be generated with the R package *spcosa* (Walvoort et al., 2023).

Stratified simple random sampling for composite samples: Simple random sampling can be applied at each stratum. The same number of samples are assigned per stratum since they are equal-area strata. If there are no budget constraints, we can analyse each sample individually. However, to reduce the laboratory costs we can create composite samples combining several samples in one composite sample from each stratum. By increasing the number of strata, we improve the spatial coverage, avoid that points are spatially clustered and likely obtain a good spatial estimate of the mean SOC stock for the area of interest. As an example, we illustrate a stratified simple random sampling at the pasture of Behialde creating 15 strata and making 3 composites from a total of 45 individual soil samples (Figure 2).

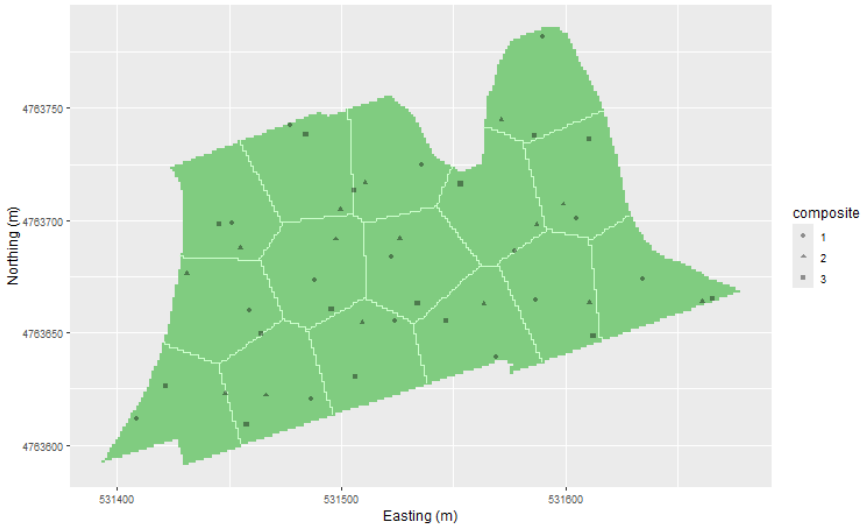

Figure 2: Stratified random sampling from geographical compact strata for preparing composite samples. The area of interest is a pasture at Behialde (Bizkaia, Spain).

Stratified simple random sampling: A selection of points from each stratum can be done with simple random sample. The result would be as in Figure 2 but without making composites (n = 45). However, instead of using the random locations for taking an individual sample, we can set up a sampling unit as in a two-stage sampling design. The location of the random points can be used as the centre of the sampling unit. Within these sampling units we can collect samples at secondary sampling points for making a composite.

Arrouays et al. (2018) designed a sampling protocol for monitoring SOC stock changes for the Integrated Carbon Observation System (ICOS) testing it at 9 CarboEurope sites (https://www.carboeurope.org/) using stratified random sampling. They used geographically compact sub-areas as strata to avoid clustering the sampling locations and to improve the accuracy of the spatial mean SOC stock. This sampling approach is a

probability sample, which allows to estimate the statistical parameters efficiently with a small sample size (Arrouays et al., 2018). They created 20 strata of equal area and at each stratum they located two circular plots of 10 m radius. These circular plots are the first-order sparse measurement points. Within each circular plot, they assigned 5 locations randomly, that are the second-order sparse measurement points, and that were combined into a composite sample. We illustrate a modified version of this protocol at Behialde (Figure 3) defining three compact strata, one plot per stratum, and 10 secondary random sampling points per circular plot. In this example, the number of strata is three because this is the minimum required by some established protocols (e.g., FAO). The number of secondary random sampling points is arbitrary (e.g., it could be 5 random sampling points). Alternatively, the second-order sampling points could be located at predetermined locations from the first-order measuring point (e.g., as in LUCAS).

a)

b)

Figure 3: Two-stage stratified random sampling from geographical compact strata. a) The first stage consists in dividing the area of interest into equal-area compact strata and selecting one point per stratum randomly. b) The second stage consists of delineating plots of 10 m radius around the locations and selecting randomly 10 points per plot. The area of interest is a pasture at Behialde (Bizkaia, Spain).

2.4 Stratification with clusters defined from environmental covariates

The inherent capacity of soil to store SOC is determined by the soil-forming factors and intrinsic soil properties like particle size distribution, mineralogy or soil type. The current SOC storage is influenced by the land use and management history, land cover and vegetation, climate, parent material and relief. Spatial ancillary data or environmental covariates that inform directly or indirectly on these factors can be used to stratify the area of interest into zones that are likely to have differences in current SOC storage or where we expect different responses to management and CFPs. The strata can be delineated combining information on the spatial distribution of SOC content and its uncertainty at the farm (De Gruijter et al., 2016) or environmental covariates, proxies of the soil-forming factors that influence SOC storage (Wiesmeier et al., 2019). At local scale, the main drivers of SOC storage are relief, soil texture and physico-chemical properties, soil microorganisms and soil fauna, land use and management (Wiesmeier et al., 2019). The proxies that are often used for stratification can include soil particle size distribution or soil texture, soil type, surface geochemistry, digital elevation models and derivate variables (slope, curvature, topographic wetness index, northness and eastness), indicators of management intensity and history (e.g., time-series of vegetation indices like normalized difference vegetation index (NDVI), yield maps, management areas). These environmental covariates or ancillary data are often available from public remote sensing databases (e.g., LANDSAT, Copernicus Sentinels). Electromagnetic and gamma radiometrics at high-resolution (proximal or remote sensing) are also very valuable for informing indirectly on soil properties and surface mineralogy and geochemistry.

Long-term series of satellite imagery are very rich in information for characterising land use and land cover changes, vegetation vigour and phenology, and proxies of productivity (e.g., NDVI). Spectral bands acquired from bare soil pixels can inform directly or indirectly on soil properties related to SOC storage and soil properties that control it (Cui et al., 2025; Loiseau et al., 2019; Zhu et al., 2024). This limits their application to arable land that have bare soils some time of the year or semi-arid areas with sparse vegetation (Roberts et al., 2019). Spectral indices that inform of soil properties cannot be calculated for permanent grasslands, croplands with cover crops or without periods of fallow, or with tree cover (e.g., agroforestry, orchards). Vegetation indices calculated from remote sensing time series can be used instead in these cases. Some indices that inform on soil properties (mineralogy, texture, SOC) among many others are shown in

Table 2. Moreover, a map of predictions of SOC concentration of SOC stocks can be used as input variable for stratification with clustering (Bettigole et al., 2023).

Table 2: Spectral indices calculated with Sentinel-2 spectral bands acquired on bare soils that can be potentially used for stratification. Selection of indices found in Loiseau et al. (2019) and Cui et al. (2025).

Spectral index	Expression	Related soil properties	References
Coloration index	(Red-Green)/(Red+Green)	Soil color	(Ray et al., 2004)
Grain size index	(Red-Blue)/(Red+Green+Blue)	Fine sand content	(Xiao et al., 2006)
Clay index	SWIR1/SWIR2	Clay	(Joint Research Centre, Hengl, 2007)
Redness Index	$Red^2/(Blue*Green^3)$	Hematite content	(Ray et al., 2004)
Carbonate Index	Red/Green	Carbonate	(Amen and Blaszczynski, 2001)
Ferrous Iron	Red/SWIR1	Ferrous iron	(Amen and Blaszczynski, 2001)

Normalised difference Geological response	(SWIR1-SWIR2)/(SWIR1+SWIR2)	Geological response (gypsum, silt)	(Nield et al., 2007)
Normalised difference Calcareous sediments	(SWIR1-Green)/(SWIR1+Green)	Calcareous Sedimentary rocks	(Nield et al., 2007)
SOC Index	Blue/(Green×Red)	Soil Organic Carbon	(Zhu et al., 2024)
Gypsum Index	(SWIR1-NIR)/(SWIR2+NIR)	Gypsum	(Wang et al., 2022)
SWIR/NIR Carbon Index	SWIR2/NIR	Soil carbon	(Zhu et al., 2024)

The strata can be used as basis for stratified random sampling to make several composites, or to locate first-order sparse measurement points (as detailed in section 2.3). This method of stratification is suggested by many soil carbon MRV protocols like the FAO-GSCOC (2020) or VM0042 (Verra, 2024). This type of **stratification can reduce the sampling variance** because the soil samples are taken from homogeneous areas, with similar SOC range within each stratum, while also capturing better the spatial variation of SOC across the monitored area. When the objective is to assess the temporal change in SOC stock **it is important to maintain the same stratification in subsequent years**, so layers that inform on current management should be avoided.

The number of strata and the minimum number of samples recommended by stratum vary among protocols, and it is related to the heterogeneity of the terrain to be sampled. FAO-GSCOC (2020) recommends creating a minimum of 3 strata and from 5 to 10 sampling locations per stratum. Although to reduce the laboratory costs, creating composite samples is allowed, maintaining a minimum of 3 composites per stratum. Other protocols do not specify a minimum number of strata or samples per stratum, although they suggest calculating the minimum number of samples needed to detect a statistically significant MDD for a given confidence level. The optimal number of clusters (strata) when applying unsupervised classification with clustering algorithms (e.g. k-means) is often selected using internal clustering quality indices like the Silhouette (Rousseeuw, 1987), Calinski-Harabasz (Calinski and Harabasz, 1974) or Dunn (Dunn, 1974) indices among many others.

We stratified the pasture at Behialde using as covariates elevation, slope, the product of northness by slope (a proxy for exposure), topographic wetness index (TWI), and NDVI (standard deviation and the median from each quarter of the year) (Figure 4). The NDVI was calculated from the Harmonized Sentinel-2 MSI (MultiSpectral Instrument, Level-2A (SR)) image collection at 10 m resolution. Processing the Sentinel-2 time series was performed with Google Earth Engine. The date of acquisition of the images ranged from 01/01/2018 to 31/12/2024, and selected images had less than 20% clouds. Clouds and cirrus pixels were masked prior calculating NDVI for each image. Then, the median of NDVI for the first (January-March), second (April-June), third (July-September) and fourth (October-December) quarters and the standard deviation of the whole time series were calculated.

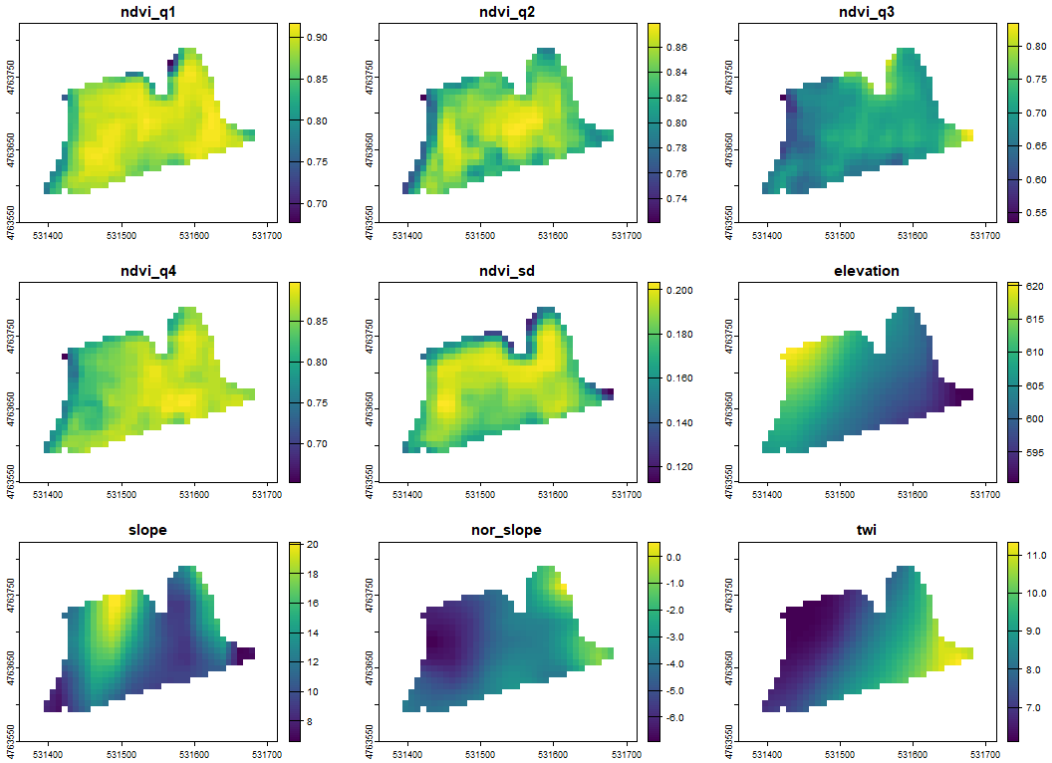

Figure 4: Covariates used for stratification using environmental covariates.

We standardised all variables (mean centred and scaled) and decorrelated the data with the Cholesky transformation (Wicklin, 2012). The latter step allows to use the Mahalanobis distance for k-means clustering, since several covariates are highly correlated (e.g., elevation and TWI, or NDVI variables). The optimal number of strata was examined with the Dunn, Calinski-Harabasz and Silhouette indices. Whereas the Dunn index proposed 2 as optimal number of strata, Silhouette and Calinski-Harabasz suggested 6 strata. The final k-means models were created with k-means clustering selecting the best of 10 initializations and k-means ++ initialization method. We generated maps for 2, 3 and 6 strata (Figure 5).

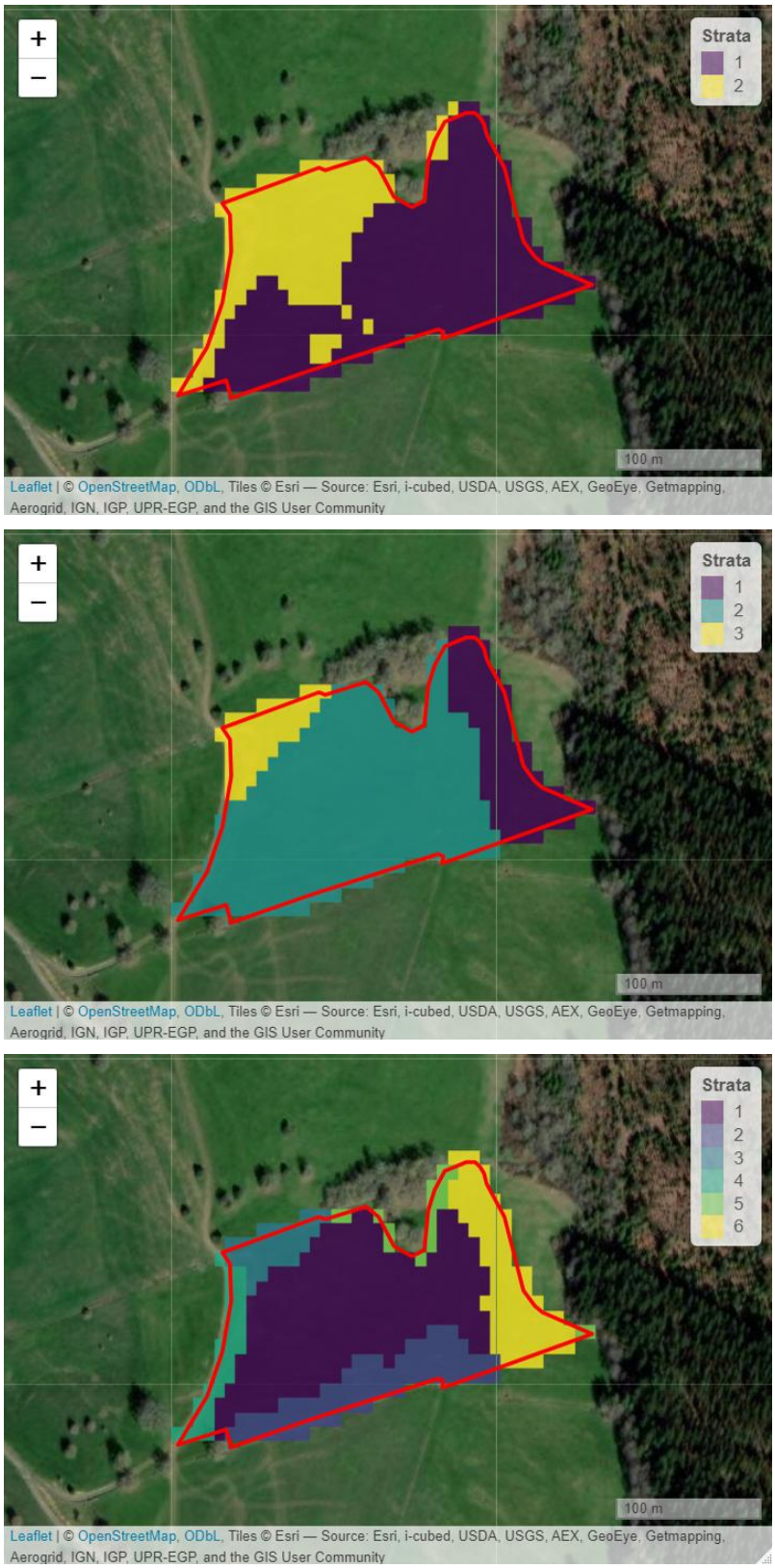

Figure 5: Stratification of Behialde pasture using environmental covariates for 2, 3 and 6 strata.

The map of 6 strata differentiates the areas near the plot boundaries, probably due to the spectral signal influenced by the dirt road and the trees (see strata numbers 4 and 5). Based on visualization of the results, we could select 2 or 3 strata. According to the protocol by the FAO-GSCOC (2020), we would select 3 strata, but the area occupied by each of them is very different (stratum 1 = 19 %, stratum 2 = 72 %, stratum 3 = 9%). However, if we selected 2 strata, given that stratum 1 covers 67% of the plot and stratum 2 occupies 33%, we could assign 3 samples proportionally to the area (2 random samples in stratum 1, and 1 sample in stratum 2) (Figure 6.a).

a)

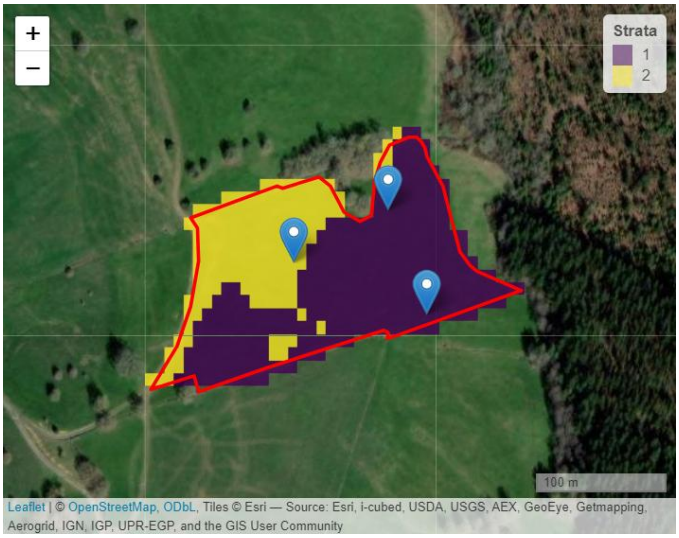

b)

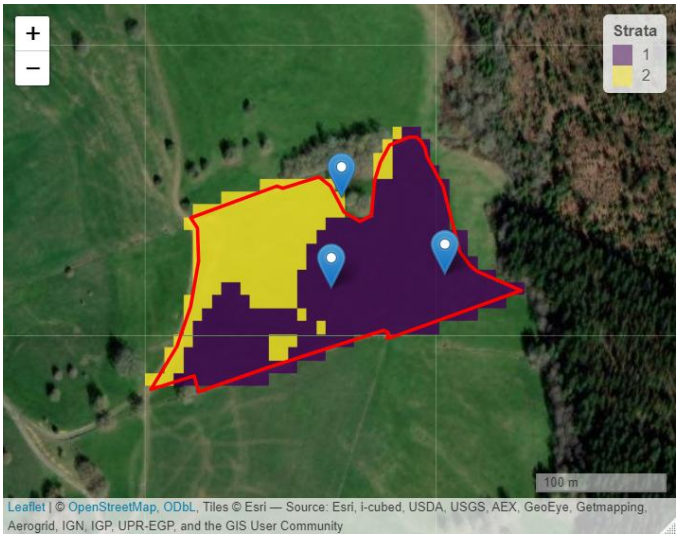

Figure 6: Stratified random sampling with allocation proportional to stratum area for Behialde. a) All sampling points fall within the plot boundaries, b) One sampling point was assigned at a pixel that had part of its area outside the boundaries of the intervention area.

2.5 Targeted sampling

This sampling approach is attractive for systems where we expect clear differences in soil properties due to management strategies (e.g., crop alleys and agroforestry), and is often used in precision agriculture for sampling soils and crop attributes. The FAO protocol (FAO, 2020) and many references in the literature refer to directed stratified sampling, targeted sampling, or zonal sampling to the approach that we define here as stratification with clusters defined from environmental covariates (section 2.4). We prefer the term "stratification with clusters defined from environmental covariates" to emphasize the underlying randomness in the selection of the sampling points, i.e., probability sampling. On the other hand, the term "targeted sampling" may be more suitable when the purpose of the sampling is to identify areas where some soil properties might be above or below critical levels, e.g., high concentration of pollutants or salinity.

For specific agroecosystems like agroforestry or orchards, targeted sampling can refer to locations with relative distances of trees where we can expect much higher SOC stocks compared to arable areas (Cardinael et al., 2017; Minarsch et al., 2024). Targeted sampling can use high resolution imagery or remote sensing data (aerial photographs, electromagnetic induction maps, management maps, etc.) for identifying different zones of SOC levels. In the case of agroforestry or orchard systems, a sketch of the different zones and general tree spacing at the site can be prepared during fieldwork.

2.6 Conditioned Latin Hypercube Sampling

Conditioned Latin Hypercube Sampling (cLHS) was adapted by Minasny and McBratney (2006) from the classic Latin Hypercube sampling algorithm to soil mapping and monitoring. This sampling approach has become very popular and very often it outperforms other stratification methods like k-means on environmental covariates or SOC predictions (Bettigole et al., 2023). cLHS optimizes the coverage of the covariate space (covariate space is the multivariate combination of the different environmental covariates within the study area). The domain of each covariate is divided into n equal sized marginal strata, where n is also the sample size. For p covariates, this results in p^n marginal strata. The bounds of the marginal strata are selected with quantiles from the evenly spaced cumulative probabilities so that the number of grid cells in each stratum is equal. An example of its application in Behialde for a sample size of 6 units is shown in Figure 7. The covariates were the same as in section 2.4 (elevation, slope, product of northness by slope, TWI, and NDVI).

The objective function of (Minasny and McBratney, 2006) has the following criteria (Malone et al., 2019):

- Matching the sample with the empirical distribution functions of the continuous ancillary variables;
- Matching the sample with the empirical distribution functions of the categorical ancillary variables; and
- Matching the sample with the correlation matrix of the continuous ancillary variables.

The cLHS has been modified to account for inaccessibility to the original sampling locations, supplement an existing dataset, or optimizing sample size (Malone et al., 2019).

Figure 7: Conditional Latin Hypercube Sampling for 6 sampling points at Behialde.

2.7 OSPATS+

De Gruijter et al. (2016b) developed a sophisticated methodology for measuring and auditing changes in SOC stocks at farm level building from a stratification method that uses a map of predictions of SOC stocks and their uncertainties (OSPATS) (De Gruijter et al., 2015). Their methodology applies a design-based approach, with stratified simple random sampling and optimal allocation of samples to strata that minimizes the sampling variance of the mean (Neyman allocation, see section 2.8). Some decisions regarding the sampling strategy are that the sampled locations differ between the initial and subsequent sampling times to reduce the risk of fraudulent practices, the SOC stock is measured directly on whole soil cores, and the soil samples are not bulked (De Gruijter et al., 2016a). The area of the farm is discretised into a fine grid, and each cell is treated as a sampling unit. The objective function is minimized by iterative re-allocation, defined with generalized distances between pairs of grid points, calculated by the difference between the predictions, the variances of the prediction errors and their covariance. The optimization criterion to select the total sample size is based on the value of information, prioritising the expected profit for the farmer (carbon credits), accounting for the added value of the samples reducing the uncertainty of the mean change in SOC and the cost of data collection, for a given level of certainty about the sequestered carbon. The information from the first sampling campaign is used to improve the predictions of the SOC map and reducing its associated uncertainty, hence reducing the final variance of the difference in mean SOC stock. There is software available for applying the stratification algorithm OSPATS in with scripts for R (Malone and Saby, 2019), the function *optimizeStrataSpatial* in the R package *SamplingStrata* (Ballin and Barcaroli, 2020) and OSPATS+ is available as a package for the programming language Julia to increase the computation speed (De Gruijter et al., 2019).

2.8 Allocation of soil samples among strata

There are several methods frequently used in the literature for assigning the number of samples among strata that Bettigole et al. (2023) summarized as follows:

- Even. The same number of samples are allocated to each stratum.
- Area-weighted sample. The number of samples are proportional to the area occupied by each stratum. If the total area of the monitoring area is *A*, given a total number of samples for our intervention area *n,* and A_h the area of stratum *h*, then the number of samples in that stratum, n_h is calculated as follows. The number of samples is rounded to integers.

$$n_h = n\frac{A_h}{\sum A_h} \qquad [1]$$

- Neyman allocation. Neyman allocation optimizes the samples allocated to each stratum (n_s) based on the total number of samples (n), mean covariate values per strata (x_s), mean covariate across all strata (x), within-strata standard deviation of covariates (σ_s), and standard deviation across all strata (σ). Instead of environmental covariates, we can apply Neyman allocation on maps of SOC stocks or concentration.

$$n_s = n\frac{x_s \cdot \sigma_s}{x \cdot \sigma} \qquad [2]$$

- Mean bias-weighted sampling. This method assigns samples with weights based on the average distance from the stratum mean SOC (or SOC observations at a stratum h, z_h) to the mean SOC at the study site ($\hat{\bar{z}}$). The method can use laboratory measurements of SOC at the site or high-resolution spatial predictions on SOC.

$$n_h = log\left(\frac{\sum|z_h - \hat{\bar{z}}|}{z_h}\right) \qquad [3]$$

Bettigole et al. (2023) recommended to avoid even allocation and creating at least 5 strata based on ancillary data for farms of area ranging between 60-230 ha.

2.9 Choice of sampling design

The inherent spatial variability of soil properties and pedogenetic conditions influencing SOC storage within a study site, the availability of SOC data, the spatial scale of the SOC monitoring project, and the availability of resources will determine our choice of sampling design (VandenBygaart, 2006). Lawrence et al. (2020) provided several questions to guide the decision of the optimal sampling approach for surveying soil properties depending on the monitoring objective, the spatial autocorrelation, the extent and scale of management within the field, availability of ancillary data and resources. We provide a simpler decision tree to guide the choice of spatial sampling approach in the context of LILAS4SOILS (Figure 8). Most SOC MRV protocols require stratification, so we have highlighted stratification based on compact geographical strata and stratification based on environmental covariates. These two methods can be combined with more systematic approaches for targeted sampling at agroforestry systems.

There are multiple studies comparing different sampling designs in terms of efficiency and accuracy for estimating change in SOC stocks (Bettigole et al., 2023; Bradford et al., 2023; Potash et al., 2023). Sampling designs that incorporate information on environmental covariates, remote sensing, soil type and spatial predictions of SOC generally improve sample efficiency in comparison to SRS, but which sampling design is

better seems to be site-dependent (Bettigole et al., 2023; Potash et al., 2023) making the generalization of the best sampling approach difficult across study areas, e.g., Bettigole et al. (2023) recommend cLHS whereas Potash et al. (2023) prefer doubly balance sampling.

The required sampling density is generally higher when the purpose of the study is mapping than when it is estimating population parameters. For mapping at field scale up to several hectares, Žížala et al. (2024) suggested that between 18 to 30 samples (0.6 - 1 sample ha^{-1}) could suffice for sampling with covariate-informed designs (e.g., cLHS o Feature Space Coverage Sampling). The required sampling density also decreases as the area of the farm or carbon farming project increases, allowing for better cost efficiency (€/ha sampling) at larger projects. A common practice for improving sampling efficiency for monitoring carbon farming projects is to group several properties (farms, fields, etc.) that can be contiguous or not, into the same project. Bradford et al. (2023) found that even at high sampling densities commonly used at MRV projects (e.g., 1.2 ha $sample^{-1}$) and moderate within-field spatial variability, the estimates of SOC change for single fields were largely inaccurate. When several fields were grouped together, the estimates of change in SOC stocks gained in robustness and accuracy at higher sampling densities and larger number of fields (Bradford et al., 2023).

Finally, the number of subsamples taken within a soil monitoring unit for preparing composites varies among existing protocols. While several studies suggest that increasing the number of subsamples bulked into a composite over five does not provide significant advantages (Arrouays et al., 2018; Lark, 2012), other protocols require a larger number of subsamples (ranging from 10 to 25) for capturing the SOC variability within the monitoring unit (Stolbovoy et al., 2007). (Stolbovoy et al., 2007). As a compromise between these alternatives, the common protocol for LILAS4SOILS proposed in this document takes 9 subsamples for preparing a composite sample per monitoring unit (see section 3.1.3.4.2).

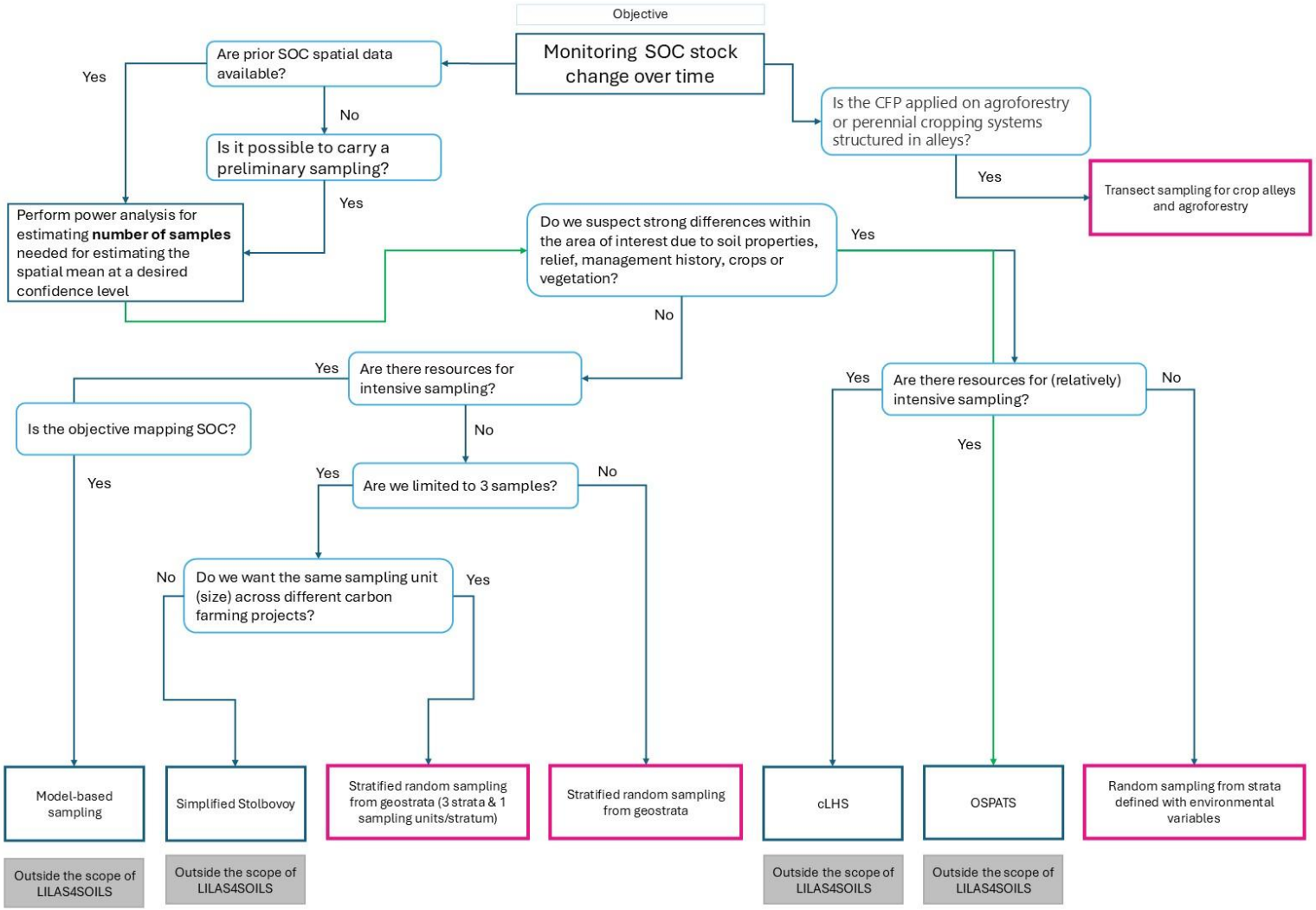

Figure 8: Simplified decision tree for selection of spatial sampling approach.

3. SOC Sampling and Monitoring Protocol

There is not a single recipe for finding the best protocol across sites. Rather that suggesting a single sampling design, this document provides guidelines for selection of the approach that will be best suited to each demo-site and living lab. For clarity we provide some definitions of the terms used in this protocol.

Demo-site: The farm or exploitation where the CFPs will be implemented, and the change in SOC stock will be monitored, modelled, and validated over the life of the carbon farming project. Indicates the general location of the project.

Intervention area: The specific area within the demo-site where the CFPs will be implemented. This area should have between 1 to 5 ha. Other spatial sampling approaches (e.g., cLHS) or increasing the number of strata and number of samples may be needed for larger intervention areas (several hundred hectares).

Sampling unit: Soil can be considered a *continuum* population that varies over space. Thus, the elementary sampling unit needs to be defined (Brus, 2022). In this sampling protocol, the sampling unit has the spatial support of a circular plot of 5 m radius. However, in the specific case of orchards, alley crops and agroforestry systems, transects can be the elementary sampling unit. We have prioritised having the **same spatial support** over the group of demo-sites across living labs in the context of LILAS4SOILS.

Sampling points: The exact locations where the soil samples are taken within the sampling units, whether they are combined to make a composite sample, or kept as an individual soil sample (e.g., for measuring bulk density and coarse fragments). The scheme of sampling points within the sampling unit is explained in detail in section 3.1.3.4.2.

3.1 Spatial boundaries of intervention area

The spatial delineation of the intervention area (area that will be used for implementing CFPs and monitored for SOC changes) should exclude the roads or buildings located within its boundaries. The delineation can be done using freely available and user-friendly software like Google Earth Pro or geographic information systems (GIS) software (ArcGIS, QGIS) with the support of the most updated satellite imagery.

The Coordinate Reference System (CRS) used when delineating the boundaries should be the most widely used in the region of study and suitable for doing the field sampling (the same as in the GPS device), but it is not strictly necessary at this stage. However, it is important to know and record the CRS (geodetic datum and coordinate system, or EPSG code). For example, OpenStreet Map and Google Maps use EPSG: 3857 (Web Mercator, with World Geodetic System 1984). Once the spatial sampling has been designed and we obtain the coordinates of the sampling points, these can be **transformed into the projection of the GPS with the correct transformation**. For example, for the pasture at Behialde (Basque Country, Spain), the CRS is EPSG:25830 (datum European Terrestrial Reference System 1989, and projection UTM Zone 30N, units in meters).

3.2 Protocol for spatial sampling

3.2.1. Stratified random sampling using environmentally defined clusters as strata

When available information on environmental covariates related to SOC storage or high-resolution maps of SOC stocks and associated uncertainty (with reliable validation statistics) are available for the intervention area and the demo-sites, stratification from environmentally defined clusters will be the preferred approach following the indications of section 2.4 and Annex A.

The resulting maps of strata need to be validated visually by the living lab coordinators based on their knowledge of the area and could also count with the assessment by the farmers as, who know well their soils. This evaluation would answer the question *Do you think these areas are different in terms of landscape, soil properties (e.g., soil texture) and the response of crops to management practices?*

The selection of the optimal number of strata can be done with internal clustering quality indices widely used in the literature (e.g., Silhouette, Calinski-Harabasz, Dunn, etc.), preferably 2-3 strata in intervention areas of 1-5 ha. While most MRV protocols set a minimum of 3 strata, the final choice should be done with careful evaluation of the results from the clustering exercise, since the surface of the intervention area is relatively small.

The **allocation of sampling units to each stratum will be proportional to their area** (section 2.8). If high-resolution and reliable maps of SOC stocks and uncertainty are the spatial layers used for stratification, Neyman allocation is also recommended.

The results of the stratification and preliminary analysis of the environmental covariates (visualization of maps, histograms, etc) may suggest that the intervention area is very homogeneous. Hence, stratification may not add valuable information for reducing the sampling variance. Sometimes, lack of time to prepare the sampling design, available data or expertise for conducting this method may limit its application. In both cases, we would select the next sampling approach, stratified random sampling from compact geostrata.

The sampling units (circular plot of 5 m radius) will be allocated with the coordinates of their centre. We start assigning the first sampling unit per stratum. If the circular plot intersects the boundary of the stratum or the monitoring area, generate a different random sample until the three plots fall within the boundaries. Then, add consecutively the additional plots per stratum keeping a minimum distance between centres of the plots of 15 m (Arrouays et al., 2018). These sampling units will be resampled at the years 3 (2027) and 4 (2028) of the project LILAS4SOILS.

3.2.2. Stratified random sampling using geographically compact sub-areas as strata

At intervention areas where the soil conditions, relief, and management history are presumed to be homogeneous, environmentally defined strata may not be necessary. Stratification with compact geostrata (Brus, 2022) would then be our selected approach following the indications of section 2.3 and Annex A. The intervention area will be divided into three compact strata of equal area and a minimum of one sampling unit (circular plot of 5 m radius) will be located randomly at each stratum. Because the strata have the same size, this allocation is also proportional to the area of the stratum. Depending on the available resources, we might expand the number of sampling units to n, and then the number of sampling units per stratum h would be $n_h = n/3$. This would improve our spatial estimate of the mean SOC and its variance.

The sampling units (circular plot of 5 m radius) will be allocated with the coordinates of their centre. We start assigning the first sampling unit per stratum. If the circular plot intersects the boundary of the stratum or the monitoring area, generate a different random sample until the three plots fall within the boundaries. Then, add consecutively the additional plots per stratum keeping a minimum distance between centres of the plots of 15 m (Arrouays et al., 2018). These sampling units will be resampled at the years 3 (2027) and 4 (2028) of the project LILAS4SOILS. At each soil monitoring unit, we will implement the field sampling protocol.

3.2.3. Crop alleys or agroforestry areas

Targeted sampling might be preferred by the coordinator of the carbon farming project in orchards or agroforestry systems that are structured in alleys to capture the effect of specific CFPs (e.g. hedgerows, lines of trees). We refer the reader to the systematic review and harmonised protocol by Minarsch et al. (2024). The intervention area should be stratified with environmental covariates or geostrata before assigning transect sampling units across the area to ensure that the variability and/or the geographical area is covered.

Minarsch et al. (2024) recommend 4 transects per alley cropping system (ACS) (i.e., equivalent to the intervention area in this protocol). In the case of LILAS4SOILS demo-sites, the minimum required will be 3 transects per intervention area or ACS due to limitations of resources. The levels of tree influence shall be considered when selecting transect positions. The location of replicated transects should be systematic rather than random. The approximate area proportions of the tree and arable/pasture strips need to be registered at the field for calculations of weighted SOC stocks at the ACS area. Field records will be preferred over delineation from high-resolution aerial photographs, but the latter are also an option.

Minarsch et al., (2024) proposed two types of composite sampling. The first composite sampling scheme (see Figure 4 C1 at Minarsch et al., (2024)) places the transects in parallel to the tree lines, establishing seven transects: one at the tree line, then three at each side (at 1 m from the edge of the tree strip, at a quarter of the arable width, and half of the arable strip). This method of composite sampling would account for the influence of trees on SOC content and bulk density. However, it increases substantially the number of analytical samples at the laboratory. In the second type (see Figure 4 C2 at Minarsch et al., (2024)), the composites are made along a transect type T3, i.e., the transect covers both sides of the interrow around the tree strip, from 7 individual samples. Four transects are placed relative to tree positions: under a tree, between two trees, and at one quarter distance to the tree line. This method of composite sampling homogenises differences in SOC content in the tree rows and the interrows. However, it is difficult to account for differences in bulk density under different vegetation cover. Hence, bias in bulk density estimates will be introduced for the calculation of SOC stocks, unless several bulk density samples are taken at different distances from the trees and averaged.

Because we can expect differences in bulk density between tree lines and the interrows, we should collect separate samples from tree strips and interrows, which also calls for creating composite samples for tree lines and interrows separately. We could simplify the method by Minarsch et al., (2024) by creating one composite at the tree line, a second composite in the middle of the interrow, and a third composite at a quarter distance from the tree line (Figure 9). This would only duplicate or triplicate the number of laboratory analyses (e.g., 3 replicate transects x 3 (tree line & 2 at interrow)). The same transects will be revisited in subsequent times.

Other agroforestry systems like dehesas or montados where trees are spread irregularly or in clusters, need a different spatial sampling design, like those presented in sections 3.2.1 and 3.2.2 or one tailored to the specific conditions of these agroecosystems.

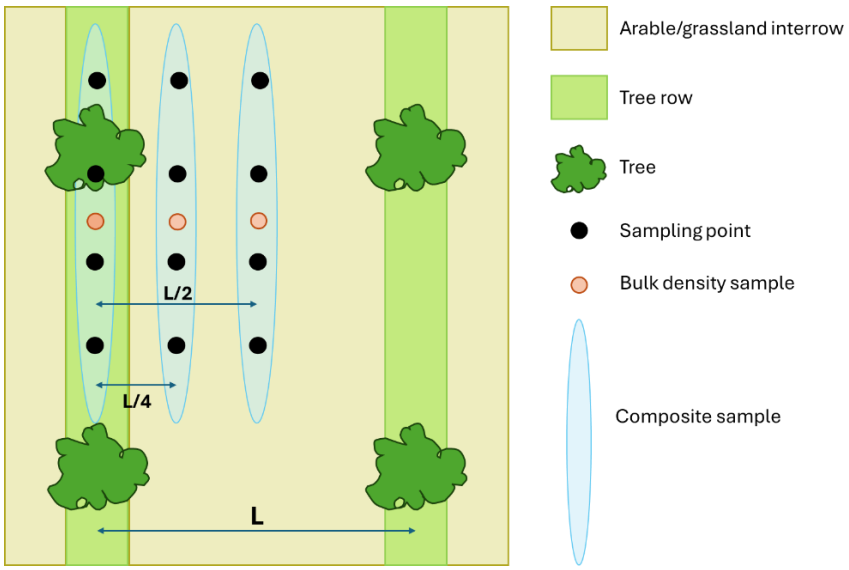

Figure 9: Modification of the composite sampling scheme C1 proposed by Minarsch et al. (2024) for soil organic carbon monitoring in temperate alley cropping systems. The patterns for making three composite samples in parallel (C1) to the tree lines – at the tree line, at a quarter of the distance between tree lines, and half the distance between tree lines. Additional bulk density samples per transect.

Alternatively, and since the sampling units will be revisited, we can place a circular or square sampling unit for creating a composite sample with a field protocol like LUCAS (European Commission, 2017) or the one described in section 3.1.3.4.2. However, the pit for taking a bulk density sample should be placed in both sampling times at an equivalent position relative to the tree line (e.g., the centre of the sampling unit is at a quarter distance to the tree line, then in subsequent times the bulk density needs to be sampled at a quarter distance from the tree line). While the spatial average of SOC stock may have a systematic error due to the bulk density, we would be able to calculate design-unbiased estimate of the temporal change of SOC.

3.2.4. What should we do if we are conducting the sampling at the field, and we find out that it is not possible to sample one of the sampling units?

- This can happen if we see the sampling plot has been strongly disturbed recently, or it is crossed by a trail, etc.
- We will avoid choosing by convenience the next sampling unit in the proximity of the theoretical one, because this would introduce bias (Brus, 2022).
- In the case we are using circular plots at compact geostrata or strata defined from environmental covariates, we will go to the field with a **second set of numbered sampling units** generated with a different randomization (e.g., different allocation of circular plots within the strata). The fieldwork

team will have an alternate set of sampling units and have the coordinates of the centre of the plots saved at the GPS.

- The sampling unit from the first set that is not suitable for sampling will be substituted by the **first sampling unit from the alternative set for that stratum** (Brus, 2022).
- Therefore, it is imperative to bring a digital or printed map with the location of both sets of sampling plots (primary and alternative) and their coordinates.

3.2.5. Resampling

It is very important that the field team records the real coordinates of the centre of the sampling units so that **the same locations can be resampled in the next field campaigns**.

In the subsequent years we will revisit the same sampling units, although with slight variation in the location of the sub-samples for making the composite samples. The selected approach is a static synchronous sampling design, suitable for identifying the trend in SOC (De Gruijter et al., 2006). Compared to other space-time designs, the sampling variance is reduced by revisiting the sampling sites because the temporal correlation is accounted for, hence improving the spatial mean estimate of SOC change (Mudge et al., 2020). Revisiting the sample sampling units improves the cost efficiency to detect change in SOC with a smaller number of samples. However, several authors have advised against resampling the same locations of fear that this might influence the intensity and spatial application of CFPs (Mudge et al., 2020). After finalisation of fieldwork, we should try to leave the sampling points as least disturbed as possible, filling the holes where coarse fragments and bulk density samples have been taken with the remaining soil.

3.3 Soil properties measured at different soil monitoring times

The complete set of soil properties for calculating SOC stock and additional indicators of several soil functions will be measured at the baseline (Time 0, year 2025) prior the implementation of the CFPs (Table 3). The same set of soil properties (except particle size distribution) will be measured at Time 2 (year 2028), to assess the change in SOC stock and associated evolution of indicators of soil functions. Soil texture is considered stable over the duration of the carbon farming project and hence is measured only at Time 0. Some properties, like particle size distribution, carbonates, and total Nitrogen (TN) are used for modelling carbon dynamics with the hybrid approach for soil carbon MRV (Table 3), and therefore they will be measured as well in the following sampling times.

At the intermediate sampling time (Time 1, year 2027), we will measure the properties needed for calculating SOC stocks, i.e., bulk density, SOC content and coarse fragments. The reason to have an intermediate sampling time just for SOC stock is that the interannual variability may obscure the trend on SOC change due to the CFPs. The need to measure only SOC or separately total carbon (TC) and carbonates will depend on the laboratory instrument (e.g., automatic measurement of total carbon with catalytic high-temperature combustion, total inorganic carbon via acidification, and total organic carbon as their difference). In soils without carbonates as determined at Time 0, it will not be necessary to measure carbonates (total inorganic carbon) at Time 1 for calculating the content of SOC, meaning that carbonates should only be measured in alkaline soils.

We acknowledge that the content of coarse fragments is more variable over short spatial range than over time. While in soils with low stoniness the determination of coarse fragments content and bulk density of

the whole soil is often calculated from the same undisturbed sample with the core method, in this protocol the sample for coarse fragments is taken next to an intact core for measuring bulk density, and we assume the coarse fragments to be similar in both samples. However, we recommend sampling coarse fragments simultaneously to SOC content and bulk density, as these three variables are needed for calculating SOC stocks (Table 3).

Table 3Bulk density has been proposed as an indicator for the *threat to soil* of soil compaction or soil structural decline (European Commission, 2023; Evangelista et al., 2023), but it is also a potential indicator for the functions of production of food and biomass, and indirectly for storage and regulation of water through its relationship with soil porosity and infiltration capacity.

Table 3: Soil properties measured at the different sampling times. The variables needed to calculate SOC stocks are measured every sampling campaign.

Time 0	Time 1	Time 2	Co-benefits / Soil functions
Particle size distribution			Carbon storage (Modelling C dynamics)
Coarse fragments	**Coarse fragments**	**Coarse fragments**	Carbon storage
Bulk density	**Bulk density**	**Bulk density**	*Soil compaction* (*threat*) Carbon storage
Soil Organic Carbon	**Soil Organic Carbon**	**Soil Organic Carbon**	Carbon storage
Total Carbon		Total Carbon	Carbon storage
Total Nitrogen		Total Nitrogen	Nutrient storage and regulation (Modelling carbon dynamics)
Carbonates		Carbonates	Carbon storage Nutrient storage and regulation (Modelling carbon dynamics)
pH		pH	Nutrient storage and regulation
Potential Mineralizable Nitrogen (PMN)		Potential Mineralizable Nitrogen (PMN)	Nutrient storage and regulation
Soil organic matter fractions (MAOM and POM)		Soil organic matter fractions (MAOM and POM)	Carbon storage Nutrient storage and regulation
Soil moisture at field water capacity (θ_{FC})		Soil moisture at field water capacity (θ_{FC})	Storage and regulation of water
Soil moisture at permanent wilting point (θ_{WP})		Soil moisture at permanent wilting point (θ_{WP})	Storage and regulation of water
16S rRNA gene amplicon sequencing		16S rRNA gene amplicon sequencing	Habitat of soil biodiversity

3.4 Protocol for field sampling

3.4.1. Conditions to select the interval of sampling dates

Soil properties (e.g., SOC, pH, soil microbial communities) responsive to management and climatic conditions have interannual and seasonal variability. Hence, the sampling campaigns must be conducted around the same month (or at least season) every sampling campaign.

In the Mediterranean, the soil can be very dry making it very difficult to operate with the soil auger or soil probe and taking intact cores. Some soil carbon MRV protocols recommend sampling in periods of low biological activity; in Mediterranean soils this may happen in summer due to the reduced soil moisture limiting the microbial activity. However, summer may be avoided for soil sampling because the time and physical effort needed for sampling will affect sampling efficiency and time management.

Sampling should avoid being conducted right after cultivation operations and practices that disturb the soil considerably or cause peaks in some soil processes and hence in soil properties used as indicators of co-benefits for CFPs (e.g. tillage, disking, seeding, fertilizer application) (Arrouays et al., 2018). Arrouays et al. (2018) recommended a minimum period of four weeks after the last ploughing for sampling in croplands. Preferably, the soil should be close to field capacity and with firm layers (Arrouays et al., 2018). The soil should not be saturated (1-3 days after the last precipitation), and the water table below the lowest sampling depth limit (30 cm). The soil should not be saturated as these soils are more susceptible to compaction during sampling.

3.4.2. Field sampling

Before going to the field, the soil survey team needs the following material for soil sampling:

- Soil probe or soil auger of at least 30 cm length
- Spade with a 20 cm blade
- Small spade
- Measuring tape of 4 m (optional)
- Field knife with flat blade
- Stainless steel rings + cylinder holder device
- Rubber mallet
- Permanent marker
- Two labelled reclosable plastic bags per sampling unit. The first for the 0-10 cm composite sample and a second one for the 10-30 cm composite sample
- Two labelled reclosable plastic bags (or simple plastic bags) per sampling unit for bulk density samples, for the 0-10 cm and 10-30 cm depth interval respectively
- Bottle of 70 % ethanol
- Paper towels
- Box to store and transport the samples.
- A cooler with ice packs to preserve samples for PMN and 16S rRNA gene amplicon sequencing.

The amount of composite sample (minimum of 500-600 g) should be enough for carrying the whole set of laboratory analyses to determine SOC stock and indicators of soil functions listed as co-benefits (Table 3).

The centre of the sampling unit (circular plot of 5 m radius) is located following the coordinates of the GPS and marked with a flag (or plastic or wooden stick). Near the centre of the plot, a soil pit is dug where individual samples for bulk density and coarse fragments are extracted following the steps explained in sections 3.4.3 and 3.4.4. at the selected depth intervals (Figure 11). The size of the pit is adapted to the local conditions (Arrouays et al., 2018).

The soil thickness considered in this protocol is the 0-30 cm of mineral soils, sampled by fixed depth intervals. Soil samples will be taken for the depth intervals 0-10 cm and 10-30 cm. Only the top 0-10 cm layer will be analysed for soil microbial biodiversity (16S rRNA gene amplicon sequencing).

Organic soil horizons are excluded from the sampling. Superficial stones, litter and grass, vegetation residues or agricultural amendments (e.g., straw), and the organic layer (O horizons) will be removed carefully with a spade, to not eliminate the superficial centimetres of the mineral soil (A or Ap horizon) (European Commission, 2017), before taking the samples of bulk density, coarse fragments and subsamples for the composite.

In the proximity of the centre of the plot, but not right next to the pit (about 50 cm apart), the first sample for the composite is extracted with a soil probe or soil auger up to 30 cm depth (Figure 10 and Figure 11). If necessary, use the rubber mallet to push the soil probe. Turn the soil probe in clockwise direction and extract it. The sample is divided by depth interval into two previously labelled, reclosable plastic bags (0-10 cm and 10-30 cm respectively) with help of a field knife (Figure 10).

Figure 10: a) Soil probe is inserted up to 30 cm in the mineral soil. b) the soil sample is divided into two pre-labelled plastic bags for the 0-10 cm and 10-30 cm composite samples. Photo credit: Patricia Gallejones.

The additional sampling points for the composite sample are located at 2 m and 4 m from the centre of the plot in the four cardinal directions: North, South, East and West (Figure 1110). In practice, we are located at the centre of the plot with a compass –which can be a physical compass or an app at the cell phone– and we identify one of the cardinal directions (e.g., North). We use the measuring tape or take two steps (approximately 2 m) into that direction to the second sampling point, where we take an additional soil

sample with the probe. The sample is partitioned by depth interval into their corresponding reclosable bags for the composite samples (Figure 109). We take two additional steps to reach 4 m from the centre of the plot, extract the third soil sample with the probe and partition it into the 0-10 cm and 10-30 cm composite samples. We return to the centre of the plot and identify the next cardinal direction (e.g., East) and take samples 4 and 5 with the same procedure. We repeat these steps until we have a composite sample from 9 sampling points (Figure 11). The principle to identify the sampling points is very similar to the field sampling manual for LUCAS, with four additional points at 4 m (European Commission, 2017).

Soil pits for bulk density and coarse fragments should be refilled after field sampling, returning the soil layers with the same order of the original horizons (Arrouays et al., 2018).

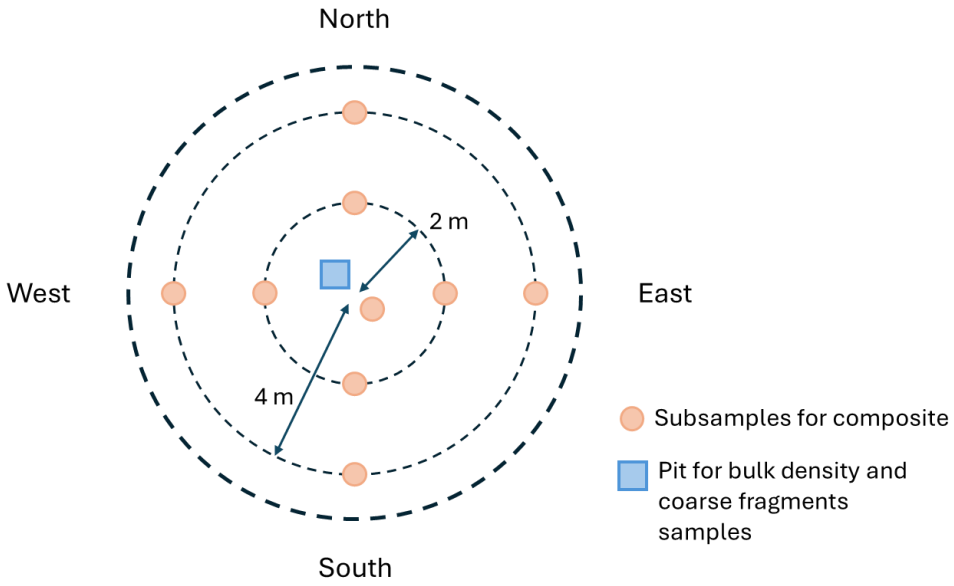

Figure 11: A circular plot of 5 m radius constitutes the sampling unit. Nine sampling points for a composite sample are located at 2 m and 4 m into the cardinal directions and near the centre of the plot. A pit for sampling bulk density and coarse fragments is dug in the centre of the plot.

3.4.3. Sampling for bulk density

Two methods are suggested for sampling bulk density depending on the stoniness: the core method (non-stony soils) and the excavation method (very stony soils). These two methods are included in the International Standard ISO-11272:1998 (replaced by ISO-11272:2017) for determination of bulk density, together with the clod method.

The core method is one of the most common methods for direct determination of bulk density (Blake and Hartge, 1986). Undisturbed soil core samples are collected using a stainless-steel coring ring of known volume taken vertically at each depth interval (0-10 cm and 10-30 cm).

Once the surface litter and grass, stones greater than 6 cm (European Commission, 2017), as well as organic horizon has been removed carefully raking with a small spade or a field knife, we place a coring ring with the bevelled edge down and we press it gently using a mallet. We can use a block of wood if the soil corer does not include a ring holder device (Figure 12). We will avoid compacting the soil by not pushing the ring

too deep into the soil. To extract the cylinder, we dig around the coring ring with a spade, making four diggings at 2-3 cm from the ring, leaving the ring in the middle of a square. We deposit carefully the soil at the side of each hole, while not stepping or disturbing the area where the soil core is. When we have excavated at the four sides of the ring, we insert the spade underneath the ring to extract it (together with surrounding soil clump) to not disturb it and loosen the soil within. We remove the excess of soil from the bottom of the cylinder and outside the edge with the field knife (European Commission, 2017) and we cut with scissors the roots that stand out of the cylinder (FAO, 2020).

The length of the cylinder may be smaller than the thickness of the horizon being sampled (e.g., 51 mm cylinder, and 0-10 cm dept interval). Hence, we can remove the top 2 cm of mineral soil before inserting the ring to sample the middle of the considered depth interval.

Figure 12: The metallic ring has an adapter holding device (a piston) to facilitate sampling for bulk density. Photo credit: Patricia Gallejones.

Following the field recommendations for soil survey for LUCAS (European Commission, 2017), if the ring is not completely filled with soil (less than 10% missing due to loss of material when removing the ring or presence of a big stone) it is possible to fill the ring with removed soil. If more than 10% of the soil is missing, discard this sample and take a new sample in its proximity, where the soil has not been disturbed. Seal the ring with a plastic lid and mark it with the code of the sampling unit to avoid confusion. Place inside a plastic bag.

A common size for the cylinders is 100 cm^3 which are suitable for soils with non or little amount of coarse fragments, since these are often underrepresented in small samples, leading to underestimation of bulk density in gravelly soils (FAO, 2020).

For the depth interval 10-30 cm, we repeat the same steps for sampling with the core method, digging to a depth near the middle of the layer (20 cm). We can profit from the holes that we made to extract the bulk density sample from the 0-10 cm, digging 10 cm more trying to leave a horizontal and flat layer at 20 cm with a horizontal stroke.

In very stony and incoherent soils, the excavation method will be used for determination of bulk density according to the International Standard ISO 11272:2017. Taking volumetric samples from the 10-30 cm as

a single piece can be challenging, so it is suggested to take two superimposed samples from 10-20 cm and 20-30 cm (Arrouays et al., 2018b).

3.4.4. Sampling for coarse fragments

The sample for measuring gravimetric coarse fragment content will be taken from the same pit dug during bulk density sampling. The sample volume must be at least 100-300 cm^3 to properly estimate the percentage of coarse fragments. For the layer 0-10 cm, a V-shaped hole will be dug to a depth of 10 cm using the spade and a slice of soil (approximately 3-cm thickness) will be taken from the side of the hole with the spade (European Commission, 2017). The slice will be trimmed at the sides to give a 3-cm wide subsample. We will place the top 10 cm in a prelabelled plastic bag after removing excess soil from the bottom (if the shovelling was too deep). This step would be done after taking the first sample of bulk density, but before taking the sample from the 10-30 cm. After we have taken the bulk density sample from the 10-30 cm, we repeat the step of sampling a slice of soil from one of the sides of the pit at 10-30 cm depth and place it in its individual prelabelled plastic bag.

3.4.5. Sampling for soil moisture at field water capacity (θ_{FC}) and at permanent wilting point (θ_{PWP})

The ISO standard for determination of soil hydraulic properties (ISO 11274:1998) includes different methods for working with altered or intact samples. If our laboratory works with altered sample for measuring soil water retention, we do not need to take an additional sample because we will use an aliquot from the composite sample. If the laboratory has the equipment for working with undisturbed soil clods (~ 10 cm^3), these can be sampled either with an additional intact core following the same procedure and depth intervals as for bulk density. Another option is to extract a “block” of soil with the help of the spade from a cleaned surface (previously gently raked with the spade) for each depth interval trying to use the natural cracks or structural divisions in the soil and place it in a plastic storage container to preserve the soil structure. We refer to the French Soil Quality Monitoring Network Manual RMQS2 (Jolivet et al., 2022) for detailed instructions. For the objectives of LILAS4SOILS, a smaller sample around 10 cm width would suffice compared to the block of soil about 20 cm width collected for the RMQS. At the laboratory, undisturbed soil clods can be extracted from the plastic container.

In soils with incoherent or very loose structure, high content of coarse fragments, coarse texture, or high content or roots and plant debris this method may be not feasible. Then, an intact core sample or measuring soil water retention characteristics from altered sample (composite) will be the option at the laboratory.

3.4.6. Preparation and conservation of samples for soil biodiversity

This section outlines the procedures for collecting soil samples for 16S rRNA gene amplicon sequencing. It is recommended that samples are paired with as many relevant environmental measurements as possible.

To ensure representative sampling, the sample for soil biodiversity will originate from the composite sample made from all the sampling points from the same sampling unit (Section 3.4.2 and Figure 11). The samples shall be transported to the laboratory as soon as possible and stored at 4°C. Prior to DNA

extraction, sieve the fresh soil samples through a 2-mm mesh as soon as possible upon arrival to the laboratory. All materials used to sieve soil samples to be used for diversity analyses need to be rinsed with 70% ethanol to prevent cross-contaminations. Sieved samples should be stored at 4°C.

Prior sending samples to DNA extraction and 16S rRNA gene amplicon sequencing, prepare a representative 10 g aliquot of soil. Cold shipping is mandatory, including cold packs.

3.4.7. Pre-processing of samples

We will have three different sample types at arrival at the laboratory: composite samples (500-600 g), coarse fragments, and bulk density (intact cores). We might have a fourth sample depending on the method for determination of θ_{PWP} and θ_{FC} (undisturbed or disturbed soil). If the water retention characteristics are determined from an undisturbed sample, we will have a second cylinder or a sealed container with soil to select soil clods with unaltered structure.

As stated aThe fresh composite sample has to be homogenised and a subsample of approximately 50 g will be stored rapidly at 4°C and used later for estimation of PMN and 16S rRNA gene amplicon sequencing. Prior these analyses it will be sieved through a 2-mm mesh to separate the fine fraction (< 2mm). If DNA extraction is not to be carried out immediately it is preferable to freeze a subsample of the fresh sample (for 16S rRNA gene amplicon sequencing) at -20 °C. The other subsample will be used for PMN and stored at 4°C. However, freezing and thawing should be avoided by doing the DNA extractions rapidly after sampling.

The remaining of composite sample (~450-550 g) will be air dried and sieved to separate coarse fragments (> 2mm). During sieving, we will pay attention for breaking aggregates > 2mm that may be confused with coarse fragments. The air-dried composite sample will be later used for measurement of particle size distribution, SOC, TC, TN, carbonates, pH and SOC fractions (and most likely θ_{PWP} and θ_{FC}).

The sample for coarse fragments is air dried and processed for determination of coarse fragment content.

The intact core for determination of bulk density is processed separately.

3.5 Laboratory analyses and calculations of soil properties for estimating SOC stocks

The preferred methods are gathered from general protocols for monitoring soil health indicators like the EU Soil Monitoring and Resilience Directive (SMD) (European Commission, 2023) and the FAO-GSOC MRV Protocol (FAO, 2020).

Table 4: Preferred soil analysis methods and International Standard or literature references for estimating indicators of soil functions, or co-benefits derived from soil-farming practices, and calculating SOC stocks.

Soil properties	Laboratory method	Type of sample (pre-processing)	Reference
Particle size distribution	Laser diffraction Method by sieving and sedimentation	Air dry	ISO 13320:2009 ISO 11277:1998

Coarse fragments	Gravimetry	Air dry	NEIKER, European Commission (2017)
Bulk density	Gravimetry	Oven dried at 105°C	ISO 11272:2017
Total Carbon	High-temperature catalysed combustion	Air dry	ISO 10694:1995
Soil Organic Carbon	High-temperature catalysed combustion	Air dry	ISO 10694:1995
Total Nitrogen	High-temperature catalysed combustion	Air dry	ISO 13878:1998
Carbonates	High-temperature catalysed combustion	Air dry	ISO 10694:1995
pH	Potentiometry	Air dry	ISO 10390:2005
Potential Mineralizable Nitrogen (PMN)	Spectrophotometry	Fresh (4°C)	Canali and Benedetti (2005); Mulvaney (1996); Powers (1980)
Soil organic matter fractions (MAOM and POM)	Size fractionation	Air dry	Cotrufo et al. (2019)
Soil moisture at field water capacity (θ_{FC})	Pressure plate	Air dry (rewetted during procedure)	ISO 11274:1998
Soil moisture at permanent wilting point (θ_{PWP})	Pressure plate	Air dry (rewetted during procedure)	ISO 11274:1998
16S rRNA gene amplicon sequencing	DNA extraction, PCR amplification, sequencing, data processing and taxonomic classification	Fresh (4°C)	NEIKER

Particle size distribution

The preferred methods for particle size distribution are sieving and sedimentation (ISO 11277:1998) or laser diffraction (ISO 13320:2009, now updated at ISO 13320:2020). Particle size fraction will be used as input variables for modelling SOC dynamics and predicting the effects of CFPs on SOC stocks with a hybrid approach.

Soil texture influences SOC storage through the role of the mineral matrix on physico-chemical stabilization mechanisms, especially clay minerals and fine silt particles (von Lützow et al., 2006; Six et al., 2002). Soil texture also controls soil hydraulic properties and is often use for estimating soil moisture at field capacity (θ_{FC}) and permanent wilting point (θ_{PWP}) with pedotransfer functions (Cousin et al., 2022; Van Looy et al., 2017), that often allow to propagate uncertainties and assess its applicability domain (Román Dobarco et al., 2019; Szabó et al., 2021).

Coarse fragments

The sample for determination of coarse fragments is sieved through a 2-mm mesh, aggregates greater than 2 mm in size are destroyed and washed to remove fine particles < 2mm. Some laboratories have automated mechanisms to sieve, destroy aggregates and wash coarse fragments (e.g., shaker sieve together with a wet sieving system). The gravimetric content of coarse fragments (> 2 mm) is calculated as the ratio of the dry mass of coarse fragments (> 2 mm) divided by the dry mass of the bulk soil ($mass_{soil}$) (fine earth + coarse fragments) and expressed in percentage (or as unitless ratio). We calculate it from the sample taken at the field for measuring coarse fragments (section 3.4.4). The bulk soil sample is air-dried to dryness and its weight is recorded. The soil is then sieved through a 2-mm mesh to separate the fine earth (< 2mm) and the coarse fragments (> 2 mm). The mass of the coarse fragments ($mass_{coarse}$) is recorded and used to

estimate the gravimetric percentage of coarse fragments (CF_{grav}) that will be used for SOC stocks calculations:

$$CF_{grav}(\%) = \frac{mass_{coarse}}{mass_{soil}}\ x\ 100 \qquad [4]$$

Note that other methods can be used to measure or estimate the volumetric content of coarse fragments but it is important to differentiate both, due to the effects on SOC stock calculations as *volumetric coarse fragment* content needs to be combined with the *bulk density of the fine earth* (Poeplau et al., 2017) (see section 3.6).

Sometimes, the gravimetric coarse fragments content and bulk density are determined from the same intact core. However, the volume of soil in the cylinder is much smaller than that sampled with the spade and can exclude larger gravel or smaller stones, hence less representative of the content of coarse fragments in the soil sampling unit. The coarse fragments content in samples taken with the spade will be relatively small, as otherwise the excavation method should have been applied for measuring bulk density and coarse fragments content. Hence, we assume that the coarse fragments content in both individual samples, (i) coarse fragments and (ii) bulk density, are equivalent but that the value from the latter is more representative.

Bulk density

Following the extraction of intact soil cores at the field, the determination of dry bulk density at the laboratory is done with the international standard ISO 11272:2017. The intact soil core is oven-dried at 105°C for at least 24 hours to eliminate soil moisture and weighted. Bulk density of the whole soil is calculated as the ratio of dried soil mass to its known volume (Blake and Hartge, 1986):

$$\rho_{Wh} = \frac{mass_{soil}}{V_{soil}} \qquad [5]$$

Where ρ_{Wh} is the bulk density of the whole soil (g cm^{-3}) while $mass_{soil}$ is the dry mass of the soil core and V_{soil} the known inner volume of the sampled soil cylinder (cm^3). Sometimes bulk density is reported in Mg m^{-3}.

Several protocols calculate the bulk density of the fine earth (< 2 mm) and use it in subsequent SOC stocks calculations (e.g., (FAO, 2020)). The mass of the fine earth ($mass_{fine}$) is easily obtained by sieving the bulk soil from the intact core through a 2-mm mesh and weighing it, but the volume of fine earth is not always measured. Only in case the intact soil core has no coarse fragments both bulk densities would be identical. Otherwise, the volume of fine earth can be calculated by subtracting the volume of coarse fragments from the volume of the whole sample. If the volume of the coarse fragments has not been measured it can be estimated assuming an average density of coarse fragments around 2.65 g cm^{-3} (Hurlbut and Klein, 1977; McKenzie et al., 2002):

$$\rho_{fine} = \frac{mass_{fine}}{V_{fine}} = \frac{mass_{soil} - mass_{coarse}}{V_{soil} - \frac{mass_{coarse}}{\rho_{coarse}}} \qquad [6]$$

Where ρ_{fine} is the bulk density of fine earth (< 2 mm), V_{fine} is the volume of cylinder occupied by fine earth (< 2 mm) and ρ_{coarse} is the density of coarse fragments. While using the density of the fine earth can ease calculations of stocks, assuming the same density for all coarse fragments irrespective of their lithology type is a source of error.

Total C, carbonates and SOC content

TC and SOC content will be determined with the international standard ISO 10694:1995 with catalysed dry combustion. Carbonate content will be also determined following ISO 10694:1995. The content of carbonates may be significant in alkaline soils. TC is determined with an elementary analyser (e.g., Soli Toc Cube, ELEMENTAR) with the combustion method. The composite sample is well homogenised and finely grinded before taking a small aliquot for the automatic analyser. The sample is ignited at high temperature furnace within a O_2 stream where the totality of C forms is oxidised. The carrier gas transports the CO_2 to an infrared detector. Total inorganic carbon (TIC) and total organic carbon (TOC) can be determined by catalysed combustion along a temperature ramp (400°C for organic carbon, 600°C for residual organic carbon and 900°C for TIC).

Total N

Total N can be determined via high-temperature combustion with an elemental analyser according to ISO 13878:1998. We prefer this method over the modified Kjeldahl method proposed by the SMD (European Commission, 2023) as it is more time efficient and can be determined simultaneously to SOC. A key argument for choosing total nitrogen determination by combustion instead of the Kjeldahl method in soils is its higher accuracy and ability to detect all nitrogen forms.

The Kjeldahl method only measures organic and ammoniacal nitrogen, ignoring other forms such as nitrates and nitrites, which can lead to an underestimation of total nitrogen content in soil samples. In contrast, combustion analysis (typically using an elemental analyzer) completely oxidizes all organic matter and converts all nitrogen present in the sample into nitrogen oxides or N_2, which are quantified with high precision.

Moreover, combustion is faster, does not require hazardous reagents (such as sulfuric acid and metallic catalysts used in Kjeldahl), and is more environmentally friendly, making it a better choice for routine and high-precision soil analysis.

pH

Soil pH can be measured from air-died soil samples (composite sample) using the international standard ISO 10390:2005. In alignment with the SMD (European Commission, 2023) we will determine pH-H_2O. pH is determined with a glass electrode in a 1:2.5 (soil:water v/v) suspension of soil in water (pH in H_2O).

Potential Mineralizable Nitrogen (PMN)

Potential mineralizable Nitrogen (PMN) is a measure of the fraction of organic nitrogen that is readily available for decomposition by microorganisms, making it available for plant growth. PMN is an indicator of soil fertility and nutrient availability and cycling. PMN can be an important indicator for organic farming practices that avoid synthetic fertilizers. In aerobic conditions, PMN is available to plants and microorganisms mainly as nitrate, whereas in anaerobic conditions it is mainly available as ammonium.

There are different methods for determination of PMN via soil incubation in aerobic or anaerobic conditions for several days. With the method of anaerobic incubation, 2.8 ml of distilled water is added to 1.5 g of

fresh soil sample, sieved at 2 mm, eliminating bubbles, and it is kept for 7 days at 40 ºC. The concentration of inorganic N (NH4+-N) is measured after KCl extraction. The samples are shaken for 1 hour after the addition of 1M KCl (extractant-to-soil ratio of 5:1). The extracts are centrifuged and analysed for $NH4^+$.

Soil organic matter (SOM) fractions

The SOM fractions, mineral-associated organic matter (MAOM) and particulate organic matter (POM) are obtained with physical fractionation following a modification of the protocol proposed by Cotrufo et al. (2019). The difference with the original protocol is that sodium hexametaphosphate is not included as dispersion agent, only glass beads are used for breaking aggregates and completely disperse the soil. Briefly, 5 g of oven dried fine earth (< 2 mm) are mixed with 100 ml of deionized water and 2g of glass beads and shaken for 18 hours with an automated shaker. The soil slurry is then rinsed through a 53 µm sieve. The fraction passing through the sieve (<53 µm) corresponds to MAOM, whereas the fraction greater than 53 µm is defined as POM. Both fractions are oven dried at 55 °C until constant weight. POM and MAOM fractions are analysed for organic carbon with an elemental analyser. The mass and SOC recovery percentage will be calculated, with acceptable ranges of 95-100 % and 85-115 % respectively.

Soil moisture at field water capacity ($\boldsymbol{\theta_{FC}}$) and at permanent wilting point ($\boldsymbol{\theta_{PWP}}$)

Soil moisture at field capacity ($\boldsymbol{\theta_{FC}}$) and at permanent wilting point ($\boldsymbol{\theta_{PWP}}$) is determined with the pressure plate method following ISO 11274:1998. The SMD suggests the ISO 11274:2019 or estimating $\boldsymbol{\theta_{FC}}$ and $\boldsymbol{\theta_{PWP}}$ with the set of pedotransfer functions for Europe developed by Tóth et al. (2015), which were updated by Szabó et al. (2021) providing uncertainty estimates.

At the laboratory, θ_{FC} is determined from disturbed or undisturbed soil samples, clods of approximate volume 10 cm^3 from each depth interval (0-10 cm and 10-30 cm). The soil clods are equilibrated at pre-determined matric potentials using a Richards pressure-plate apparatus for several days (ISO 11274:2019 recommends 5-7 days) (Cousin et al., 2022). The soil clods are then weighed: i) immediately after extraction from the pressure-plate (wet weight at a determined matric potential), and ii) after they have been dried at 105°C for 48 h (dry weight) to determine the gravimetric soil water content (Cousin et al., 2022). The traditionally recognised soil matric potential for permanent wilting point is -1500 kPa (pF = 4.2) (Richards and Weaver, 1943), whereas field capacity is assumed to be the soil moisture at -33 kPa or -10 kPa (pF = 2.5 and pF = 2.0) (Bruand et al., 2004; Cousin et al., 2022). Cousin et al. (2022) recommend using undisturbed soil samples for determination of θ_{FC} as the clod retains unaltered its structure, whereas θ_{PWP} can be measured from sieved or disturbed samples.

16S rRNA gene amplicon sequencing

DNA extraction. Use the DNeasy PowerSoil Pro Kit (Qiagen) for DNA extraction (https://www.qiagen.com/us/products/discovery-and-translational-research/dna-rna-purification/dna-purification/microbial-dna/dneasy-powersoil-pro-kit?catno=47014) following the manufacturer's instructions, starting from 0.25 g of soil and with a final elution volume of 100 µL.

DNA quantification and quality check. DNA quality should be checked with NanoDrop, OD 260/280 should be between 1.8-2.0. A Qubit fluorometer or similar is preferred for quantification, with a minimum

requirement of 10 ng uL-1**PCR and sequencing.** The recommended PCR primer set for amplifying the V4 region of the 16S rRNA gene (Caporaso et al., 2011) is:

- Forward primer 515F: 5′-GTGCCAGCMGCCGCGGTAA-3′
- Reverse primer 806R: 5′-GGACTACHVGGGTWTCTAAT-3′

Carry out PCR reactions with 15 µL of Phusion High - Fidelity PCR Master Mix, 0.2 µM of forward and reverse primers and about 10 ng template DNA. Thermal cycling consists of an initial denaturation at 98 ºC for 1 min, followed by 30 cycles of denaturation at 98 ºC for 10 s, annealing at 50 ºC for 30 s, and elongation at 72 ºC for 30 s and 72 ºC for 5 min.

Purify the PCR products using magnetic bead purification. Mix samples in equidensity ratios based on the concentration of PCR products.

While sequencing providers may vary, we recommend using a service that employs Illumina sequencing platforms.

Each sample should yield a minimum of 50,000 sequence reads. Raw sequences should be deposited to the European Nucleotide Archive and/or Zenodo.

Bioinformatics. Assign paired-end reads to samples based on their unique barcode and truncate by cutting off the barcode and primer sequences. Merge paired-end reads using FLASH (http://ccb.jhu.edu/software/FLASH/) (Magoč and Salzberg, 2011). Quality filter the raw tags using the fastp software to obtain high-quality Clean Tags (Bokulich et al., 2013). Compare the tags with the Silva reference database (https://www.arb-silva.de/) to detect chimera sequences, then obtain the Effective Tags by removing the chimera sequences with the vsearch package (https://github.com/torognes/vsearch) (Edgar et al., 2011). For the Effective Tags obtained previously, denoise with DADA2 module in the QIIME2 software to obtain initial ASVs (Amplicon Sequence Variants). Perform species annotation using QIIME2 software and Silva Database.

3.6 Calculation of SOC stocks

The formulas to calculate the estimators of the population of interest change depending on the sampling design. We are assuming at this section that we apply stratified random sampling. We start by calculating the SOC stock at a single soil sampling unit

The SOC density (Mg C ha^{-1}) for depth layer *i* at a sampling unit is calculated as:

$$SOC_{density.i} = SOC_i \; x \; \rho_{Wh,i} \; x \left(1 - CF_{grav,i}\right) x \; thickness_i \; x \; 0.1 \qquad [7]$$

Where SOC_i is the SOC content of the fine earth (< 2 mm) (mg C g^{-1} soil < 2mm), $\rho_{Wh,i}$ is the bulk density of whole soil (g soil cm^{-3}) at layer *i*, $CF_{grav,i}$ is the ratio of gravimetric coarse fragments to bulk soil (hence units of $1 - CF_{grav,i}$ is g soil < 2mm/ g soil) at depth interval *i*, $thickness_i$ is the thickness of depth interval *i* (cm) and 0.1 the conversion factor (1 mg C cm^{-2} = 0.1 Mg C ha^{-1}). Notice that when the bulk density is of the fine earth, the coarse fragments ratio is volumetric (Poeplau et al., 2017), otherwise there would be a systematic error of the SOC stocks.

Alternatively, if the $mass_{fine}$ has been determined from a sample (e.g., intact core) of known volume, equation 7 can be simplified to equation 8 as per Poeplau et al. (2017):

$$SOC_{density.i}\ (Mg\ C\ ha^{-1}) = SOC_i\ (mg\ C\ g^{-1}_{soil<2mm})\ x\ \frac{mass_{fine}\ (g_{soil<2mm})}{V_{soil}\ (cm^3)}\ x\ thickness_i\ (cm)\ x\ 0.1\ \left(\frac{Mg\ C\ cm^2}{mg\ C\ ha}\right) \quad [8]$$

With simple random sampling within strata, the estimator of the mean SOC stock density for each stratum *h* and depth interval *i* is the unweighted sample mean (Arrouays et al., 2018b; Brus, 2022):

$$\widehat{\overline{SOC}}_{h,i} = \overline{SOC}_{S_{h,i}} = \frac{1}{n_{h,i}} \sum_{k \in S_{h,i}} SOC_{k,h,i} \quad [9]$$

where $\widehat{\overline{SOC}}_{h,i}$ is the mean SOC density for the stratum *h* and depth interval *i*, $\overline{SOC}_{S_{h,i}}$ is the unweighted mean of the sample $S_{h,i}$, $n_{h,i}$ is the number of sampling units in stratum *h*, *k* is a sampling unit from the sample $S_{h,i}$ and $SOC_{k,h,i}$ is the SOC density of sampling unit *k* and depth interval *i* from stratum *h* calculated with equation 7.

The estimator of the mean SOC density (Mg C ha^{-1}) at the intervention area is calculated with the formula for the stratified random sampling, averaging the values from each stratum with their relative weights:

$$\widehat{\overline{SOC}}_i = \sum_{h=1}^{H} w_h\ \widehat{\overline{SOC}}_{h,i} \quad [10]$$

where $\widehat{\overline{SOC}}_i$ is the estimator of the mean SOC stock density for depth interval *i*, *H* is the total number of strata, w_h is the weight for stratum *h*. When the allocation of sampling units has been done proportional to the area, w_h is the relative area of the stratum, and if the stratification was done with equal area geostrata the weights are the same across all strata.

The sampling variance is a measurement of the random error associated to the sampling strategy, and it quantifies our uncertainty about the population mean, i.e., the mean SOC density at an intervention area (Brus, 2022). The square root of the sampling variance is the standard error. The sampling variance of the mean SOC density for the intervention area is obtained by weighted averaging of the sampling variances of each stratum. The weights must be squared (Brus, 2022):

$$\hat{V}\left(\widehat{\overline{SOC}}_i\right) = \sum_{h=1}^{H} w_h^2\ \hat{V}\left(\widehat{\overline{SOC}}_{h,i}\right) \quad [11]$$

Where $\hat{V}\left(\widehat{\overline{SOC}}_{h,i}\right)$ is the estimated sampling variance of the mean SOC density of stratum *h* and layer *i* (Arrouays et al., 2018b; Brus, 2022):

$$\hat{V}\left(\widehat{\overline{SOC}}_{h,i}\right) = \frac{1}{n_h(n_h-1)} \sum_{k=1}^{n_h} \left(SOC_{k,h,i} - \widehat{\overline{SOC}}_{h,i}\right)^2 \quad [12]$$

3.7 Equivalent soil mass

Temporal changes on soil bulk density are expected as a result from the CFPs that may hinder the effects of the CFPs on the estimated change in SOC stocks. Therefore, it is recommended to provide the SOC stocks

in equivalent soil mass (ESM) basis as recommended by some SOC MVR standards (FAO, 2020; Verra, 2024) and the scientific literature (Bradford et al., 2023; Von Haden et al., 2020; Wendt and Hauser, 2013). With the ESM approach, the SOC stocks are assessed relative to a constant soil mass per unit area, expressed as Mg ha^{-1}, and possible changes in bulk density are compensated by changes in sampled depth (Loubet et al., 2025). For a specific depth interval *i*, the mass of fine earth per unit area (FSS_i) is calculated dividing the dry mass of the fine earth ($mass_{fine,i}$) by the area sampled by the probe or auger, S_i (Wendt and Hauser, 2013). The SOC mass of a depth interval *i* per unit area, $M_{SOC,i}$, is the product of the fine earth mass and SOC content:

$$M_{SOC,i} = FSS_i \; x \; SOC_i \; x \; 10^{-3} \qquad [13]$$

Where $M_{SOC,i}$ is expressed in Mg C ha^{-1}, the mass of fine earth (FSS_i) is expressed in Mg ha^{-1} and the content of SOC in fine earth, SOC_i is in $g\ C\ kg^{-1}_{soil<2mm}$, with the conversion factor 10^{-3} kg soil to Mg soil and g C to Mg C. We can express equation 13 from the measurements of the soil auger sample:

$$M_{SOC,i} = FSS_i \; x \; SOC_i = \frac{mass_{fine,i}}{S_i} \; x \; SOC_i = \frac{mass_{fine,i}}{\pi \left(\frac{D}{2}\right)^2} \; x \; SOC_i \qquad [14]$$

Where the mass of fine earth, $mass_{fine,i}$, corresponds to the mass from the sample (e.g., cylinder or auger) in g, the sampled area is in cm^2, the SOC_i the content of SOC in $mg\ C\ g^{-1}_{soil<2mm}$, D is the inner diameter of the cylinder (cm). indicating the units and the conversion factor in equation 14:

$$M_{SOC,i}(Mg\ C\ ha^{-1}) = \frac{mass_{fine,i}\,(g_{soil<2mm})}{\pi \left(\frac{D}{2}\right)^2 (cm^2)} \; x \; SOC_i \left(mg\ C\ g^{-1}_{soil<2mm}\right) x \; 0.1 \left(\frac{Mg\ C\ cm^2}{mg\ C\ ha}\right) \qquad [15]$$

Because we are sampling the depth intervals 0-10 cm and 10-30 cm, the cumulative SOC stock of 0-30 cm is calculated and then transformed into SOC stock for a reference soil mass that is maintained constant over sampling times. Values for the reference soil mass can be that from the decompacted situation after project development (FAO, 2020), or soil mass at the baseline (Loubet et al., 2025). Wendt and Hauser (2013) provided a spreadsheet to estimate the ESM using a using cubic spline function. Von Haden et al. (2020) developed an R script that uses cubic spline interpolations and mineral soil masses to calculate ESM-based SOC stocks. Similarly, Ferchaud et al. (2023) developed the R script *SimpleESM* to ease calculations of ESM-based SOC stocks.

3.8 Calculation of SOC stock change

The change of the mean SOC stocks between two sampling times t1 and t0 ($\overline{\Delta SOC}$) is calculated as the spatial mean of SOC stock for a given time ($\widehat{\overline{SOC}}_{t1}$) minus the spatial mean SOC stock from a previous survey ($\widehat{\overline{SOC}}_{t0}$).

$$\overline{\Delta SOC} = \widehat{\overline{SOC}}_{t1} - \widehat{\overline{SOC}}_{t0} \qquad [16]$$

We are using a static synchronous approach, and the same soil sampling units are revisited in consecutive campaigns. Hence, we calculate the change in SOC stock at each sampling unit *k*, followed by averaging by stratum *h* and at the intervention area with weights proportional to strata areas.

$$\widehat{\overline{\Delta SOC}} = \sum_{h=1}^{H} w_h \, \widehat{\overline{\Delta SOC}}_h = \sum_{h=1}^{H} w_h \frac{1}{n_h} \sum_{k=1}^{n_h} \Delta SOC_k \qquad [17]$$

The variance of the mean change in SOC stock can be derived from the properties of variance:

$$\hat{V}\left(\widehat{\overline{\Delta SOC}}\right) = \hat{V}\left(\widehat{\overline{SOC}}_{t1}\right) + \hat{V}\left(\widehat{\overline{SOC}}_{t0}\right) - 2Cov\left(\widehat{\overline{SOC}}_{t1}, \widehat{\overline{SOC}}_{t0}\right) \qquad [18]$$

Where $\hat{V}\left(\widehat{\overline{SOC}}_{t1}\right)$ and $\hat{V}\left(\widehat{\overline{SOC}}_{t0}\right)$ are respectively the variances of the mean SOC stock for time t1 and t0 calculated with equation 12, and $Cov\left(\widehat{\overline{SOC}}_{t1}, \widehat{\overline{SOC}}_{t0}\right)$ is the covariance of the two mean estimators (Brus, 2014).

3.9 Measuring and modelling changes in SOC

4.9.1. Measure and Model

The baseline SOC stocks at the intervention areas are calculated for Time 0 (2025) before the implementation of CFPs. Measure and model approaches use robust and validated process-based models (e.g., RothC, AGM) for predicting changes in SOC stocks caused by the CFPs. These models should be able to simulate the effects of extreme climatic events (e.g., droughts) on SOC dynamics that can explain SOC accrual values different than those anticipated during planning of the carbon farming project. The ARMOSA process-based crop model (Perego et al., 2013) has been used to assess the effects of conservation agriculture on SOC dynamics in comparison to conventional agricultural practices (Valkama et al., 2020) using as input data on climate, soil properties, management and crop type. The simulations allow to assess the effects of carbon farming in comparison with the baseline scenario (conventional agriculture).

4.9.2. Measure and Re-measure

The baseline SOC stocks are measured at intervention areas at Time 0 and control plots where the soil characteristics, relief, climate and agricultural system are similar to the intervention area. It is possible that at the control plot and at the intervention area some practices of conservation agriculture or regenerative agriculture are already adopted (e.g., reduced tillage). The management at Time 0 defines our baseline conditions. However, we assume additional practices that will further improve soil condition and carbon storage will be adopted only at the intervention area (e.g., improved crop rotation). The SOC stocks will be remeasured at Time 1 and Time 2 at both control plots and intervention areas, allowing for the incorporation of dynamic baselines (Bradford et al., 2023). This is particularly important for cases where process-based models are not sufficiently calibrated or validated. The significance of the changes in SOC stocks can be assessed with a t-test with the adequate degrees of freedom (Loubet et al., 2025). The t-value is calculated as:

$$t = \frac{\widehat{\overline{SOC}}_{t0} - \widehat{\overline{SOC}}_{t1}}{\sqrt{\hat{V}\left(\widehat{\overline{SOC}}_{t0}\right) + \hat{V}\left(\widehat{\overline{SOC}}_{t1}\right) - 2Cov\left(\widehat{\overline{SOC}}_{t1}, \widehat{\overline{SOC}}_{t0}\right)}} \qquad [19]$$

Where the variance refers to the sampling variance at the intervention area (accounting for the sample size).

3.10 Establishment of baseline SOC values

In some situations, the identification and monitoring of control plots near the intervention areas may not be possible because the agricultural management in the region is predominantly of regenerative agriculture, or due to limited funding. There are several methods for setting baseline values of SOC stocks for a particular land use and pedoclimatic context, which generally rely on similarity metrics for soil-forming factors and soil properties between the area of interest and its neighbouring region. Digital soil mapping (DSM) frameworks and concepts like genoforms and phenoforms (Rossiter and Bouma, 2018) and their analogous genosoils and phenosoils (Huang et al., 2018), digital terron mapping (Carré and McBratney, 2005; Malone et al., 2014), pedogenon mapping (Román Dobarco et al., 2021), or homosoils (Mallavan et al., 2010; Nenkam et al., 2023) can be useful for these situations. These DSM frameworks have in common that the soil-forming factors and soil properties are represented by spatially exhaustive covariates (e.g., digital elevation models and derived terrain attributes, lithology maps, climate gridded data, etc.) as per the *scorpan* model (McBratney et al., 2003). *Scorpan* models establish quantitative relationships between soil properties or soil classes (response variables) and seven predictive factors: other soil properties (*s*), climate (*c*), organisms (*o*), relief (*r*), parent material (p), time (a) and spatial position (*n*).

Pedogenon maps define classes with homogeneous soil-forming factors for a given reference time (i.e., temporal baseline) applying unsupervised classification to a set of quantitative regionalised covariates. The underlying assumption is that within each class the long-term pedogenetic processes are similar and hence would result in similar soil capacity to store SOC and similar resilience to management and land use history. Maps of pedogenon classes can be defined from local (Jang et al., 2022) to continental scale (Román Dobarco et al., 2023). Then, they can be combined with high-resolution spatial data on land use (e.g., CORINE Land Cover at 100 m (European Environment Agency, 2019), CLCplus Backbone at 10 m (European Environment Agency, 2024)) to derive subclasses where we assume similar inherent capacity and pedogenesis, but substantial differences in soil properties and functions due to management history, i.e., *phenosoils*. Pedogenon, genosoil, and phenosoil maps have been used to assess the change in SOC stock at local scale linked to agricultural activities and set SOC sequestration potential (Jang et al., 2023), and more recently to assess SOC dynamics at continental scale (Styc et al., 2025). Thus, **pedogenon and phenosoils maps can be populated with SOC legacy data** from public national, European or global soil datasets (e.g., LUCAS (Orgiazzi et al., 2018), Carbosol (Llorente et al., 2018), IGCS (Inventaire, Gestion et Conservation des Sols)(Arrouays et al., 2004), etc.) **ongoing projects** (e.g., BENCHMARKS, AI4SOILHEALTH, MARVIC) **and targeted sampling to set baseline levels by phenosoil class**. Baseline levels of SOC content and stocks for each phenosoil can be determined from the distribution of available SOC data (e.g., median SOC stocks, inter-quantile range) and used for their respective demo-sites.

Digital terron maps are also created applying unsupervised classification models (e.g., k-means, fuzzy clustering) to landscape attributes and soil property maps (e.g., clay, pH, mineralogy) to define soil-landscape units that can be used for land capability assessment or agricultural management zones, often with emphasis on vineyards as per the terroir concept (Malone et al., 2014). Similarly, digital terron maps developed at local or regional scale and combined with legacy soil datasets and land use can be used as strata for setting up baselines of SOC stocks for the local (or regional) pedoclimatic and landscape conditions. The concept of homosoils can be useful for areas with sparse soil data, by identifying areas of the world that have similar soils and may have available soil data. The baseline SOC stocks for specific land uses or agricultural systems by homosoils type can be transferred to geographically distant areas with the same homosoils.

It is possible that a demo-site or intervention area is located over several phenosoils, terron classes, or soil types (World Reference Base system of soil classification (WRB, 2022)), if there is high heterogeneity of soil characteristics within the intervention area. The intra-site variability may have been captured by the stratification based on environmental covariates. **Baseline SOC stocks identified for the local or regional pedoclimatic and landscape condition can be used as input for modelling the trend for BAU scenario with a hybrid approach** and propagate uncertainty.

3.11 Available resources and tutorials on sampling design and implementation in R

Tutorial by David Rossiter on using the package *spcosa* in R for stratified random sampling using compact geographical strata:
https://www.css.cornell.edu/faculty/dgr2/_static/files/R_html/SpatialCoverageSampling_Tutorial.html

Tutorial on how to implement *conditioned Latin Hypercube Sampling* (cLHS) with R by Dave White (2018) (NRCS, USDA):
https://ncss-tech.github.io/soil-pit/sandbox/dave/clhs.html

Online book by the Soil Survey Staff (31/01/2025) *Statistics for Soil Survey* (NRCS and National Cooperative Soil Survey):
https://ncss-tech.github.io/stats_for_soil_survey/book/
With a chapter dedicated to different spatial sampling strategies and their implementation in R:
https://ncss-tech.github.io/stats_for_soil_survey/book/sampling.html#sampling-strategies

Online book by dick Brus (2023) *Spatial Sampling with R*:
https://dickbrus.github.io/SpatialSamplingwithR/

Online book by Richard Arnold et al. (2025) on *Sample Survey* for the course STAT 392 at the Victoria University of Wellington and at Statistics New Zealand:
https://homepages.ecs.vuw.ac.nz/~rarnold/STAT392/SampleSurveysBook/_book/

References

Amen, A., Blaszczynski, J., 2001. Integrated Landscape Analysis. U.S. Department of the Interior, Bureau of Land Management. National Science and Technology Center, Denver, CO, pp. 2–20.

Arrouays, D., Hardy, R., Schnebelen, N., Le Bas, C., EIMBERCK, M., Roque, J., Grolleau, É., Pelletier, A., Doux, J., Lehmann, S., Saby, N., King, D., Jamagne, M., Rat, D., Stengel, P., 2004. Le programme inventaire gestion et conservation des sols en France. Etude Gest. Sols 11, 187–197.

Arrouays, D., Saby, N.P.A., Boukir, H., Jolivet, C., Ratié, C., Schrumpf, M., Merbold, L., Gielen, B., Gogo, S., Delpierre, N., Vincent, G., Klumpp, K., Loustau, D., 2018. Soil sampling and preparation for monitoring soil carbon. Int. Agrophysics 32, 633–643. https://doi.org/10.1515/intag-2017-0047

Batjes, N.H., 1996. Total carbon and nitrogen in the soils of the world. Eur. J. Soil Sci. 47, 151–163. https://doi.org/10.1111/j.1365-2389.1996.tb01386.x

Bell, S.M., Terrer, C., Barriocanal, C., Jackson, R.B., Rosell-Melé, A., 2021. Soil organic carbon accumulation rates on Mediterranean abandoned agricultural lands. Sci. Total Environ. 759, 143535. https://doi.org/10.1016/j.scitotenv.2020.143535

Bettigole, C., Hanle, J., Kane, D.A., Pagliaro, Z., Kolodney, S., Szuhay, S., Chandler, M., Hersh, E., Wood, S.A., Basso, B., Goodwin, D.J., Hardy, S., Wolf, Z., Covey, K.R., 2023. Optimizing Sampling Strategies for Near-Surface Soil Carbon Inventory: One Size Doesn't Fit All. Soil Syst. 7, 27. https://doi.org/10.3390/soilsystems7010027

Blake, G.R., Hartge, K.H., 1986. Bulk Density, in: Methods of Soil Analysis, SSSA Book Series. pp. 363–375. https://doi.org/10.2136/sssabookser5.1.2ed.c13

Blum, W.E.H., 2005. Functions of Soil for Society and the Environment. Rev. Environ. Sci. Biotechnol. 4, 75–79. https://doi.org/10.1007/s11157-005-2236-x

Bokulich, N.A., Subramanian, S., Faith, J.J., Gevers, D., Gordon, J.I., Knight, R., Mills, D.A., Caporaso, J.G., 2013. Quality-filtering vastly improves diversity estimates from Illumina amplicon sequencing. Nat. Methods 10, 57–59. https://doi.org/10.1038/nmeth.2276

Boschetto, R.G., Mohamed, R.M., Arrigotti, J., 2010. Vulnerability to Desertification in a Sub-Saharan Region: A First Local Assessment in Five Villages of Southern Region of Malawi. Ital. J. Agron. 5, 91–101. https://doi.org/10.4081/ija.2010.s3.91

Bradford, M.A., Eash, L., Polussa, A., Jevon, F.V., Kuebbing, S.E., Hammac, W.A., Rosenzweig, S., Oldfield, E.E., 2023. Testing the feasibility of quantifying change in agricultural soil carbon stocks through empirical sampling. Geoderma 440, 116719. https://doi.org/10.1016/j.geoderma.2023.116719

Bruand, A., Duval, O., Cousin, I., 2004. Estimation des propriétes de retention en eau des sols à partir de la base de donnees SOLHYDRO: Une première proposition combianant le type d'horizon, sa texture et sa densite apparente. Etude Gest. Sols 323–34.

Brus, D.J., 2022. Spatial Sampling with R, 1st ed. Chapman and Hall/CRC, Boca Raton. https://doi.org/10.1201/9781003258940

Brus, D.J., 2021. Statistical approaches for spatial sample survey: Persistent misconceptions and new developments. Eur. J. Soil Sci. 72, 686–703. https://doi.org/10.1111/ejss.12988

Brus, D.J., 2014. Statistical sampling approaches for soil monitoring. Eur. J. Soil Sci. 65, 779–791. https://doi.org/10.1111/ejss.12176

Brus, D.J., De Gruijter, J.J., 2013. Effects of spatial pattern persistence on the performance of sampling designs for regional trend monitoring analyzed by simulation of space–time fields. Comput. Geosci. 61, 175–183. https://doi.org/10.1016/j.cageo.2013.09.001

Bünemann, E.K., Bongiorno, G., Bai, Z., Creamer, R.E., De Deyn, G., De Goede, R., Fleskens, L., Geissen, V., Kuyper, T.W., Mäder, P., Pulleman, M., Sukkel, W., Van Groenigen, J.W., Brussaard, L., 2018. Soil quality – A critical review. Soil Biol. Biochem. 120, 105–125. https://doi.org/10.1016/j.soilbio.2018.01.030

Calinski, T., Harabasz, J., 1974. A dendrite method for cluster analysis. Commun. Stat. - Theory Methods 3, 1–27. https://doi.org/10.1080/03610927408827101

Canali, S., Benedetti, A., 2005. Soil Nitrogen Mineralization, in: Microbiological Methods for Assesing Soil Quality. CABI Publishing, Cambridge, USA, pp. 127–135.

Cardinael, R., Chevallier, T., Cambou, A., Béral, C., Barthès, B.G., Dupraz, C., Durand, C., Kouakoua, E., Chenu, C., 2017. Increased soil organic carbon stocks under agroforestry: A survey of six different sites in France. Agric. Ecosyst. Environ. 236, 243–255. https://doi.org/10.1016/j.agee.2016.12.011

Carré, F., McBratney, A.B., 2005. Digital terron mapping. Geoderma 128, 340–353. https://doi.org/10.1016/j.geoderma.2005.04.012

Chappell, A., Baldock, J.A., Viscarra Rossel, R.A., n.d. Sampling soil organic carbon to detect change over time. CSIRO, Canberra, Australia.

Commission of the European Communities, 2006. Proposal For a Directive of the European Parliament and of the Council, Establishing a Framework For the Protection of Soil and Amending Directive 2004/35/EC COM 231 final, Brussels.

Cotrufo, M.F., Ranalli, M.G., Haddix, M.L., Six, J., Lugato, E., 2019. Soil carbon storage informed by particulate and mineral-associated organic matter. Nat. Geosci. 12, 989–994. https://doi.org/10.1038/s41561-019-0484-6

Cousin, I., Buis, S., Lagacherie, P., Doussan, C., Le Bas, C., Guérif, M., 2022. Available water capacity from a multidisciplinary and multiscale viewpoint. A review. Agron. Sustain. Dev. 42, 46. https://doi.org/10.1007/s13593-022-00774-8

Cui, Z., Chen, S., Hu, B., Wang, N., Zhai, J., Peng, J., Bai, Z., 2025. High-Accuracy Mapping of Soil Organic Carbon by Mining Sentinel-1/2 Radar and Optical Time-Series Data with Super Ensemble Model. Remote Sens. 17. https://doi.org/10.3390/rs17040678

De Gruijter, J.J., Bierkens, M.F.P., Brus, D.J., Knotters, M., 2006. Sampling for Natural Resource Monitoring. Springer Berlin Heidelberg, Berlin, Heidelberg. https://doi.org/10.1007/3-540-33161-1

De Gruijter, J.J., McBratney, A.B., Minasny, B., Wheeler, I., Malone, B.P., Stockmann, U., 2016. Farm-scale soil carbon auditing. Geoderma 265, 120–130. https://doi.org/10.1016/j.geoderma.2015.11.010

De Gruijter, J.J., Wheeler, I., Malone, B.P., 2019. Using model predictions of soil carbon in farm-scale auditing- A software tool. Agric. Syst. 169, 24–30. https://doi.org/10.1016/j.agsy.2018.11.007

Directorate-General for Climate Action, European Commission, 2025. Carbon Removals and Carbon Farming. URL https://climate.ec.europa.eu/eu-action/carbon-removals-and-carbon-farming_en (accessed 3.26.25).

Dixon, R.K., Solomon, A.M., Brown, S., Houghton, R.A., Trexier, M.C., Wisniewski, J., 1994. Carbon Pools and Flux of Global Forest Ecosystems. Science 263, 185–190. https://doi.org/10.1126/science.263.5144.185

Drobnik, T., Greiner, L., Keller, A., Grêt-Regamey, A., 2018. Soil quality indicators – From soil functions to ecosystem services. Ecol. Indic. 94, 151–169. https://doi.org/10.1016/j.ecolind.2018.06.052

Dunn†, J.C., 1974. Well-Separated Clusters and Optimal Fuzzy Partitions. J. Cybern. 4, 95–104. https://doi.org/10.1080/01969727408546059

Edgar, R.C., Haas, B.J., Clemente, J.C., Quince, C., Knight, R., 2011. UCHIME improves sensitivity and speed of chimera detection. Bioinformatics 27, 2194–2200. https://doi.org/10.1093/bioinformatics/btr381

European Commission, 2023. ANNEXES to the proposal for a Directive of the European Parliament and of the Council on Soil Monitoring and Resilience (Soil Monitoring Law). COM(2023) 416 final.

European Commission. Joint Research Centre., 2017. LUCAS 2018: soil component : sampling instructions for surveyors. Publications Office, LU.

European Environment Agency, 2024. CLC+Backbone 2021 (raster 10 m), Europe, 3-yearly, Jun. 2024. https://doi.org/10.2909/71FC9D1B-479F-4DA1-AA66-662A2FFF2CF7

European Environment Agency, 2019. CORINE Land Cover 2018 (raster 100 m), Europe, 6-yearly- version 2020_20u1, May 2020. https://doi.org/10.2909/960998C1-1870-4E82-8051-6485205EBBAC

European Parliament, Council of the European Union, 2024. Regulation (EU) 2024/3012 of the European Parliament and of the Council of 27 November 2024 establishing a Union certification framework for permanent carbon removals, carbon farming and carbon storage in products.

Evangelista, S.J., Field, D.J., McBratney, A.B., Minasny, B., Ng, W., Padarian, J., Dobarco, M.R., Wadoux, A.M.J.-C., 2023. A proposal for the assessment of soil security: Soil functions, soil services and threats to soil. Soil Secur. 10, 100086. https://doi.org/10.1016/j.soisec.2023.100086

FAO, 2020. A protocol for measurement, monitoring, reporting and verification of soil organic carbon in agricultural landscapes. FAO. https://doi.org/10.4060/cb0509en

Ferchaud, F., Chlebowski, F., Mary, B., 2023. SimpleESM: R script to calculate soil organic carbon and nitrogen stocks at Equivalent Soil Mass.

Friedlingstein, P., O'Sullivan, M., Jones, M.W., Andrew, R.M., Hauck, J., Landschützer, P., Le Quéré, C., Li, H., Luijkx, I.T., Olsen, A., Peters, G.P., Peters, W., Pongratz, J., Schwingshackl, C., Sitch, S., Canadell, J.G., Ciais, P., Jackson, R.B., Alin, S.R., Arneth, A., Arora, V., Bates, N.R., Becker, M., Bellouin, N., Berghoff, C.F., Bittig, H.C., Bopp, L., Cadule, P., Campbell, K., Chamberlain, M.A., Chandra, N., Chevallier, F., Chini, L.P., Colligan, T., Decayeux, J., Djeutchouang, L.M., Dou, X., Duran Rojas, C., Enyo, K., Evans, W., Fay, A.R., Feely, R.A., Ford, D.J., Foster, A., Gasser, T., Gehlen, M., Gkritzalis, T., Grassi, G., Gregor, L., Gruber, N., Gürses, Ö., Harris, I., Hefner, M., Heinke, J., Hurtt, G.C., Iida, Y., Ilyina, T., Jacobson, A.R., Jain, A.K., Jarníková, T., Jersild, A., Jiang, F., Jin, Z., Kato, E., Keeling, R.F., Klein Goldewijk, K., Knauer, J., Korsbakken, J.I., Lan, X., Lauvset, S.K., Lefèvre, N., Liu, Z., Liu, J., Ma, L., Maksyutov, S., Marland, G., Mayot, N., McGuire, P.C., Metzl, N., Monacci, N.M., Morgan, E.J., Nakaoka, S.-I., Neill, C., Niwa, Y., Nützel, T., Olivier, L., Ono, T., Palmer, P.I., Pierrot, D., Qin, Z., Resplandy, L., Roobaert, A., Rosan, T.M., Rödenbeck, C., Schwinger, J., Smallman, T.L., Smith, S.M., Sospedra-Alfonso, R., Steinhoff, T., Sun, Q., Sutton, A.J., Séférian, R., Takao, S., Tatebe, H., Tian, H., Tilbrook, B., Torres, O., Tourigny, E., Tsujino, H., Tubiello, F., Van Der Werf, G., Wanninkhof, R., Wang, X., Yang, D., Yang, X., Yu, Z., Yuan, W., Yue, X., Zaehle, S., Zeng, N., Zeng, J., 2025. Global Carbon Budget 2024. Earth Syst. Sci. Data 17, 965–1039. https://doi.org/10.5194/essd-17-965-2025

Guerrero, C., Lorenzetti, R., 2021. Use of composite samples and NIR spectroscopy to detect changes in SOC contents. Geoderma 396, 115069. https://doi.org/10.1016/j.geoderma.2021.115069

Herrick, J.E., Wander, M.M., 1998. Relationships between soil organic carbon and soil quality in cropped and rangeland soils: The importance of distribution, composition and soil biological activity, in: Soil Processes and the Carbon Cycle. CRC Press.

Huang, J., McBratney, A.B., Malone, B.P., Field, D.J., 2018. Mapping the transition from pre-European settlement to contemporary soil conditions in the Lower Hunter Valley, Australia. Geoderma 329, 27–42. https://doi.org/10.1016/j.geoderma.2018.05.016

Hurlbut, C.S., Klein, C., 1977. Manual of mineralogy (after James D. Dana). Wiley.

Jang, H.J., Dobarco, M.R., Minasny, B., Campusano, J.P., McBratney, A., 2023. Assessing human impacts on soil organic carbon change in the Lower Namoi Valley, Australia. Anthropocene 43, 100393. https://doi.org/10.1016/j.ancene.2023.100393

Jang, H.J., Román Dobarco, M., Minasny, B., McBratney, A., Jones, E., 2022. Developing and testing of pedogenons in the lower Namoi valley, NSW, Australia. Geoderma 428. https://doi.org/10.1016/j.geoderma.2022.116182

Jobbágy, E.G., Jackson, R.B., 2000. The vertical distribution of soil organic carbon and its relation to climate and vegetation. Ecol. Appl. 10, 423–436. https://doi.org/10.1890/1051-0761(2000)010[0423:TVDOSO]2.0.CO;2

Joint Research Centre: Institute for Environment and Sustainability, Hengl, T., 2007. A practical guide to geostatistical mapping of environmental variables. Publications Office.

Jolivet, C., Almeida Falcon, J.-L., Berché, P., Boulonne, L., Fontaine, M., Gouny, L., Lehmann, S., Maitre, B., Ratié, C., Schellenberger, E., Soler-Dominguez, N., 2022. French Soil Quality Monitoring Network Manual RMQS2: second metropolitan campaign 2016–2027. https://doi.org/10.17180/KC64-NY88

Kopittke, P.M., Berhe, A.A., Carrillo, Y., Cavagnaro, T.R., Chen, D., Chen, Q.-L., Román Dobarco, M., Dijkstra, F.A., Field, D.J., Grundy, M.J., He, J.-Z., Hoyle, F.C., Kögel-Knabner, I., Lam, S.K., Marschner, P., Martinez, C., McBratney, A.B., McDonald-Madden, E., Menzies, N.W., Mosley, L.M., Mueller, C.W., Murphy, D.V., Nielsen, U.N., O'Donnell, A.G., Pendall, E., Pett-Ridge, J., Rumpel, C., Young, I.M., Minasny, B., 2022. Ensuring planetary survival: the centrality of organic carbon in balancing the multifunctional nature of soils. Crit. Rev. Environ. Sci. Technol. 52, 4308–4324. https://doi.org/10.1080/10643389.2021.2024484

Kwiatkowska-Malina, J., 2018. Functions of organic matter in polluted soils: The effect of organic amendments on phytoavailability of heavy metals. Appl. Soil Ecol. 123, 542–545. https://doi.org/10.1016/j.apsoil.2017.06.021

Lal, R., 2010. Managing Soils and Ecosystems for Mitigating Anthropogenic Carbon Emissions and Advancing Global Food Security. BioScience 60, 708–721. https://doi.org/10.1525/bio.2010.60.9.8

Lark, R.M., 2012. Some considerations on aggregate sample supports for soil inventory and monitoring. Eur. J. Soil Sci. 63, 86–95. https://doi.org/10.1111/j.1365-2389.2011.01415.x

Lawrence, P.G., Roper, W., Morris, T.F., Guillard, K., 2020. Guiding soil sampling strategies using classical and spatial statistics: A review. Agron. J. 112, 493–510. https://doi.org/10.1002/agj2.20048

Lehmann, J., Bossio, D.A., Kögel-Knabner, I., Rillig, M.C., 2020. The concept and future prospects of soil health. Nat. Rev. Earth Environ. 1, 544–553. https://doi.org/10.1038/s43017-020-0080-8

Liptzin, D., Norris, C.E., Cappellazzi, S.B., Bean, G.M., Cope, M., Greub, K.L.H., Rieke, E.L., Tracy, P.W., Aberle, E., Ashworth, A., Bañuelos Tavarez, O., Bary, A.I., Baumhardt, R.L., Borbón Gracia, A., Brainard, D.C., Brennan, J.R., Briones Reyes, D., Bruhjell, D., Carlyle, C.N., Crawford, J.J.W., Creech, C.F., Culman, S.W., Deen, B., Dell, C.J., Derner, J.D., Ducey, T.F., Duiker, S.W., Dyck, M.F., Ellert, B.H., Entz, M.H., Espinosa Solorio, A., Fonte, S.J., Fonteyne, S., Fortuna, A.-M., Foster, J.L., Fultz, L.M., Gamble, A.V., Geddes, C.M., Griffin-LaHue, D., Grove, J.H., Hamilton, S.K., Hao, X., Hayden, Z.D., Honsdorf, N., Howe, J.A., Ippolito, J.A., Johnson, G.A., Kautz, M.A., Kitchen, N.R., Kumar, S., Kurtz, K.S.M., Larney, F.J., Lewis, K.L., Liebman, M., Lopez Ramirez, A., Machado, S., Maharjan, B., Martinez Gamiño, M.A., May, W.E., McClaran, M.P., McDaniel, M.D., Millar, N., Mitchell, J.P., Moore, A.D., Moore, P.A., Mora Gutiérrez, M., Nelson, K.A., Omondi, E.C., Osborne, S.L., Osorio Alcalá, L., Owens, P., Pena-Yewtukhiw, E.M., Poffenbarger, H.J., Ponce Lira, B., Reeve, J.R., Reinbott, T.M., Reiter, M.S., Ritchey, E.L., Roozeboom, K.L., Rui, Y., Sadeghpour, A., Sainju, U.M., Sanford, G.R., Schillinger, W.F., Schindelbeck, R.R., Schipanski, M.E., Schlegel, A.J., Scow, K.M., Sherrod, L.A., Shober, A.L., Sidhu, S.S., Solís Moya, E., St Luce, M., Strock, J.S., Suyker, A.E., Sykes, V.R., Tao, H., Trujillo Campos, A., Van Eerd, L.L., Van Es, H., Verhulst, N., Vyn, T.J., Wang, Y., Watts, D.B., Wright, D.L., Zhang, T., Morgan, C.L.S., Honeycutt, C.W., 2022. An evaluation of carbon indicators of soil health in long-term agricultural experiments. Soil Biol. Biochem. 172, 108708. https://doi.org/10.1016/j.soilbio.2022.108708

Llorente, M., Rovira, P., Merino, A., Rubio, A., Turrión, M.B., Badía, D., Romanya, J., González, J., Cortina, J.A., 2018. The CARBOSOL Database: a georeferenced soil profile analytical database for Spain. https://doi.org/10.1594/PANGAEA.884517

Loiseau, T., Chen, S., Mulder, V.L., Román Dobarco, M., Richer-de-Forges, A.C., Lehmann, S., Bourennane, H., Saby, N.P.A., Martin, M.P., Vaudour, E., Gomez, C., Lagacherie, P., Arrouays, D., 2019. Satellite data integration for soil clay content modelling at a national scale. Int. J. Appl. Earth Obs. Geoinformation 82, 101905. https://doi.org/10.1016/j.jag.2019.101905

Loubet, B., Saby, N.P., Gebleh, M., Buysse, P., Chenu, J.-P., Ratie, C., Jolivet, C., Kalalian, C., Levavasseur, F., Munera-Echeverri, J.-L., Lafont, S., Loustau, D., Papale, D., Nicolini, G., Winck, B., Arrouays, D., 2025. Carbon soil stock change in an intensive crop field near Paris reveals significant carbon losses. https://doi.org/10.5194/egusphere-2025-592

Lützow, M.V., Kögel-Knabner, I., Ekschmitt, K., Matzner, E., Guggenberger, G., Marschner, B., Flessa, H., 2006. Stabilization of organic matter in temperate soils: mechanisms and their relevance under different soil conditions – a review. Eur. J. Soil Sci. 57, 426–445. https://doi.org/10.1111/j.1365-2389.2006.00809.x

Magoč, T., Salzberg, S.L., 2011. FLASH: fast length adjustment of short reads to improve genome assemblies. Bioinformatics 27, 2957–2963. https://doi.org/10.1093/bioinformatics/btr507

Mallavan, B.P., Minasny, B., McBratney, A.B., 2010. Homosoil, a Methodology for Quantitative Extrapolation of Soil Information Across the Globe, in: Boettinger, J.L., Howell, D.W., Moore, A.C., Hartemink, A.E., Kienast-Brown, S. (Eds.), Digital Soil Mapping. Springer Netherlands, Dordrecht, pp. 137–150. https://doi.org/10.1007/978-90-481-8863-5_12

Malone, B.P., Hughes, P., McBratney, A.B., Minasny, B., 2014. A model for the identification of terrons in the Lower Hunter Valley, Australia. Geoderma Reg. 1, 31–47. https://doi.org/10.1016/j.geodrs.2014.08.001

Malone, B.P., Minansy, B., Brungard, C., 2019. Some methods to improve the utility of conditioned Latin hypercube sampling. PeerJ 7, e6451. https://doi.org/10.7717/peerj.6451

McBratney, A.B., Mendonça Santos, M.L., Minasny, B., 2003. On digital soil mapping. Geoderma 117, 3–52. https://doi.org/10.1016/S0016-7061(03)00223-4

McKenzie, N., Coughlan, K., Cresswell, H., 2002. Soil Physical Measurement and Interpretation for Land Evaluation. CSIRO Publishing. https://doi.org/10.1071/9780643069879

Minarsch, E.-M.L., Schierning, P., Wichern, F., Gattinger, A., Weckenbrock, P., 2024. Transect sampling for soil organic carbon monitoring in temperate alley cropping systems - A review and standardized guideline. Geoderma Reg. 36, e00757. https://doi.org/10.1016/j.geodrs.2024.e00757

Minasny, B., McBratney, A.B., 2018. Limited effect of organic matter on soil available water capacity. Eur. J. Soil Sci. 69, 39–47. https://doi.org/10.1111/ejss.12475

Minasny, B., McBratney, A.B., 2006. A conditioned Latin hypercube method for sampling in the presence of ancillary information. Comput. Geosci. 32, 1378–1388. https://doi.org/10.1016/j.cageo.2005.12.009

Mudge, P., McNeill, S., Hedley, C., Roudier, P., Poggio, M., Malone, B.P., Smith, P., McNally, S., Beare, M., Schipper, L., 2020. Design of an on-farm soil carbon benchmarking and monitoring approach for individual pastoral farms. MPI Technical Paper No: 2020/02., Ministry for Primary Industries. ed.

Mulvaney, R.L., 1996. Nitrogen-Inorganic forms, in: Methods of Soil Analysis. Part 3 - Chemical Methods. Madison, WI, USA, pp. 1123–1184.

Nenkam, A.M., Wadoux, A.M.J.-C., Minasny, B., McBratney, A.B., Traore, P.C.S., Whitbread, A.M., 2023. Using homosoils to enrich sparse soil data infrastructure: An example from Mali. CATENA 223, 106862. https://doi.org/10.1016/j.catena.2022.106862

Nield, S.J., Boettinger, J.L., Ramsey, R.D., 2007. Digitally Mapping Gypsic and Natric Soil Areas Using Landsat ETM Data. Soil Sci. Soc. Am. J. 71, 245–252. https://doi.org/10.2136/sssaj2006-0049

Orgiazzi, A., Ballabio, C., Panagos, P., Jones, A., Fernández-Ugalde, O., 2018. LUCAS Soil, the largest expandable soil dataset for Europe: a review. Eur. J. Soil Sci. 69, 140–153. https://doi.org/10.1111/ejss.12499

Perego, A., Giussani, A., Sanna, M., Fumagalli, M., Carozzi, M., Alfieri, L., Brenna, S., Acutis, M., 2013. The ARMOSA simulation crop model: Overall features, calibration and validation results. Ital. J. Agrometeorol. 23–38.

Poeplau, C., Vos, C., Don, A., 2017. Soil organic carbon stocks are systematically overestimated by misuse of the parameters bulk density and rock fragment content. SOIL 3, 61–66. https://doi.org/10.5194/soil-3-61-2017

Potash, E., Guan, K., Margenot, A.J., Lee, D., Boe, A., Douglass, M., Heaton, E., Jang, C., Jin, V., Li, N., Mitchell, R., Namoi, N., Schmer, M., Wang, S., Zumpf, C., 2023. Multi-site evaluation of stratified and balanced sampling of soil organic carbon stocks in agricultural fields. Geoderma 438, 116587. https://doi.org/10.1016/j.geoderma.2023.116587

Powers, R.F., 1980. Mineralizable Soil Nitrogen as an Index of Nitrogen Availability to Forest Trees. Soil Sci. Soc. Am. J. 44, 1314–1320. https://doi.org/10.2136/sssaj1980.03615995004400060037x

Ray, S.S., Singh, J.P., Das, G., Panigrahy, S., 2004. Use of high resolution remote sensing data for generating site-specific soil management plan. Presented at the Int. Arch. Photogramm. Remote Sensing Spatial Inf. Syst., Istanbul, pp. 127–131.

Richards, L.A., Weaver, L.R., 1943. Fifteen-atmosphere percentage as related to the permanent wilting percentage. Soil Sci. 56, 331–340. https://doi.org/10.1097/00010694-194311000-00002

Roberts, D., Wilford, J., Ghattas, O., 2019. Exposed soil and mineral map of the Australian continent revealing the land at its barest. Nat. Commun. 10, 5297. https://doi.org/10.1038/s41467-019-13276-1

Román Dobarco, M., Cousin, I., Le Bas, C., Martin, M.P., 2019. Pedotransfer functions for predicting available water capacity in French soils, their applicability domain and associated uncertainty. Geoderma 336, 81–95. https://doi.org/10.1016/j.geoderma.2018.08.022

Román Dobarco, M., McBratney, A., Minasny, B., Malone, B., 2021. A modelling framework for pedogenon mapping. Geoderma 393, 115012. https://doi.org/10.1016/j.geoderma.2021.115012

Román Dobarco, M., Padarian Campusano, J., McBratney, A.B., Malone, B., Minasny, B., 2023. Genosoil and phenosoil mapping in continental Australia is essential for soil security. Soil Secur. 13. https://doi.org/10.1016/j.soisec.2023.100108

Rossiter, D.G., Bouma, J., 2018. A new look at soil phenoforms – Definition, identification, mapping. Geoderma 314, 113–121. https://doi.org/10.1016/j.geoderma.2017.11.002

Rousseeuw, P.J., 1987. Silhouettes: A graphical aid to the interpretation and validation of cluster analysis. J. Comput. Appl. Math. 20, 53–65. https://doi.org/10.1016/0377-0427(87)90125-7

Scharlemann, J.P., Tanner, E.V., Hiederer, R., Kapos, V., 2014. Global soil carbon: understanding and managing the largest terrestrial carbon pool. Carbon Manag. 5, 81–91. https://doi.org/10.4155/cmt.13.77

Six, J., Conant, R.T., Paul, E.A., Paustian, K., 2002. Stabilization mechanisms of soil organic matter: Implications for C-saturation of soils. Plant Soil 241, 155–176. https://doi.org/10.1023/A:1016125726789

Smith, P., Davis, S.J., Creutzig, F., Fuss, S., Minx, J., Gabrielle, B., Kato, E., Jackson, R.B., Cowie, A., Kriegler, E., Van Vuuren, D.P., Rogelj, J., Ciais, P., Milne, J., Canadell, J.G., McCollum, D., Peters, G., Andrew, R., Krey, V., Shrestha, G., Friedlingstein, P., Gasser, T., Grübler, A., Heidug, W.K., Jonas, M., Jones, C.D., Kraxner, F., Littleton, E., Lowe, J., Moreira, J.R., Nakicenovic, N., Obersteiner, M., Patwardhan, A., Rogner, M., Rubin, E., Sharifi, A., Torvanger, A., Yamagata, Y., Edmonds, J., Yongsung, C., 2016. Biophysical and economic limits to negative CO2 emissions. Nat. Clim. Change 6, 42–50. https://doi.org/10.1038/nclimate2870

Soil Survey Staff, 2025. Statistics for Soil Survey. NRCS.

Stolbovoy, V., Montanarella, L., Filippi, N., Jones, A., Gallego, J., Grassi, G., 2007. Soil sampling protocol to certify the changes of organic carbon stock in mineral soil of the European Union. Version 2. (No. EUR 21576 EN/2). Office for Official Publications of the European Communities, Luxembourg.

Stolbovoy, V., Montanarella, L., Filippi, N., Selvaradjou, S., Panagos, P., Gallego, J., 2005. Soil Sampling Protocol to Certify the Changes of Organic Carbon Stock in Mineral Soils of European Union. Office for Official Publications of the European Communities, Luxembourg.

Styc, Q., Minasny, B., Jang, H.J., McBratney, A., 2025. Modelling Soil Organic Carbon Dynamics at the Continental Extent Using Pedogenon Mapping. Eur. J. Soil Sci. 76, e70070. https://doi.org/10.1111/ejss.70070

Szabó, B., Weynants, M., Weber, T.K.D., 2021. Updated European hydraulic pedotransfer functions with communicated uncertainties in the predicted variables (euptfv2). Geosci. Model Dev. 14, 151–175. https://doi.org/10.5194/gmd-14-151-2021

Tóth, B., Weynants, M., Nemes, A., Makó, A., Bilas, G., Tóth, G., 2015. New generation of hydraulic pedotransfer functions for Europe. Eur. J. Soil Sci. 66, 226–238. https://doi.org/10.1111/ejss.12192

Valkama, E., Kunypiyaeva, G., Zhapayev, R., Karabayev, M., Zhusupbekov, E., Perego, A., Schillaci, C., Sacco, D., Moretti, B., Grignani, C., Acutis, M., 2020. Can conservation agriculture increase soil carbon sequestration? A modelling approach. Geoderma 369, 114298. https://doi.org/10.1016/j.geoderma.2020.114298

Van Looy, K., Bouma, J., Herbst, M., Koestel, J., Minasny, B., Mishra, U., Montzka, C., Nemes, A., Pachepsky, Y.A., Padarian, J., Schaap, M.G., Tóth, B., Verhoef, A., Vanderborght, J., Van Der Ploeg, M.J., Weihermüller, L., Zacharias, S., Zhang, Y., Vereecken, H., 2017. Pedotransfer Functions in Earth System Science: Challenges and Perspectives. Rev. Geophys. 55, 1199–1256. https://doi.org/10.1002/2017RG000581

VandenBygaart, A.J., 2006. Monitoring soil organic carbon stock changes in agricultural landscapes: Issues and a proposed approach. Can. J. Soil Sci. 86, 451–463. https://doi.org/10.4141/S05-105

Verra, 2024. VM0042 Improved Agricultural Land Management, v2.1.

Vogel, H.-J., Eberhardt, E., Franko, U., Lang, B., Ließ, M., Weller, U., Wiesmeier, M., Wollschläger, U., 2019. Quantitative Evaluation of Soil Functions: Potential and State. Front. Environ. Sci. 7, 164. https://doi.org/10.3389/fenvs.2019.00164

Von Haden, A.C., Yang, W.H., DeLucia, E.H., 2020. Soils' dirty little secret: Depth-based comparisons can be inadequate for quantifying changes in soil organic carbon and other mineral soil properties. Glob. Change Biol. 26, 3759–3770. https://doi.org/10.1111/gcb.15124

Vrebos, D., Jones, A., Lugato, E., O'Sullivan, L., Schulte, R., Staes, J., Meire, P., 2021. Spatial evaluation and trade-off analysis of soil functions through Bayesian networks. Eur. J. Soil Sci. 72, 1575–1589. https://doi.org/10.1111/ejss.13039

Walvoort, D., Brus, D., de Gruijter, J., 2023. spcosa: Spatial Coverage Sampling and Random Sampling from Compact Geographical Strata. R package version 0.4-2, https://CRAN.R-project.org/package=spcosa.

Wang, N., Peng, J., Xue, J., Zhang, X., Huang, J., Biswas, A., He, Y., Shi, Z., 2022. A framework for determining the total salt content of soil profiles using time-series Sentinel-2 images and a random forest-temporal convolution network. Geoderma 409, 115656. https://doi.org/10.1016/j.geoderma.2021.115656

Wendt, J.W., Hauser, S., 2013. An equivalent soil mass procedure for monitoring soil organic carbon in multiple soil layers. Eur. J. Soil Sci. 64, 58–65. https://doi.org/10.1111/ejss.12002

Wicklin, R., 2012. Use the Cholesky transformation to correlate and uncorrelate variables. URL https://blogs.sas.com/content/iml/2012/02/08/use-the-cholesky-transformation-to-correlate-and-uncorrelate-variables.html

Wiesmeier, M., Urbanski, L., Hobley, E., Lang, B., Von Lützow, M., Marin-Spiotta, E., Van Wesemael, B., Rabot, E., Ließ, M., Garcia-Franco, N., Wollschläger, U., Vogel, H.-J., Kögel-Knabner, I., 2019. Soil organic carbon storage as a key function of soils- A review of drivers and indicators at various scales. Geoderma 333, 149–162. https://doi.org/10.1016/j.geoderma.2018.07.026

WRB, I.W.G., 2022. World Reference Base for Soil Resources. International soil classification system for naming soils and creating legends for soil maps., 4th edition. ed. International Union of Soil Sciences, Vienna, Austria.

Xiao, J., Shen, Y., Tateishi, R., Bayaer, W., 2006. Development of topsoil grain size index for monitoring desertification in arid land using remote sensing. Int. J. Remote Sens. 27, 2411–2422. https://doi.org/10.1080/01431160600554363

Zamanian, K., Zhou, J., Kuzyakov, Y., 2021. Soil carbonates: The unaccounted, irrecoverable carbon source. Geoderma 384, 114817. https://doi.org/10.1016/j.geoderma.2020.114817

Zhu, Y., Qi, L., Wu, Z., Shi, P., 2024. Spectra-based predictive mapping of soil organic carbon in croplands: Single-date versus multitemporal bare soil compositing approaches. Geoderma 449, 116987. https://doi.org/10.1016/j.geoderma.2024.116987

Zickfeld, K., MacIsaac, A.J., Canadell, J.G., Fuss, S., Jackson, R.B., Jones, C.D., Lohila, A., Matthews, H.D., Peters, G.P., Rogelj, J., Zaehle, S., 2023. Net-zero approaches must consider Earth system impacts to achieve climate goals. Nat. Clim. Change 13, 1298–1305. https://doi.org/10.1038/s41558-023-01862-7

Žížala, D., Princ, T., Skála, J., Juřicová, A., Lukas, V., Bohovic, R., Zádorová, T., Minařík, R., 2024. Soil sampling design matters-Enhancing the efficiency of digital soil mapping at the field scale. Geoderma Reg. 39, e00874. https://doi.org/10.1016/j.geodrs.2024.e00874

Zwetsloot, M.J., Van Leeuwen, J., Hemerik, L., Martens, H., Simó Josa, I., Van De Broek, M., Debeljak, M., Rutgers, M., Sandén, T., Wall, D.P., Jones, A., Creamer, R.E., 2021. Soil multifunctionality: Synergies and trade-offs across European climatic zones and land uses. Eur. J. Soil Sci. 72, 1640–1654. https://doi.org/10.1111/ejss.13051

Annex A

Applying the soil sampling protocol with R

Sampling design by Stolbovoy et al (2007)

The first step is to install the packages that we will use to run the script. If you don't have R and RStudio installed in your computer, you can do it following this link: *https://posit.co/download/rstudio-desktop/*

```
install.packages(c('readr','sf','terra','leaflet','tidyverse','units'))
```

Once the packages we will use are installed, we load them into the R session.

```
library(readr)
library(sf)
library(terra)
library(tidyverse)
library(units)
```

We will set out working directory. This is the folder where we will store the output of the script. Change the path to a directory at your computer. In my case:

```
setwd("~/LILAS4SOIL/RScripts/tutorial")
```

We will load the shapefile with the boundaries of our study area (the field, pasture, vineyard, or orchard that we want to monitor for SOC change. for this, we use the sf package for spatial features. change the path and name of your shapefile. We use the field at Behialde as in the previous examples. The object tells us that the Coordinate reference system is ETRS89 / UTM zone 30N.

```
polygon <- sf::st_read("O:/Cambio
Climatico/SUELOS_SOC_STOLBOVOY/2024_Behialde_LILAS4SOILS/Behialde_04_GL_aukera1.shp")

## Reading layer `Behialde_04_GL_aukera1' from data source
##   `O:\Cambio
Climatico\SUELOS_SOC_STOLBOVOY\2024_Behialde_LILAS4SOILS\Behialde_04_GL_aukera1.shp'
##   using driver `ESRI Shapefile'
 ## Simple feature collection with 1 feature and 22 fields
 ## Geometry type: POLYGON
 ## Dimension:     XY
 ## Bounding box:  xmin: 531393.4 ymin: 4763591 xmax: 531678.4 ymax: 4763786
 ## Projected CRS: ETRS89 / UTM zone 30N
```

We can measure the area as well with the package units, in hectares.

```
field_area <- sf::st_area(polygon)
 my_area <- sum(units::set_units(field_area, ha),na.rm=TRUE)
 ## Area in hectares
 my_area

## 2.723046 [ha]
```

Load a custom R function to create the sampling design at any plot.

```
source("~/LILAS4SOIL/RScripts/tutorial/stolbovoy_function.R")
```

Apply this function to your study area. Here I named “polygon” my study area, and I use it as input for the function for the option “field_shp”. You need to specify the EPSG code of your zone as input for “crs_t”. We will be working with a projected CRS. For example, for the Basque Country (Spain) we use the EPSG:25830 (ETRS89 / UTM zone 30N) (*https://spatialreference.org/ref/epsg/25830/*). The coordinates that we will use with the GPS to locate the sampling points at the field will use this CRS, so it is important that we set it right. Finally, we need to specify the number of cells that we want to sample. We use the recommendations by Stolbovoy et al. (2007) of three sampling units for a plot between 1-5 ha.

```
Stolbovoy_test <- stolbovoy_sf_function(field_shp = polygon,
                                        Ncells = 3,
                                        crs_t = 25830)
```

We can examine several outputs. They are stored as elements of a list in Stolbovoy_test. First, if we want to visualize the location of the study area with satellite imagery.

```
Stolbovoy_test$field_map
```

If we want to visualize the grid, and how the numbers vary from 0-100 (with a continuous palette. The darker colours correspond to the grid cells with lower numbers.)

```
Stolbovoy_test$grid_map
```

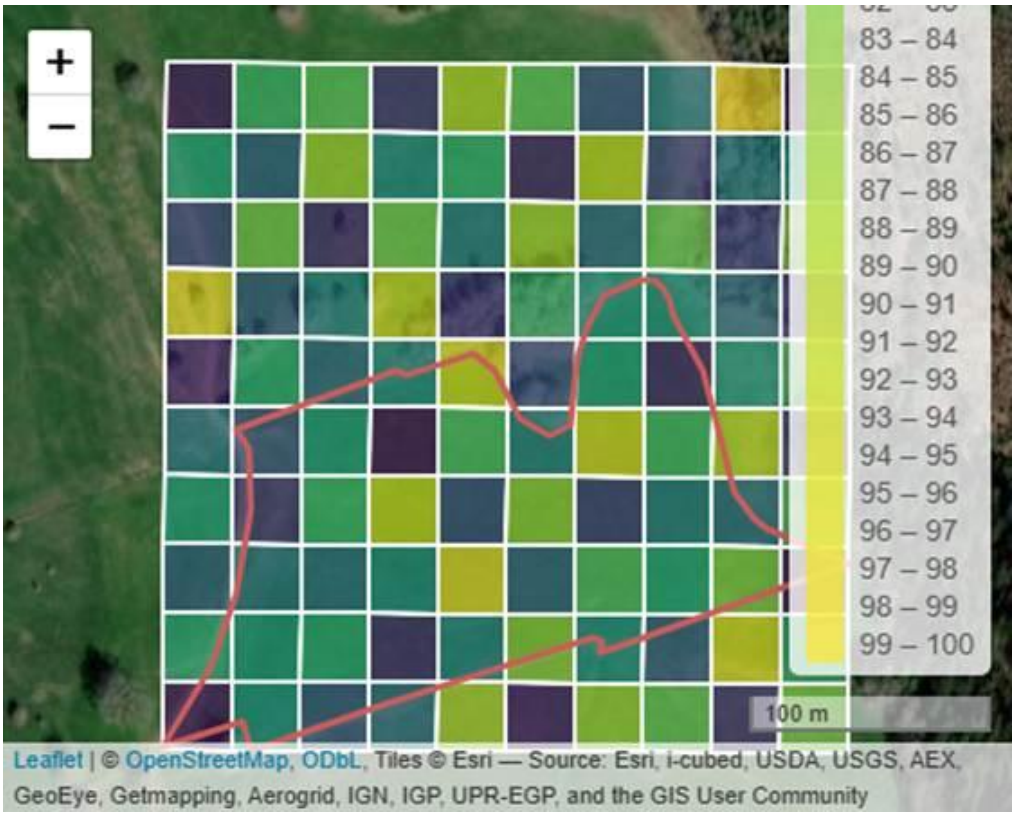

Next, if you want to see the selected cells.

```
Stolbovoy_test$stolbovoy_map
```

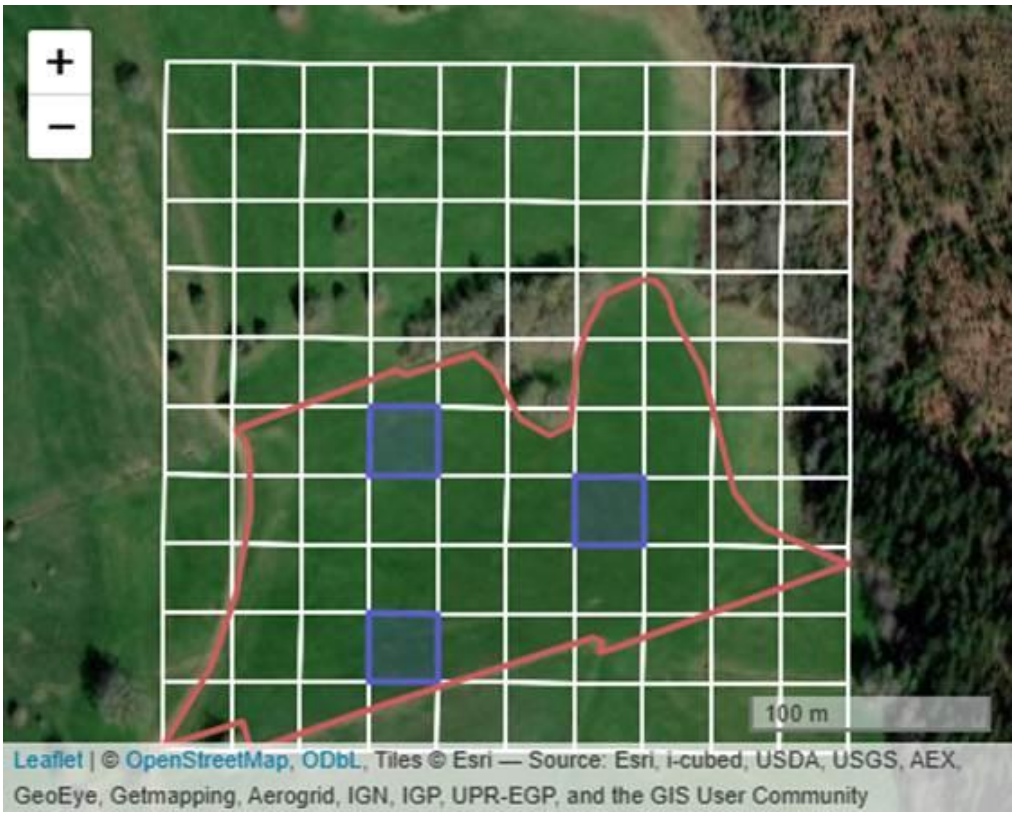

and the sampling points (25 points in this example).

```
Stolbovoy_test$stolbovoy_points
```

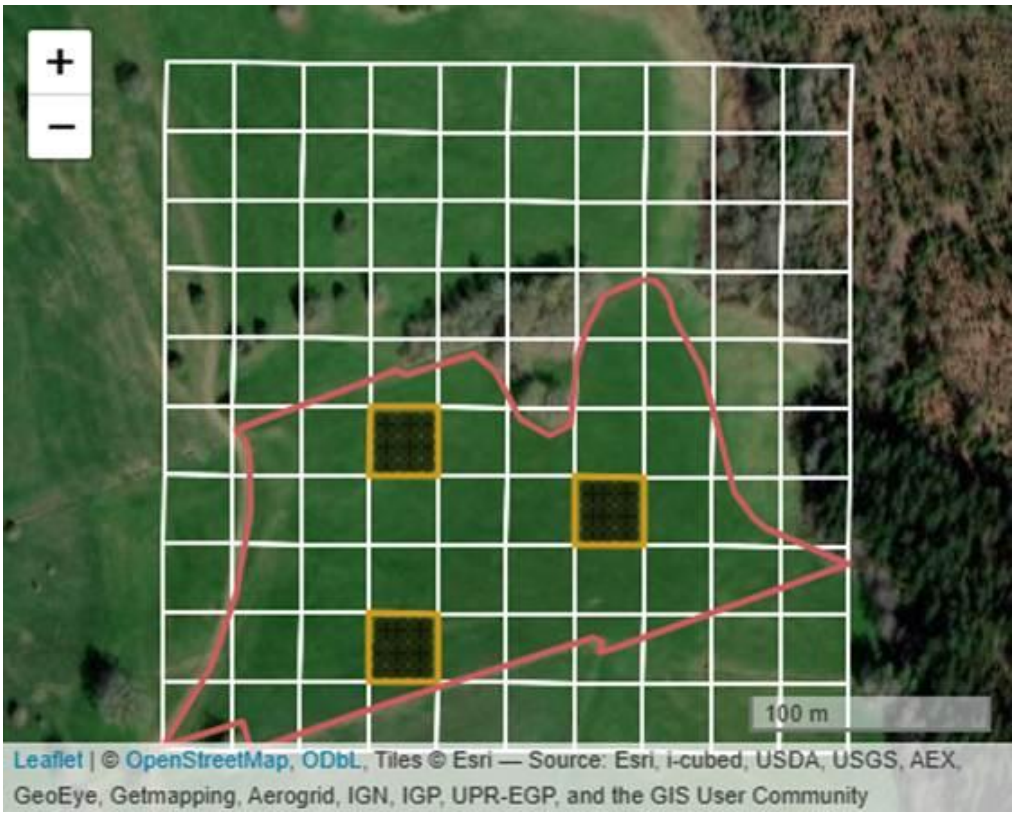

There is a table called “summary_table” that summarizes the information, indicating the coordinates (X, Y), the number of the grid cell, the type of point, “centroid”, “vertex”, or “sampling point”, and the distance between sampling points (Gs/6).

```
summary_table <- Stolbovoy_test$summary_table

### To see the first 10 observations of the table
summary_table[1:10,]

##           X       Y Grid_Cell     type dist_sampling_points
## 1  531493.2 4763719         1 centroid                   NA
## 2  531493.2 4763634        11 centroid                   NA
## 3  531578.6 4763691        17 centroid                   NA
## 4  531478.9 4763705         1   vertex                   NA
## 5  531507.4 4763705         1   vertex                   NA
## 6  531507.4 4763733         1   vertex                   NA
## 7  531478.9 4763733         1   vertex                   NA
## 8  531478.9 4763619        11   vertex                   NA
## 9  531507.4 4763619        11   vertex                   NA
## 10 531507.4 4763648        11   vertex                   NA

write_excel_csv(x = summary_table, file = "summary_table.csv", col_names = TRUE,
delim = ";")
```

We can export it into a csv file.

```
write_excel_csv(x = summary_table, file = "summary_table.csv", col_names = TRUE,
delim = ";")
```

You can further export the vertices into a shapefile accessing "Stolbovoy_test$Selection_Stolbovoy" and open it with other GIS software (ArcGIS, QGIS, etc.).

```
st_write(Stolbovoy_test$Selection_Stolbovoy,
         append=FALSE,
         dsn = "Selection_Stolbovoy.shp",
         driver = "ESRI Shapefile")


## Writing layer `Selection_Stolbovoy' to data source
##   `Selection_Stolbovoy.shp' using driver `ESRI Shapefile'
## Writing 3 features with 1 fields and geometry type Polygon.
```

We can also access and export the sampling points within each cell individually at "Stolbovoy_test$coordinates_Sampling_points". The third column of this table gives the grid cell number.

```
sampling_points <- Stolbovoy_test$coordinates_Sampling_points

head(sampling_points)

##          X       Y Grid_Cell           type dist_sampling_points
## 1 531493.2 4763719         1 sampling point             4.749121
## 2 531497.9 4763719         1 sampling point             4.749121
## 3 531502.7 4763719         1 sampling point             4.749121
## 4 531488.4 4763719         1 sampling point             4.749121
## 5 531483.7 4763719         1 sampling point             4.749121
## 6 531497.9 4763724         1 sampling point             4.749121

write_excel_csv(x = sampling_points, file = "sampling_points.csv", col_names = TRUE,
delim = ";")
```

If we want them as shapefile, we can transform them into a spatial object and export. Again, you need to substitute in the following code the appropriate EPSG code for your zone. At "dsn" we specify the destination. You can give here the name of the file to save the sampling points and the path to your directory.

```
sampling_points_sf <- sampling_points %>%
   st_as_sf(coords = c("X", "Y"), crs = 25830)

st_write(sampling_points_sf,
         append=FALSE,
```

```
          dsn = "sampling_points.shp",
         driver = "ESRI Shapefile")

## Warning in abbreviate_shapefile_names(obj): Field names abbreviated for ESRI
## Shapefile driver

## Deleting layer `sampling_points' using driver `ESRI Shapefile'
## Writing layer `sampling_points' to data source
##   `sampling_points.shp' using driver `ESRI Shapefile'
## Writing 75 features with 3 fields and geometry type Point.
```

If you also want to export the grid and explore it with another GIS software

```
st_write(Stolbovoy_test$grid,
          append=FALSE,
          dsn="stolbovoy_grid.shp",
          driver = "ESRI Shapefile")

## Writing layer `stolbovoy_grid' to data source
##   `stolbovoy_grid.shp' using driver `ESRI Shapefile'
## Writing 100 features with 1 fields and geometry type Polygon.
```

Stratified random sampling from compact geographical strata

We will create compact geostrata using the tutorial found at *https://cran.r-project.org/web/packages/spcosa/vignettes/spcosa.html* (Walvoort et al., 2023). Before using the pakage spcosa make sure you have Java installed at your computer with the version compatible with your computer. Install the packages rJava and spcosa and load them.

```
install.packages(c('rJava','spcosa'))
library(rJava)
library(spcosa)

## Warning: package 'spcosa' was built under R version 4.4.3
```

The study area should be in UTM projection. We can project it if it is not. We also transform the simple feature (package sf) into a spatial object (package sp), which works with spcosa.

```
polygon_utm <- st_transform(polygon, 25830)
### Transform to spatial
field_sp <- as_Spatial(polygon_utm)
```

In the case of LILAS4SOILS, we can adapt the protocol by Arrouays et al (2018) placing two sampling plots per strata, and only 3 strata instead of 20. We start by dividing the study area into equal-area compact geostrata. The number of strata is set with nStrata = 3. We set the seed to a number of our choice, to ensure reproducibility. We can tell the function the number of initializations that we want

to do (nTry = 10), and the function returns the best result. The number of grid cells into which is divided the study area is controlled with nGridCells. Higher value of nGridCells results in higher resolution for our strata. This step can take some time.

```
set.seed(3354)
stratification <- stratify(field_sp,
                           nStrata = 3,
                           equalArea = TRUE,
                           nTry = 10,
                           nGridCells = 20000)
```

We can plot the resulting strata

```
plot(stratification) +
   scale_x_continuous(name = "Easting (m)") +
   scale_y_continuous(name = "Northing (m)")

## Scale for x is already present.
## Adding another scale for x, which will replace the existing scale.
## Scale for y is already present.
## Adding another scale for y, which will replace the existing scale.
```

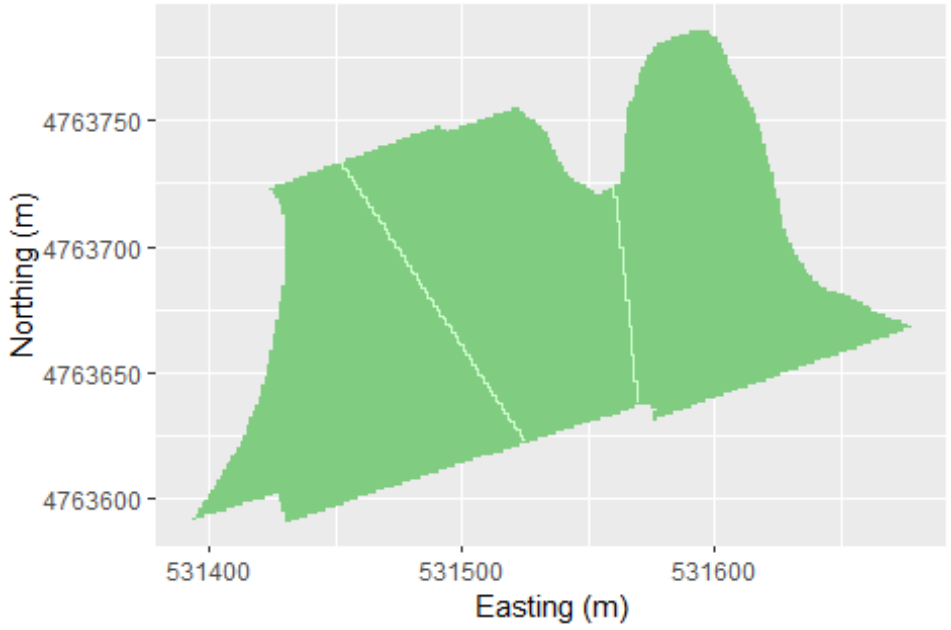

The next step will place randomly six sampling units in total. We can decide to locate more than one sampling unit per stratum, e.g., two units per stratum is set with n = 2. By changing the number within set.seed() we generate a different random sampling.

```
set.seed(546)
sampling_pattern <- spsample(stratification, n = 2)
plot(stratification, sampling_pattern)+
   ggplot2::scale_x_continuous(name = "Easting (m)") +
   ggplot2::scale_y_continuous(name = "Northing (m)")

## Scale for x is already present.
## Adding another scale for x, which will replace the existing scale.
## Scale for y is already present.
## Adding another scale for y, which will replace the existing scale.
```

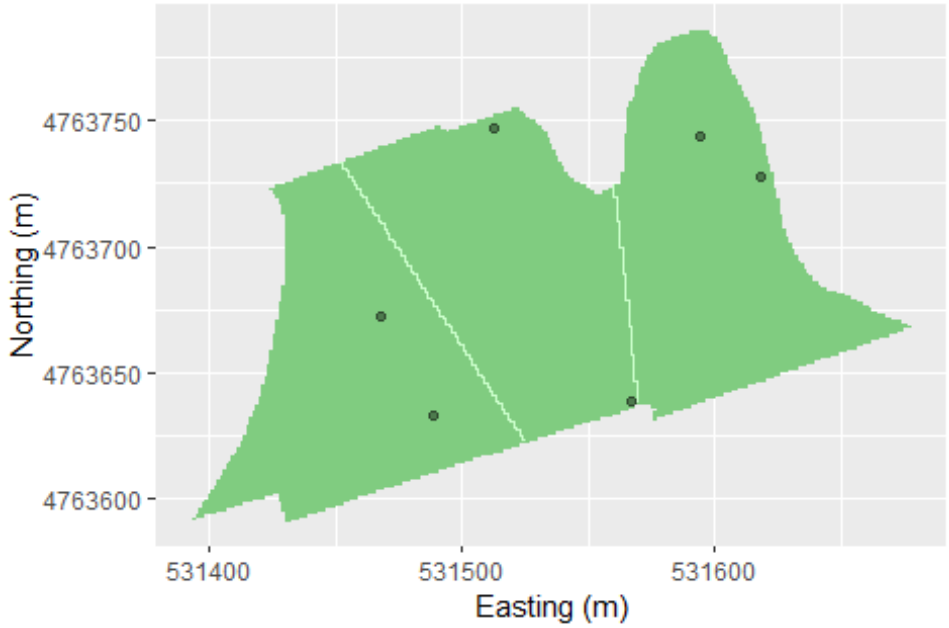


```
set.seed(943)
sampling_pattern <- spsample(stratification, n = 2)
plot(stratification, sampling_pattern)+
   ggplot2::scale_x_continuous(name = "Easting (m)") +
   ggplot2::scale_y_continuous(name = "Northing (m)")

## Scale for x is already present.
## Adding another scale for x, which will replace the existing scale.
## Scale for y is already present.
## Adding another scale for y, which will replace the existing scale.
```

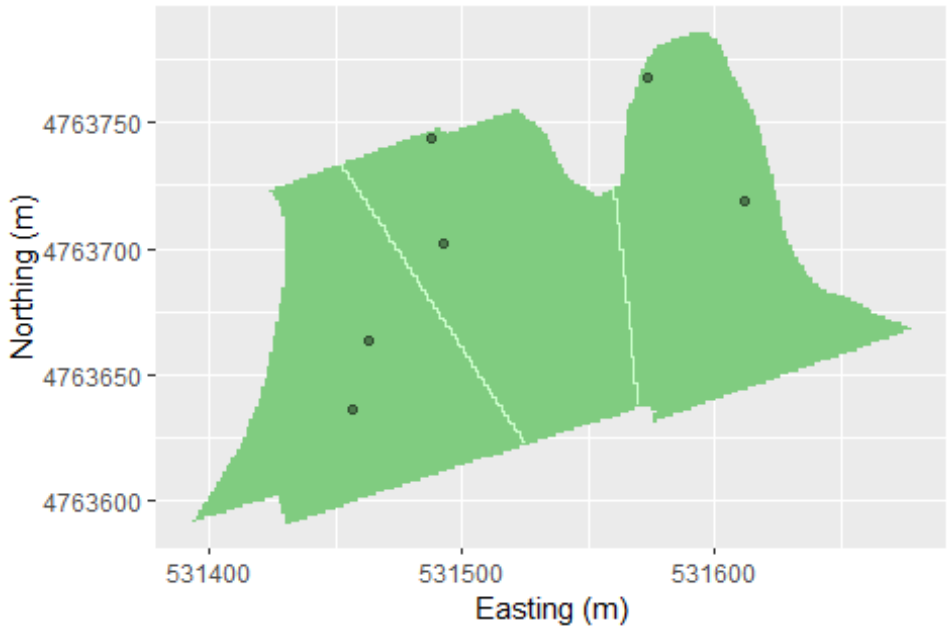

We need to extract the coordinates of the sampling points and create a multipoint object.

```
#getNumberOfStrata(stratification)

sampling_points <- as(sampling_pattern, "data.frame")

### Create multipoint
points_sf <- sf::st_multipoint(x = as.matrix(sampling_points), dim = "XYZ")
points_sf <- sf::st_sfc(points_sf, crs = 25830)

colnames(sampling_points) <- c("X", "Y")

sampling_points

##          X       Y
## 1 531573.5 4763768
## 2 531612.1 4763718
## 3 531487.5 4763744
## 4 531492.2 4763702
## 5 531463.3 4763664
## 6 531456.3 4763636
```

We can also visualize how would a 5 m radius plot look like, creating a buffer of 5 m around the centre of the sampling unit. We can use this to see if the sampling units overlap the boundaries of the strata or among themselves.

```
### Create buffer. Let´s see if they overlap
sampling_plots <- st_buffer(points_sf, dist = 5)
#plot(sampling_plots)

### Create buffer. Let´s see if they overlap
sampling_plots_wgs84 <- st_transform(sampling_plots, crs = 4326)
polygon_wgs_84 <- st_transform(polygon, crs = 4326)

leaflet(sampling_plots_wgs84) %>%
  addTiles() %>%
  addProviderTiles('Esri.WorldImagery') %>%
  addPolygons(color = "#d19a1a",
              fillColor = "#d19a1a",
              weight =4,
              opacity = 0.3,
              group="Sampling plots") %>%
  addPolygons(data=polygon_wgs_84,
              color = "#cd5c5c",
              fillColor = "transparent",
              weight =2,
              opacity = 1,
              group="polygon") %>%
  addScaleBar(
     position =  "bottomright",
     options = scaleBarOptions(metric=TRUE, imperial =FALSE, maxWidth = 200)
   )
```

In the previous example, two plots overlap with the boundaries of the study area. We generate the second sampling by changing the seed,

```
set.seed(665)
sampling_pattern <- spsample(stratification, n = 2)
sampling_points <- as(sampling_pattern, "data.frame")

### Create multipoint
points_sf <- st_multipoint(x = as.matrix(sampling_points), dim = "XYZ")
points_sf <- st_sfc(points_sf, crs = 25830)

### Create buffer. Let´s see if they overlap
sampling_plots <- st_buffer(points_sf, dist = 5)
#plot(sampling_plots)

### Create buffer. Let´s see if they overlap
sampling_plots_wgs84 <- st_transform(sampling_plots, crs = 4326)
polygon_wgs_84 <- st_transform(polygon, crs = 4326)

leaflet(sampling_plots_wgs84) %>%
  addTiles() %>%
  addProviderTiles('Esri.WorldImagery') %>%
  addPolygons(color = "#d19a1a",
              fillColor = "#d19a1a",
```

```
              weight =4,
              opacity = 0.3,
              group="Sampling plots") %>%
  addPolygons(data=polygon_wgs_84,
              color = "#cd5c5c",
              fillColor = "transparent",
              weight =2,
              opacity = 1,
              group="polygon") %>%
  addScaleBar(
     position =  "bottomright",
     options = scaleBarOptions(metric=TRUE, imperial =FALSE, maxWidth = 200)
   )
```

Stratified random sampling from strata created form environmental covariates

This method starts by loading the layers with the ancillary data of environmental covariates. We start with the NDVI layers created in Google Earth Engine. We assume that for your demo-site you have previously created or compiled the environmental covariates.

```
### Load the Sentinel-2 NDVI indices
library(terra)
```

```
ndvi_dir <- "C:/Users/mroman/OneDrive - Neiker,
S.A/Documentos/LILAS4SOIL/Covariates/Behialde/"

ndvi_q1 <- terra::rast(paste0(ndvi_dir,"NDVIq1_median.tif"))
ndvi_q2 <- terra::rast(paste0(ndvi_dir,"NDVIq2_median.tif"))
ndvi_q3 <- terra::rast(paste0(ndvi_dir,"NDVIq3_median.tif"))
ndvi_q4 <- terra::rast(paste0(ndvi_dir,"NDVIq4_median.tif"))
ndvi_sd <- terra::rast(paste0(ndvi_dir,"NDVI_sd.tif"))

ndvi <- c(ndvi_q1, ndvi_q2, ndvi_q3, ndvi_q4, ndvi_sd)
names(ndvi) <- c("ndvi_q1", "ndvi_q2", "ndvi_q3", "ndvi_q4", "ndvi_sd")
```

The spatial resolution of Sentinel-2 is around 10 m. We load the relief derivatives with the terra package. Candidate covariates for stratification are elevation, slope, easterness, northerness, the product of slope by northerness, topographic wetness index (TWI), and mid slope position.

```
### Load slope, DEM, northness, etc... Relief
relief_dir <- "C:/Users/mroman/OneDrive - Neiker,
S.A/Documentos/LILAS4SOIL/Covariates/Euskadi/Relief/"
dem <- terra::rast(paste0(relief_dir,"mdt_lidar_2017_25m_etrs89.tif"))
slope <- terra::rast(paste0(relief_dir,"slope.tif"))
northerness <- terra::rast(paste0(relief_dir,"northerness.tif"))
easterness <- terra::rast(paste0(relief_dir,"easterness.tif"))
nor_slope <- terra::rast(paste0(relief_dir,"nor_slope.tif"))
twi <- terra::rast(paste0(relief_dir,"twi_saga.tif"))
mid_slope <- terra::rast(paste0(relief_dir,"mid_slope.tif"))
r <- c(dem, slope, northerness, easterness, nor_slope, mid_slope, twi)

## Warning: [rast] CRS do not match

names(r) <- c("elevation", "slope", "northerness", "easterness", "nor_slope",
"mid_slope", "twi")
plot(r)
```

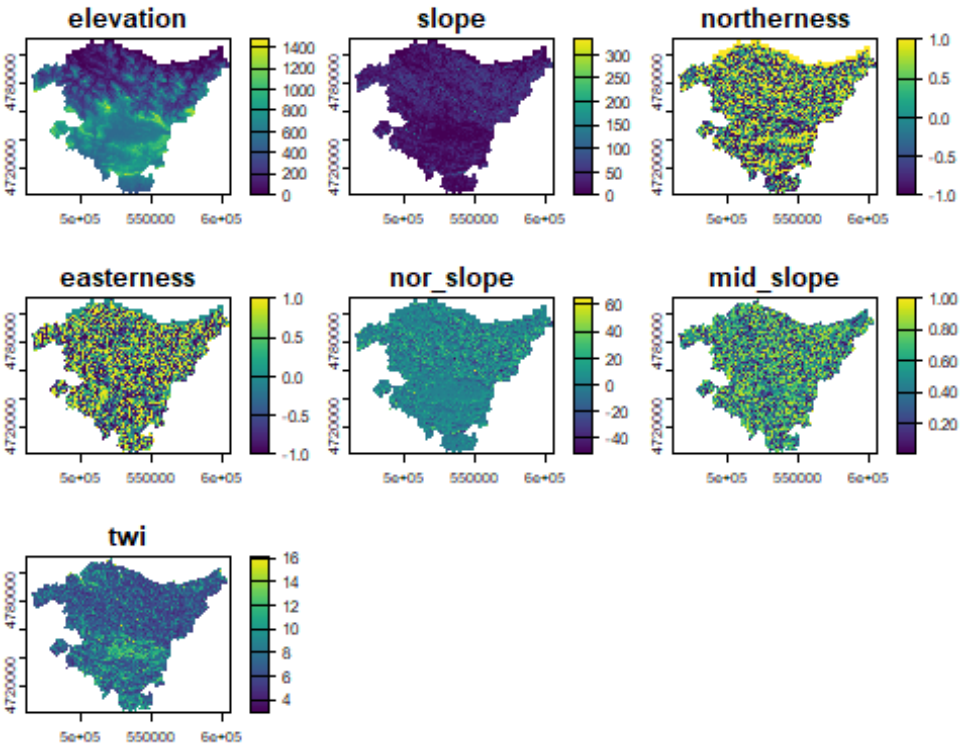

These layers are available for the whole of Euskadi. Now we process the covariates so that all have the same resolution, CRS and extent. The NDVI layers are in EPSG:4326, we project them to EPSG:25830 with bilinear resampling because they are continuous variables.

```
### Resample the NDVI layers to EPSG 25830
ndvi_utm30N <- terra::project(ndvi, "EPSG:25830", method="bilinear")
```

The relief covariates are cropped to the extent of the pasture, our study area at Behialde. We resample them to the same extent as the Setinel-2 NDVI layer, and create a mask, making NA the cells outside the study area.

```
### Crop and resample the relief variables to the same extent and resolution
r_Behialde <- terra::crop(r, ndvi_utm30N)
r_Behialde <- terra::resample(r_Behialde, ndvi_utm30N, method ="bilinear")

mask_fun <- function(x) {ifelse(is.na(x), NA, 1)}
mask_Behialde <- app(ndvi_utm30N[[1]],mask_fun)

covars <- c(ndvi_utm30N,r_Behialde)

## Warning: [rast] CRS do not match

covars_behialde <- mask(covars, mask_Behialde)
names(covars_behialde) <- c("ndvi_q1", "ndvi_q2", "ndvi_q3", "ndvi_q4", "ndvi_sd",
```

```
                              "elevation", "slope", "northness", "eastness",
                              "nor_slope", "mid_slope", "twi")

plot(covars_behialde)
```

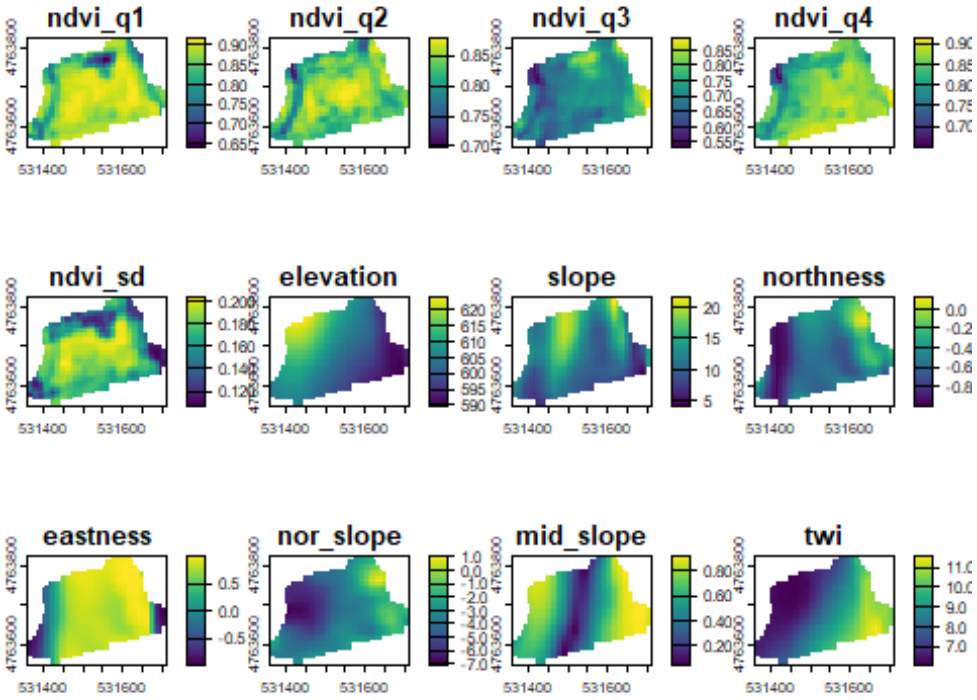

After visual examination of the covariates at Behialde, I decided to use elevation, slope, the product of northerness by slope, and TWI together with the NDVI variables, and mask the pixels that fall outside the boundaries of the pasture.

```
### Elevation, slope, northness x slope, TWI
input_c <- subset(covars_behialde,c("ndvi_q1", "ndvi_q2", "ndvi_q3", "ndvi_q4",
"ndvi_sd", "elevation", "slope", "nor_slope", "twi"))

### Use only pixels that fall within the boundaries
input_c <- terra::mask(input_c, polygon)
```

Before doing k-means clustering, we perform the inverse Cholesky transformation. This transformation decorrelates the data and as a result, the Euclidean distance calculated on the decorrelated variables is equivalent to the Mahalanobis distance calculated on the original variables. First we scale the variables, transform the raster layers into a data frame, and keep the coordinates.

```
### Scale variables
input_s <- scale(input_c, center = TRUE, scale = TRUE)
input_df <- as.data.frame(input_s, xy=TRUE)
input_df_coords <- input_df[,1:2]
```

Now we apply the inverse Cholesky transformation with matrix algebra.

```
### Apply the inverse Cholesky transformation
C <- chol(var(as.matrix(input_df[,3:ncol(input_df)])))
input_df.rs <- as.matrix(input_df[,3:ncol(input_df)]) %*% solve(C)
```

I do some preliminary analyses to select the optimal number of clusters. We have said that the minimum would be around 3. But this needs to be checked on a case-by-case basis. The package Nbclust offers calculating many internal clustering quality indices. By saying index = "all" we calculate all available indices. You can change the index to see the results for Silhouette, Dunn, or your preferred index. The input data is the data frame with the rescaled covariate data, input_df.rs. We apply k-means clustering. We will test between 2 to 6 clusters.

```
### I apply the function NBClust to select the optimal number of clusters
library(NbClust)
set.seed(2233)
res <-NbClust::NbClust(input_df.rs,
             distance = "euclidean",
             min.nc=2, max.nc=6,
             method = "kmeans",
             index = "all")


## *******************************************************************
## * Among all indices:
## * 7 proposed 2 as the best number of clusters
## * 2 proposed 3 as the best number of clusters
## * 2 proposed 4 as the best number of clusters
## * 3 proposed 5 as the best number of clusters
## * 10 proposed 6 as the best number of clusters
##
##                     ***** Conclusion *****
##
## * According to the majority rule, the best number of clusters is  6
##
##
## *******************************************************************
```

The Dunn index suggests 2 clusters as the optimal. The Silhouette and the Calinksi-Harabasz suggest 6 clusters as optimal. With the package ClusterR and the function KMeans_rcpp we perform clustering for n=2,3,6.

```
library(ClusterR)
```

```
## Warning: package 'ClusterR' was built under R version 4.4.3

set.seed(1990)
kmeans_2 <- ClusterR::KMeans_rcpp(input_df.rs,
                                  clusters = 2,
                                  num_init = 10,
                                  max_iters = 5000,
                                  fuzzy = FALSE,
                                  initializer = 'kmeans++',
                                  verbose = F)

set.seed(1995)
kmeans_3 <- ClusterR::KMeans_rcpp(input_df.rs,
                                  clusters = 3,
                                  num_init = 10,
                                  max_iters = 5000,
                                  fuzzy = FALSE,
                                  initializer = 'kmeans++',
                                  verbose = F)

set.seed(1984)
kmeans_6 <- ClusterR::KMeans_rcpp(input_df.rs,
                                  clusters = 6,
                                  num_init = 10,
                                  max_iters = 5000,
                                  fuzzy = FALSE,
                                  initializer = 'kmeans++',
                                  verbose = F)
```

Now that we have created different stratifications, we map them applying the function predict_KMeans to the rescaled raster layers.

```
strata_map <- function(input_s, kmeans_model){

### Map strata
### Transform into a dataframe
tile.df <- as.data.frame(input_s, row.names=NULL, optional=FALSE, xy=TRUE,
na.rm=FALSE)

### For each new pixel, I first have to rescale its values
## Take out the coordinates
tile.df.coords <- tile.df[,1:2]
tile.df <- tile.df[,3:ncol(tile.df)]

# Rescale the data with CLORPT.df (sample from the stack covariates that was used to
calibrate the kmeans in the first place)
tile.df.rs <- as.matrix(tile.df) %*% solve(C)
tile.df.rs <- as.data.frame(tile.df.rs)

### Predict cluster assignment
```

```
### Extract the index of the dataframe rows that are na/nan/Inf
df.na <- which(apply(tile.df.rs, MARGIN = 1, FUN = function(x) {any(is.na(x))}))

### Create empty prediction column
tile.df.rs$cluster <- NA

### If K is more than one instead of km.pedogenon.rcpp being a kmeans model, it would
be a list of models
### km.pedogenon.rcpp[[m]]$centroids
### predict in those rows where there are not na
tile.df.rs[-df.na, ]$cluster  <- ClusterR::predict_KMeans(data = tile.df.rs[-
df.na,1:(ncol(tile.df.rs)-1)],
                                                          CENTROIDS =
kmeans_model$centroids)
### Assign the values to a new raster
k.pred <- setValues(input_s[[1]], tile.df.rs$cluster)
names(k.pred) <- "Strata"
return(k.pred) # Return this
}


strata2 <- strata_map(input_s, kmeans_model = kmeans_2)
strata3 <- strata_map(input_s, kmeans_model = kmeans_3)
strata6 <- strata_map(input_s, kmeans_model = kmeans_6)
```

Now we can visualize the strata with leaflet. For that, we resample the layers to EPSG:4326 first.

```
### Plot with leaflet
library(leaflet)

#### Visualization
behialde_wgs84 <- sf::st_transform(polygon, 4326)
strata2_wgs84 <- terra::project(strata2,"EPSG:4326", method="near")
strata3_wgs84 <- terra::project(strata3,"EPSG:4326", method="near")
strata6_wgs84 <- terra::project(strata6,"EPSG:4326", method="near")

levels(strata2_wgs84) <- data.frame(id=1:2, strata=c("1", "2"))
levels(strata3_wgs84) <- data.frame(id=1:3, strata=c("1", "2", "3"))
levels(strata6_wgs84) <- data.frame(id=1:6, strata=c("1", "2", "3","4", "5", "6"))

library(leaflet)
library(terra)
library(sf)
library(viridisLite)

## Warning: package 'viridisLite' was built under R version 4.4.3

# Define color palette
pal2 <- colorFactor(palette = viridisLite::viridis(2),
                    domain = terra::values(strata2_wgs84),
                    na.color = "transparent")
```

```
leaflet(behialde_wgs84) %>%
  addTiles() %>%
  addProviderTiles('Esri.WorldImagery') %>%
  addPolygons(color = "red",
              fillColor = "transparent",
              weight =3,
              opacity = 1) %>%
  addScaleBar(position =  "bottomright",
              options = scaleBarOptions(metric=TRUE, imperial =FALSE, maxWidth =
200)) %>%
  addRasterImage(strata2_wgs84,
                 project = FALSE,
                 colors = pal2,
                 opacity = 0.8) %>%
  addLegend(pal = pal2,
            values = values(strata2_wgs84),
            title = "Strata")
```

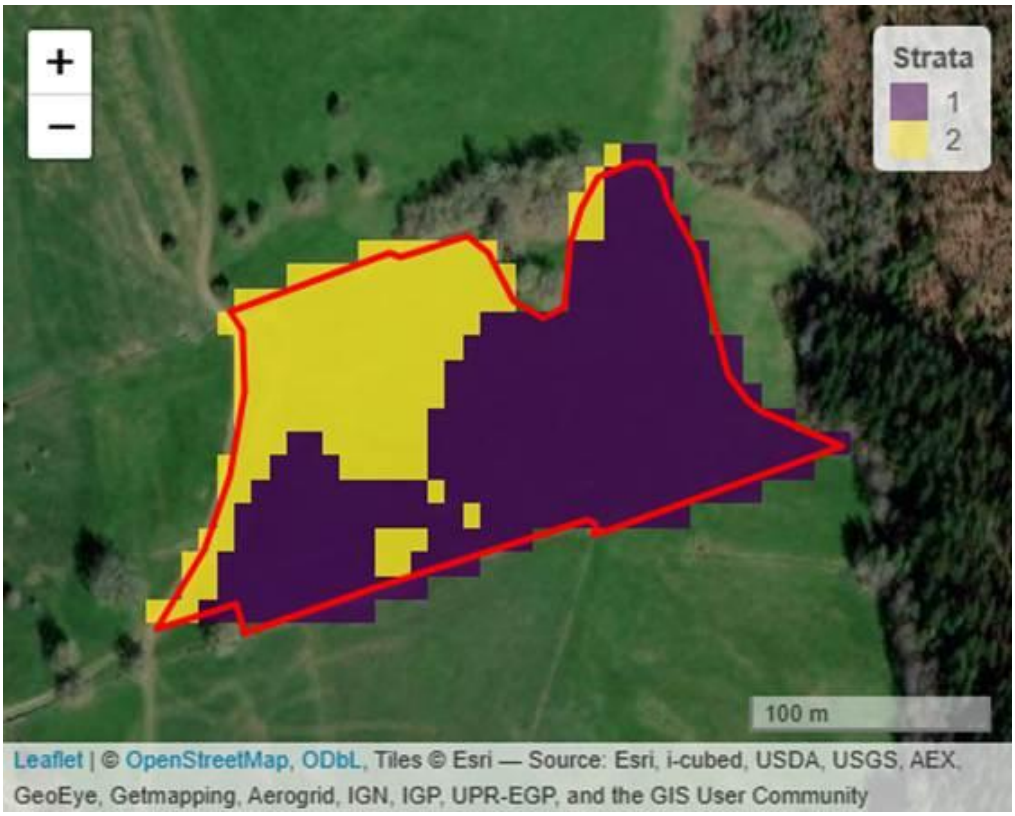


```
pal3 <- colorFactor(palette = viridisLite::viridis(3),
                    domain = terra::values(strata3_wgs84),
                    na.color = "transparent")
```

```
leaflet(behialde_wgs84) %>%
  addTiles() %>%
  addProviderTiles('Esri.WorldImagery') %>%
  addPolygons(color = "red",
              fillColor = "transparent",
              weight =3,
              opacity = 1) %>%
  addScaleBar(position =  "bottomright",
              options = scaleBarOptions(metric=TRUE, imperial =FALSE, maxWidth =
200)) %>%
  addRasterImage(strata3_wgs84,
                 project = FALSE,
                 colors = pal3,
                 opacity = 0.8) %>%
  addLegend(pal = pal3,
            values = values(strata3_wgs84),
            title = "Strata")
```

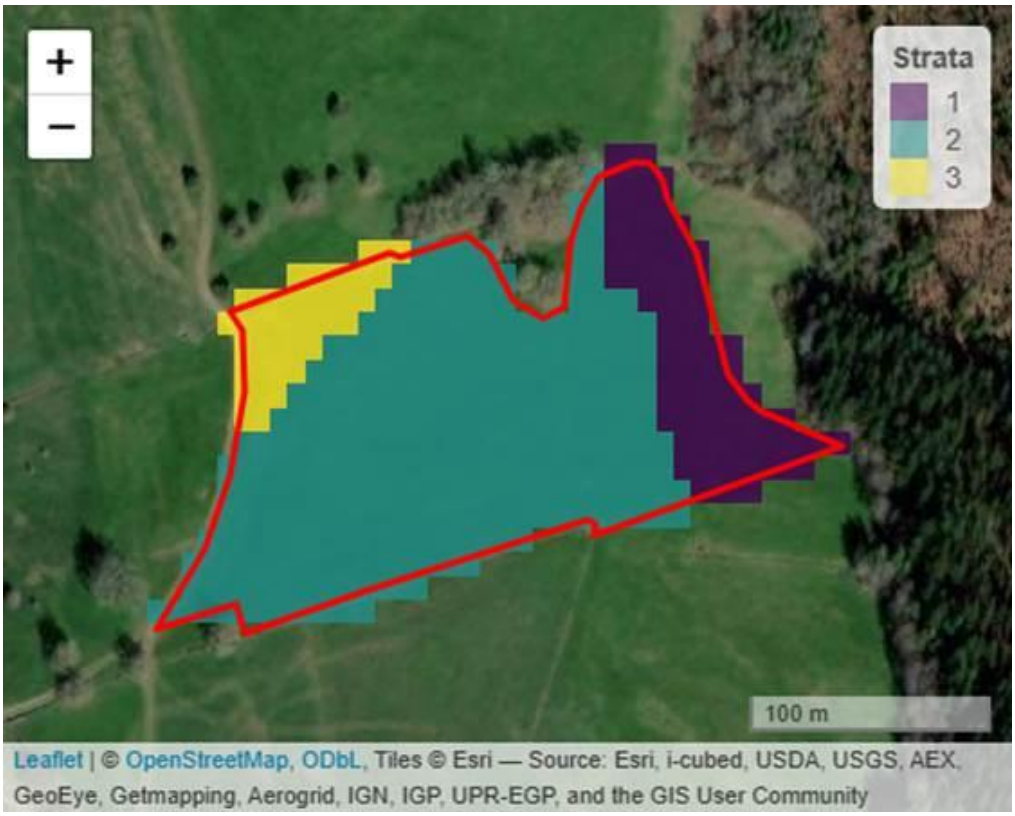


```
pal6 <- colorFactor(palette = viridisLite::viridis(6),
                    domain = terra::values(strata6_wgs84),
                    na.color = "transparent")
```

```
leaflet(behialde_wgs84) %>%
  addTiles() %>%
  addProviderTiles('Esri.WorldImagery') %>%
  addPolygons(color = "red",
              fillColor = "transparent",
              weight =3,
              opacity = 1) %>%
  addScaleBar(position =  "bottomright",
              options = scaleBarOptions(metric=TRUE, imperial =FALSE, maxWidth =
200)) %>%
  addRasterImage(strata6_wgs84,
                 project = FALSE,
                 colors = pal6,
                 opacity = 0.8) %>%
  addLegend(pal = pal6,
            values = values(strata6_wgs84),
            title = "Strata")
```

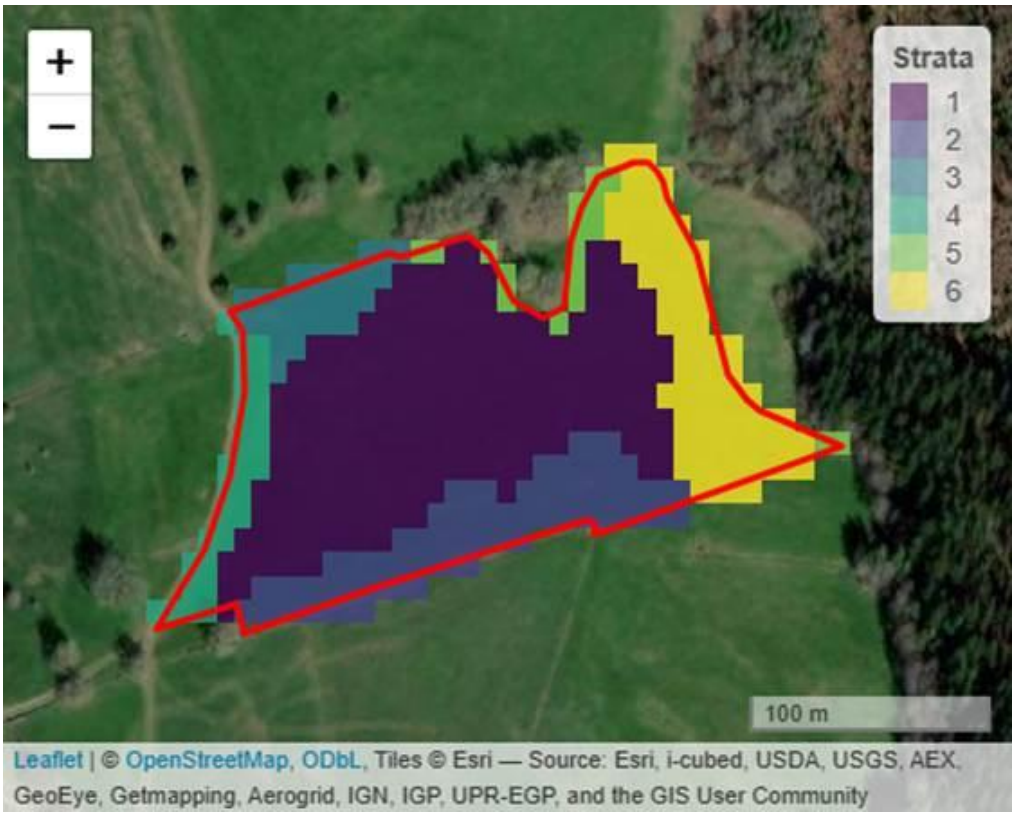

After visual comparison of the different stratification, we decide to use two strata at Behialde.

Proportional allocation of soil samples to strata

We will assign the number of samples to each stratum proportionally to the area they occupy. With a quick script, we see that stratum 1 would get approximately two thirds of the samples by the study area whereas stratum 2 would get one third. The stratification with three strata with proportional allocation would assign 19%, 72%, and 9% of samples to strata 1, 2, and 3 respectively.

```
### Transform the raster layer with the tw strata to a dataframe
library(tidyr)
library(dplyr)

area_2 <- as.data.frame(strata2)

n_sample <- area_2 %>%
   group_by(Strata) %>%
   summarise(., sample_perc = round(n()/nrow(area_2)*100,digits=1))

n_sample

## # A tibble: 2 × 2
##   Strata sample_perc
##    <dbl>       <dbl>
## 1      1        66.9
## 2      2        33.1

area_3 <- as.data.frame(strata3)

n_sample_3 <- area_3 %>%
   group_by(Strata) %>%
   summarise(., sample_perc = round(n()/nrow(area_3)*100,digits=1))

n_sample_3

## # A tibble: 3 × 2
##   Strata sample_perc
##    <dbl>       <dbl>
## 1      1        18.9
## 2      2        72
## 3      3         9.1
```

How can I take 2 random samples in strata 1 and one random sample in strata 2?

Let's say that we have budget for 6 sampling units, that would result in 4 sampling units at stratum 1 and 2 sampling units at stratum 2. We can allocate a random sampling with the function strata from package sampling. There are many other packages that allow for simple random sampling or stratified random sampling with R. The code was adapted from *https://dickbrus.github.io/SpatialSamplingwithR/STSI.html#STSI*

```
n_sample <- area_2 %>%
   group_by(Strata) %>%
```

```
   summarise(., sample_perc = round(n()/nrow(area_2)*100,digits=1),
             n_sample = round(n()/nrow(area_2)*6,digits=0))

n_sample

## # A tibble: 2 × 3
##   Strata sample_perc n_sample
##    <dbl>       <dbl>    <dbl>
## 1      1        66.9        4
## 2      2        33.1        2

### Assign the sampling units with the sampling package
library(sampling)

## Warning: package 'sampling' was built under R version 4.4.3

### Transform to ata.frame
strata2_df <- as.data.frame(strata2,xy = TRUE, na.rm = TRUE)

### Order by strata number
strata2_df <- dplyr::arrange(strata2_df, Strata)

### Assign sampling units by strata (remember the dataframe has to be in order of
stratum value)
set.seed(55)
sampling_units <- sampling::strata(data=strata2_df, ### Dataframe with the
stratification data
              stratanames = "Strata", ### Vector with the name of the strata variable
              size = n_sample$n_sample, ### Vector with the sample size per strata
              method = "srswor") # Simple random sampling without replacement

## Now with getdata we obtain the information (coordinates, stratum ID) of the
sampling units
# getdata(strata2_df, sampling_units)

### If we want to add more randomness in terms of coordinates (because we were
sampling from the center of the grid, but the real population is infinite).

StratifiedRandomSample <- getdata(strata2_df, sampling_units)%>%
   mutate(X = x %>% jitter(amount = res(strata2)[1] / 2),
          Y = y %>% jitter(amount = res(strata2)[2] / 2))

StratifiedRandomSample

##            x       y Strata ID_unit       Prob Stratum        X       Y
## 62  531557.2 4763715      1      62 0.01230769       1 531553.9 4763717
## 163 531533.1 4763666      1     163 0.01230769       1 531536.2 4763667
## 244 531541.2 4763642      1     244 0.01230769       1 531537.7 4763645
## 257 531452.7 4763634      1     257 0.01230769       1 531451.2 4763635
## 375 531452.7 4763723      2     375 0.01242236       2 531451.3 4763721
## 401 531460.8 4763706      2     401 0.01242236       2 531460.5 4763706
```

Visualization of sampling points

We plot the sampling points with leaflet. We can also make a buffer of 5 m radius to check if the plots overlap.

```
# Convert back to an sf object for spatial operations
sampled_points_sf <- st_as_sf(StratifiedRandomSample, coords = c("X", "Y"), crs =
"EPSG:25830")

sampled_points_wgs84 <- st_transform(sampled_points_sf, 4326)

### Plot it
leaflet(behialde_wgs84) %>%
  addTiles() %>%
  addProviderTiles('Esri.WorldImagery') %>%
  addPolygons(color = "red",
              fillColor = "transparent",
              weight =3,
              opacity = 1) %>%
  addScaleBar(position =  "bottomright",
               options = scaleBarOptions(metric=TRUE, imperial =FALSE, maxWidth =
200)) %>%
  addRasterImage(strata2_wgs84,
                 project = FALSE,
                 colors = pal2,
                 opacity = 0.8) %>%
  addLegend(pal = pal2,
            values = values(strata2_wgs84),
            title = "Strata") %>%
  addMarkers(data =sampled_points_wgs84)
```

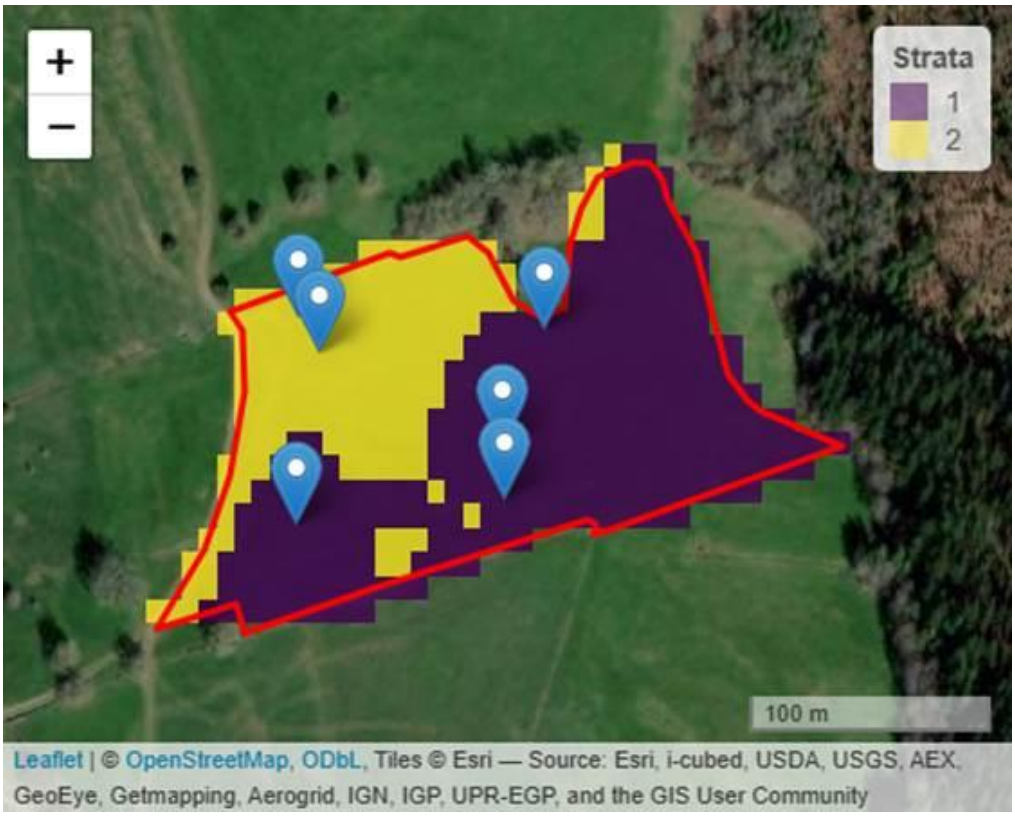

Conditioned Latin Hypercube Sampling

Taking the same environmental covariates that for k-means stratification, we will assign sampling units with cLH using the clhs package.

```
library(clhs)

## Warning: package 'clhs' was built under R version 4.4.3

covars_input_df <- as.data.frame(input_c, xy=TRUE, na.rm=TRUE)

set.seed(886)
res <- clhs(x = covars_input_df[,3:ncol(covars_input_df)],
            size = 6,
            iter = 50000, temp = 1, tdecrease = 0.95,
            length.cycle = 10, progress = FALSE, simple = FALSE)

behialde_CLH <- covars_input_df[res$index_samples, ]
```

The location of the cLHS. We set 6 sampling units, but we could have taken as many as desired by changing the input “size”.

```
# Convert back to an sf object for spatial operations
cLHS_points_sf <- st_as_sf(behialde_CLH, coords = c("x", "y"), crs = "EPSG:25830")

cLHS_points_wgs84 <- st_transform(cLHS_points_sf, 4326)

### Plot it
leaflet(behialde_wgs84) %>%
addTiles() %>%
  addProviderTiles('Esri.WorldImagery') %>%
  addPolygons(color = "red",
              fillColor = "transparent",
              weight =3,
              opacity = 1) %>%
  addScaleBar(position =  "bottomright",
               options = scaleBarOptions(metric=TRUE, imperial =FALSE, maxWidth =
200)) %>%
  addMarkers(data =cLHS_points_wgs84)
```